

THE CRYSTAL CHEMISTRY OF THE HOMOLOGOUS SERIES



by

JUDITH JENKINS KOHATSU

S.B. M.I.T.

(1969)

Submitted in Partial Fulfillment of the Requirements

for the Degree of

DOCTOR OF PHILOSOPHY

at the

Massachusetts Institute of Technology

September, 1973

Signature of Author.....

Signature redacted

Department of Metallurgy and Materials Science

August 13, 1973

Certified by

Signature redacted

Thesis Supervisor

Accepted by

Signature redacted

Chairman, Departmental Committee on Graduate Students



Abstract

THE CRYSTAL CHEMISTRY OF THE HOMOLOGOUS SERIES



by

JUDITH JENKINS KOHATSU

Submitted to the Department of Metallurgy and Materials Science on August 13, 1973 in partial fulfillment of the requirements for the degree of Doctor of Philosophy.

The plagionite group consists of four minerals, fülöppite ($\text{Pb}_3\text{Sb}_8\text{S}_{15}$), plagionite ($\text{Pb}_5\text{Sb}_8\text{S}_{17}$), heteromorphite ($\text{Pb}_7\text{Sb}_8\text{S}_{19}$), and semseyite ($\text{Pb}_9\text{Sb}_8\text{S}_{21}$), which form an homologous series. Two lattice constants remain essentially invariant throughout the series, while the third increases uniformly as the Pb content increases. Semseyite, whose crystal structure was determined in detail in this work, is monoclinic, space group C 2/c with $a=13.603(3)$, $b=11.936(8)$, $c=24.435(7)$ Å, $\beta=106.047(10)^\circ$, $\rho(\text{meas.})=6.03 \text{ gcm}^{-3}$ and $\rho(\text{cal})=6.12 \text{ gcm}^{-3}$ for $Z=4$. Intensity data was recorded both with a four-circle counter diffractometer and photographically by equi-inclination Weissenberg films. The structure was solved with the symbolic addition procedure and refined by least-squares techniques to $R=10.0\%$ for 1827 observable reflections. The asymmetric unit contains 20 atoms. Two Pb atoms are coordinated by six S atoms, one Pb atom by five S atoms and one Pb atom by seven S atoms in octahedral-like configuration. A fifth Pb atom has an irregular 8-fold coordination which may be described as a square antiprism. Three of the four independent Sb atoms have square pyramidal coordination; a fourth forms a trigonal pyramidal group. Of the eleven independent S atoms, five have octahedral-like configuration, five tetrahedral and one square-pyramidal. The structure is composed of slabs of PbS-like structure which run parallel to (112) and $(\bar{1}\bar{1}\bar{2})$ alternately along c and extend indefinitely along $[1\bar{1}0]$ and $[110]$ respectively.

From study of the structures of plagionite and semseyite a model was created which could predict the structures of heteromorphite and fülöppite, in projection. The model involves two types of addition of Pb at a previously Sb site. The interaxial angle β is correctly predicted as well as the change in $c \sin \beta$ and the density increase. An extension of the plagionite group past semseyite is predicted as possible synthetic materials.

Thesis Supervisor: Bernhardt John Wuensch

Title: Associate Professor of Ceramics

Table of Contents

	Page
Abstract.....	2
List of Figures	4
List of Tables	5
Acknowledgements	6
Chapter I Prologue	8
Chapter II Introduction	9
Chapter III The Experimental Work	23
Chapter IV Initial Structure Determination	29
Chapter V Structure Refinement with new Data	40
Chapter VI Description of the Structure	53
Chapter VII Semseyite, Stibnite, Galena, and Plagionite	81
Chapter VIII The Homologous Series $Pb_{3+2n}Sb_8S_{15+2n}$..	91
Appendix A Film Methods versus Counter Techniques...	106
Appendix B The Concept of the Direct Method	110
Appendix C The Program INTEN	117
Bibliography	131
Biographical Note	133

List of Figures

	Page
Figure 1 Density and Volume Variation of the Plagionite Group.....	20
Figure 2 Composite E-map for metal positions	37
Figure 3 Pb coordination Polyhedra-Semseyite.....	56
Figure 4 Sb coordination Polyhedra-Semseyite.....	62
Figure 5 S coordination Polyhedra-Semseyite.....	66
Figure 6 (010) Projection Semseyite	76
Figure 7 (112) Projection Semseyite	77
Figure 8 (112) Projection Plagionite	84
Figure 9 (010) Projection Plagionite	85
Figure 10 Comparison of Metal Polyhedra in Semseyite with Those in Plagionite.....	87
Figure 11 "Making" Plagionite from Semseyite.....	89
Figure 12 Addition Process 1.....	92
Figure 13 Addition Process 2.....	94
Figure 14 "Making" Heteromorphite from Semseyite....	97
Figure 15 Predicted (010) Projection Heteromorphite.	98
Figure 16 "Making" Plagionite from Heteromorphite..	100
Figure 17 "Making" Fülöppite from Plagionite.....	101
Figure 18 Predicted (010) projection Fülöppite.....	102
Figure 19 Schematic (112) Projections for the Plagionite Group.....	103
Figure 20 Making Para-Heteromorphite from Semseyite	105

List of Tables

	Page
Table 1 Comparison of Pb-As-S System with Pb-Sb-S System	14
Table 2 Cell Dimensions of the Plagionite Group.....	19
Table 3 Semseyite Lattice Constants	25
Table 4 Statistical Distribution of E's Calculated from Wilson Plot	32
Table 5 Assignment of Symbolic Signs	33
Table 6 Sign Combinations and Contradiction Indices...	34
Table 7 Atomic Parameters Initial Refinement.....	38
Table 8 Shifts of Counter Metal Positions From Film Data Positions	42
Table 9 Atomic Parameters	43
Table 10 Principal Axes and Orientations of Thermal Vibration Ellipsoids	48
Table 11 Comparison of F_{obs} with F_{cal}	49
Table 12 Statistical Distribution of E's Calculated from Wilson Plot (counter data).....	52
Table 13 Pb-S Bond Distances and Angles	57
Table 14 Sb-S Bond Distances and Angles	63
Table 15 Sulfur-Metal Bond Distances and Angles.....	68
Table 16 Sulfur-Sulfur Contact Distances	73
Table 17 Densities and changes of $c \sin \beta$ of the Plagionite Group	95
Appendix B	
Table 1 Phase Determination by an Inequality	112

Acknowledgements

The author likes to express her deep appreciation to Professor B.J.Wuensch of the Ceramics Division of the Department of Metallurgy and Materials Science for suggesting the present work. His academic advice and help with experimental problems was greatly appreciated. Moreover, the author would like to thank him for his role, knowingly or unknowingly, as match-maker. His friendship is highly prized.

The author would also like to thank Professor C.Frondel of Harvard University for providing the crystal of semseyite. She would like to acknowledge Dr. John Jambor of the Canadian Geological Survey for supplying material of fülöppite and heteromorphite and powder films. She is grateful to Professor Klaus Eriks of Boston University for allowing her to use their autophotodensitometer. Dr. Charles T. Prewitt kindly allowed her use of equipment in his laboratory also.

The author is also indebted to Mr. Al Freker for keeping the x-ray equipment in running order - a monumental job. He also constructed many useful accessories. The author also thanks Mr. D. Fellows for lettering many of the figures and for preparing the graphs.

She is grateful to Donna Wicks who typed the many tables and to Barbara Baker who helped in the typing of the manuscript.

The author gratefully thanks the members of the Ceramics division for their aid and abettance. She is particularly

indebted to the members of the "Wuensch" group, past and present, who helped her weather the many storms of a structure determination.

Of all people she is indebted to a former fellow student and crystallographer and now her husband, Iwao. He prepared the many laborious drawings for the manuscript. In addition he provided many helpful crystallographic ideas. She also appreciates his collaboration in many of the computer programs.

While a student the author was supported by NSF contract GA 1549 and a teaching assistantship sponsored by the Department of Metallurgy and Materials Science.

Chapter 1

Prologue

In this era of pragmatism and practicality man is pressed to justify his actions. Such is the case for the layman and the scientist. The scientific community thinks, not altogether unwillingly, in terms of marketability. They offer apologia for their heritage, neglecting the dictum of their very name, scire - to know.

This thesis does not concede its dignity to the idols of profits and patentability. The minerals of the plagionite group will probably never be of industrial significance. Their study, however, contributes to a most practical goal - the extension of the knowledge of matter. Without such basic extensions man's world of gadgetry would not have been built.

Chapter 11

Introduction

Sulfur is one of the most prevalent compounds of our environment. Much of the organic facet of the chemistry of sulfur and many of its simpler inorganic compounds have been thoroughly detailed and studied. However, the more complex inorganic compounds with their potential for solid state innovation have not been exhaustively catalogued, much less completely studied. One of the most complicated sulfide families to suffer this lack of attention is the sulfosalt group.

Sulfosalts are minerals characterized by the combination of one or more metal atoms with sulfur and a Group V element such as As, Sb, or Bi. Their compositions may be formalized as $X_m Z_n S_p$, with Z the Group V element and X usually being Pb, Ag, Cu, and occasionally a transition metal Zn or Hg. The integers, m, n, and p, frequently bear no simple relationship among themselves, and large numbers of intermediate compounds exist in a given pseudo-binary system (e.g. 18 in PbS - Sb₂S₃).

Of the 150 of these minerals described in the literature, fewer than a quarter have been structurally analyzed. The results of these analyses seriously question the adequacy of the simple crystal chemical models usually used to predict structure. Bonding description is no longer a simple question of isolating first and second nearest neighbors. In the sulfosalt compounds the sulfur coordination of the metal atoms form almost a continuum

rather than discrete neighbors. Such is the case for Bi - coordination in aikinite (2.663, 2.734, 2.996, 3.117, 3.531 Å) and Bi(4) in gladiolite (2.61, 2.83, 2.99, 3.49 Å) for example. (Kohatsu, I., 1971) Coordination polyhedra are frequently distorted from ideal geometric configurations. The sulfur coordination of a given metal is often not unique; Sb for example can be three -, four -, or five-coordinated by S. Two different coordination schemes may even occur in a single compound (e.g. Sb_2S_3). (Nowacki, 1971) Such idiosyncrasies as these can not be predicted by the same crystal chemical theories that so well handle the structural and bonding properties of sulfur's fellow group member, oxygen. Thus much needs to be studied and more structural data gathered to complete the picture for sulfur.

Complete characterization of the sulfosalt compounds is hampered by inherent material difficulties. X-ray analysis is initially hindered by the scarcity of material suitable for study. Many of the minerals are rare with only a few (1 or 2) known crystals available for study. Even certain common minerals occur as twins, intergrowths, or bundles of fibers, making them unsuitable for single crystal work. Synthesis of these compounds would be an alternative. However, such work has usually been unsuccessful. The exact composition of many of the compounds is still in question making synthesis difficult. Moreover, minute traces of metals, apparently minor constituents in the sulfosalts, are usually found. Whether these are merely impurities or are required to

stabilize a mineral phase has not been conclusively ascertained in most cases. For example, Hall (1967) found that polybasite, $\text{Ag}_{16}\text{As}_2\text{S}_{11}$, was stable only when 3.1 - 7.6 wt. per cent Cu is present. The task is further complicated by the fact that the sulfosalts are low temperature phases and reactions are difficult both to initiate and to carry to completion. When synthesis proceeds with a small measure of success, the result is usually a multiphase mixture rather than good single crystals. Thus while artificially manufacturing the desired mineral is theoretically a good means of relieving the scarcity of suitable material, it has not reached the stage where it is a practical solution. X-ray analysis of the sulfosalts is still limited by the discovery of good single crystals of naturally-occurring minerals.

After this initial barrier is overcome, the solution and subsequent refinement of the sulfosalt structures is hampered by the high x-ray absorptivity of the materials. Many of these minerals contain large amounts of Pb and/or Bi - both having high mass absorption coefficients. Values up to 1500 cm^{-1} are not uncommon for Pb sulfosalts in Cu K_{α} x-radiation. The effect of the presence of these metals is to absorb portions of the incident and scattered x-ray beams, consequently weakening them. The depletion of intensity can be four or five orders of magnitude even for minute (10^{-2} cm) sample sizes. Correction for this effect requires an extremely accurate description of the crystal shape. On the other hand, a very small crystal must be selected to minimize the

effect. Thus the precise description of the intricate crystal shape has become most difficult. Consequences of improper correction for absorption are severe for these highly absorbing materials. The R-value, the residual error, an indicator of the correctness of the proposed structure, is in these instances limited by the absorption correction. Failure to make an accurate correction limits the preciseness of the data, which in turn limits one's ability to precisely determine the coordinates of atoms in the structure. In the case of Pb - or Bi - containing sulfosalts, the locating of the "electronically weak" sulfur is particularly difficult. Such a problem is comparable to the one faced by organic crystallographers in locating hydrogen positions. Even if the correction would be exact, the intensity data are weak due to absorption and the relative standard deviations due to counting statistics are large. This also limits the preciseness of the determination. Poor absorption correction also limits the precision with which bond distances may be measured. In Pb-Bi sulfosalts this is especially critical since both Pb and Bi have similar scattering powers and may be identified only by their coordination geometry. Imprecise correction for absorption can also appear as anomalous anisotropic thermal motion of the atoms. The detection of such real thermal motion is of importance in discussing bonding characteristics and a pseudo-effect can lead to confusing and often wrong interpretation.

Due to these inherent difficulties little is known of sulfo-

salt crystal chemistry. The study of a Pb-Sb sulfosalt group was therefore undertaken. Eighteen minerals are known in the Pb - Sb - S system compared with only nine in the companion Pb-As - S system. (Table 1) All but one of the arsenic structures are known. Only one Sb-structure, plagionite $Pb_5Sb_8S_{17}$ (Cho, 1969) is known; however, two others, zinkenite $Pb_6Sb_{14}S_{27}$ (Takeda, 1971, Takeda, 1964) and boulangierite (Born and Hellner, 1960), $Pb_5Sb_4S_{11}$, have been partially determined. Among the sulfantimonides and sulfarsenides isostructuralism and solid substitution are often common. However, in the Pb-Sb-S and Pb-As-S systems, isostructuralism is seen not to be prevalent; no doubt because of the difference in relative sizes of the As and Sb coordination polyhedra with respect to the Pb polyhedron. Limited As substitution is still possible. (Table 1)

Due to the paucity of data much is uncertain about the polyhedral coordination of Sb by S in the presence of Pb. Arsenic in similar environments invariably assumes a trigonal pyramidal configuration, while bismuth, the other commonly occurring Group V element, invariably has a square pyramid of five sulfurs in a [1+2+2] arrangement. Antimony is known to assume both coordinations and can do so in a single structure, stibnite (Sb_2S_3). Therefore, more information is needed to interpret correctly the widely varying number of phases in the two systems.

More interestingly than merely amassing structural data, semseyite $Pb_9Sb_8S_{21}$, the subject of the current work, has pro-

TABLE 1

Comparison of Pb-As-S System with Pb-Sb-S System

Reduced Composition Pb_xMyS		$\text{PbS-As}_2\text{S}_3$ <u>Mineral</u>	$\text{PbS-Sb}_2\text{S}_3$ <u>Mineral</u>
.600	.267	gratonite $\text{Pb}_9\text{As}_4\text{S}_{15}$ (1,2)	
.565	.304	jordanite $\text{Pb}_{13}\text{As}_7\text{S}_{23}$ (?) (3)	gercronite $\text{Pb}_{13}(\text{Sb},\text{As})_8\text{S}_{23}$
.500	.333		falkmanite $\text{Pb}_3\text{Sb}_2\text{S}_6$
.454	.363		boulangerite $\text{Pb}_5\text{Sb}_4\text{S}_{11}$ (?) (4)
.444	.370		sterryite $\text{Pb}_{12}(\text{Sb},\text{As})_{10}\text{S}_{27}$ (?)
.429	.381		semseyite $\text{Pb}_9\text{Sb}_8\text{S}_{21}$
.425	.550		sorbyite $\text{Pb}_{17}(\text{Sb},\text{As})_{22}\text{S}_{40}$ (?)
.415	.390		madocite $\text{Pb}_{17}\text{Sb}_{16}\text{S}_{41}$ (?)
.400	.400	dufrenoyite $\text{Pb}_2\text{As}_2\text{S}_5$ (5)	veenite $\text{Pb}_2(\text{Sb},\text{As})_2\text{S}_5$
.379	.414		dadsonite $\text{Pb}_{11}\text{Sb}_{12}\text{S}_{29}$

Table 1
(continued)

Comparison of Pb-As-S System with Pb-Sb-S System

Reduced Composition Pb_xMyS	$\text{PbS-As}_2\text{S}_3$ <u>Mineral</u>	$\text{PbS-Sb}_2\text{S}_3$ <u>Mineral</u>
.372 .419		playfairite $\text{Pb}_{16}\text{Sb}_{18}\text{S}_{43}$ (?)
.368 .421		heteromorphite $\text{Pb}_7\text{Sb}_8\text{S}_{19}$
.361 .426		launayite $\text{Pb}_{22}\text{Sb}_{26}\text{S}_{61}$ (?)
.350 .450	rathite Ia $\text{Pb}_9\text{As}_{13}\text{S}_{28}$ (6)	
.322 .456	rathite II $\text{Pb}_9\text{As}_{13}\text{S}_{28}$	
.306 .473	acentric baumhauerite $\text{Pb}_{11}\text{As}_{17}\text{S}_{36}$ (7)	
.300 .500	rathite I $(\text{Pb},\text{Tl})_3\text{As}_5\text{S}_{10}$ (8)	
.300 .500	rathite III $\text{Pb}_3\text{As}_5\text{S}_{10}$ (9)	
.294 .491		plagionite $\text{Pb}_5\text{Sb}_8\text{S}_{17}$ (10)
.280 .480		robinsonite $\text{Pb}_7\text{Sb}_{12}\text{S}_{25}$ (?)

Table 1
(continued)

Comparison of Pb-As-S System with Pb-Sb-S System

Reduced Composition Pb_xMyS	$\text{PbS-As}_2\text{S}_3$ <u>Mineral</u>	$\text{PbS-Sb}_2\text{S}_3$ <u>Mineral</u>
.278 .500	centric baumhauerite $\text{Pb}_5\text{As}_9\text{S}_{18}$	
.273 .485		guettardite $\text{Pb}_9(\text{Sb,As})_{16}\text{S}_{33}$ (?)
.250 .500	scleroclase PbAs_2S_4 (11)	twinnite $\text{Pb}(\text{Sb,As})_2\text{S}_4$
.222 .519		zinkenite $\text{Pb}_6\text{Sb}_{14}\text{S}_{27}$ (?) (13,12)
.222 .556	hutchinsonite $(\text{Pb,Tl})_2\text{As}_5\text{S}_9$ (14)	
.200 .553		fülöppite $\text{Pb}_3\text{Sb}_8\text{S}_{15}$

TABLE 1
continued

- (1) Rosch (1963)
- (2) Ribar and Nowacki (1969)
- (3) Wuensch and Nowacki (1966)
- (4) Born and Hellner (1960)
- (5) Marumo and Nowacki (1967)
- (6) LeBihan (1962)
- (7) Engel and Nowacki (1969)
- (8) LeBihan (1962)
- (9) LeBihan (1962)
- (10) Wuensch and Cho (1970)
- (11) Iitaka and Nowacki (1961)
- (12) Takeda and Sadanaga (1964)
- (13) Takeda and Sadanaga (1964)
- (14) Takeuchi (1965)

posed structural relationships with the one known structure, plagionite $Pb_5Sb_8S_{17}$. It has been suggested that fülöppite $Pb_3Sb_8S_{15}$, plagionite, heteromorphite $Pb_7Sb_8S_{19}$, and semseyite form an homologous series. It may be characterized as $Pb_{3+n}Sb_8S_{15+n}$ with $n=0$ (fülöppite) to $n=3$ (semseyite). Two of the lattice constants, a and b , remain essentially invariant while the third, c , increases uniformly with n . (Table 2) Jambor (1969) has shown that the volume and the densities (both measured and calculated) increase uniformly with n . (Figure 1) He also points out that $(c \sin \beta)$ increases more uniformly than c as n increases. The probable space group for all the members of the series is $C2/c$ with $Z=4$. As one proceeds from fülöppite to semseyite, one observes an increasingly perfect $\{112\}$ cleavage.

Not only do the minerals of the plagionite group show similar characteristics, but as a group they are likewise dissimilar from the other Pb-Sb sulfosalts. The plagionite minerals occur as tabular, lozenge-like crystals rather than fibrous needles as do most other Pb-Sb sulfosalts. The plagionite group minerals do not exhibit the common $4 A^\circ$ (or multiple) translation indicative of the direction of a stibnite-like chain as do many Sb and all Bi sulfosalts. Lastly they have no As analogues, nor do they permit As substitution although both of these traits are not uncommon in the Sb sulfosalts. Thus it appears that relationships must exist among the structures of these four minerals. If the

TABLE 2

Cell Dimensions of the Plagionite Group

	a	b	c	β	c sin β
Fülöppite	13.41 Å	11.71	16.90	94°43'	16.8 Å
Plagionite	13.49	11.87	19.98	107°10'	19.1 Å
Heteromorphite	13.60	11.93	21.22	90°50'	21.2 Å
Semseyite	13.60	11.94	24.45	106°2'	23.5 Å

(after Jambor (1969))

FIGURE 1
Density Variation in the Plagionite Group

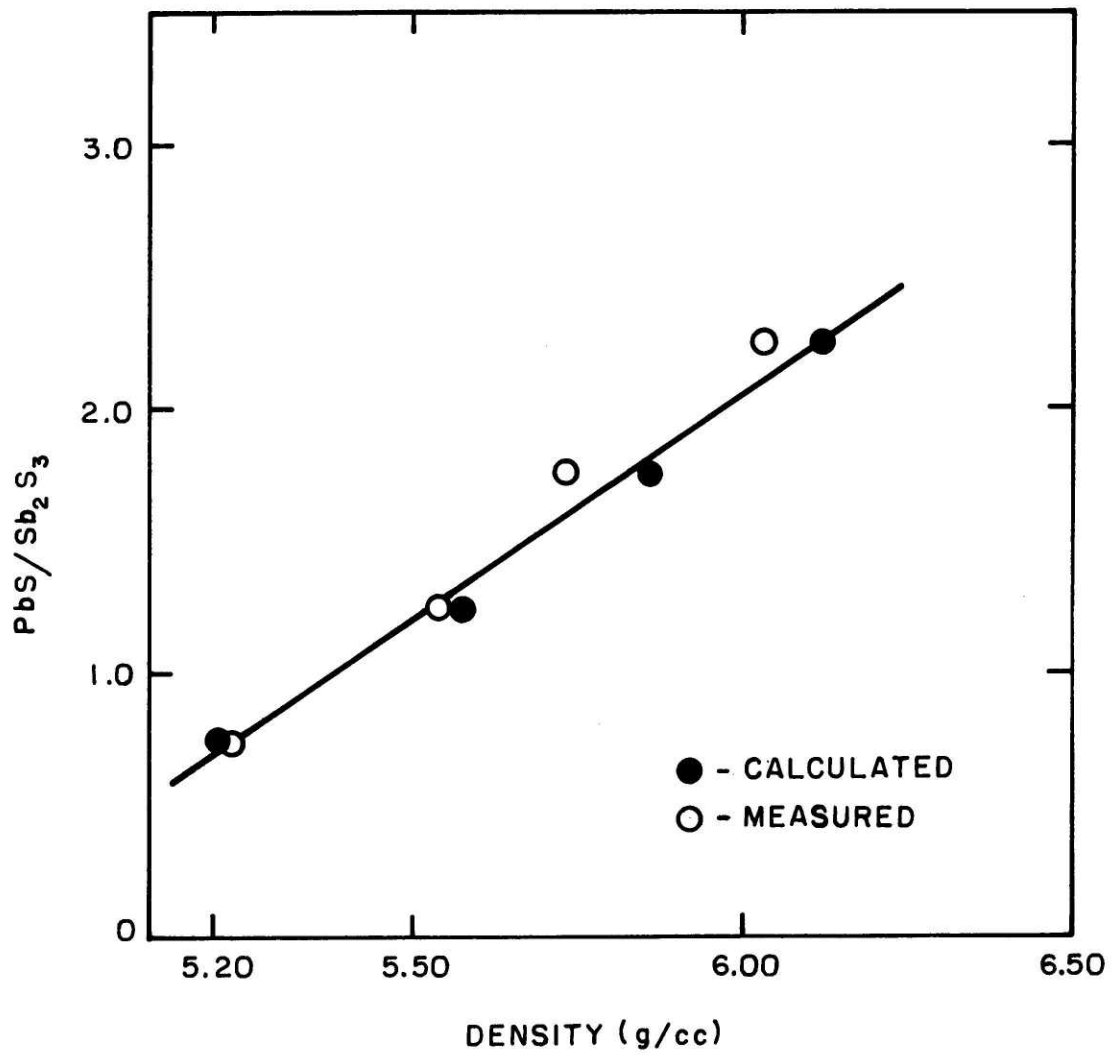
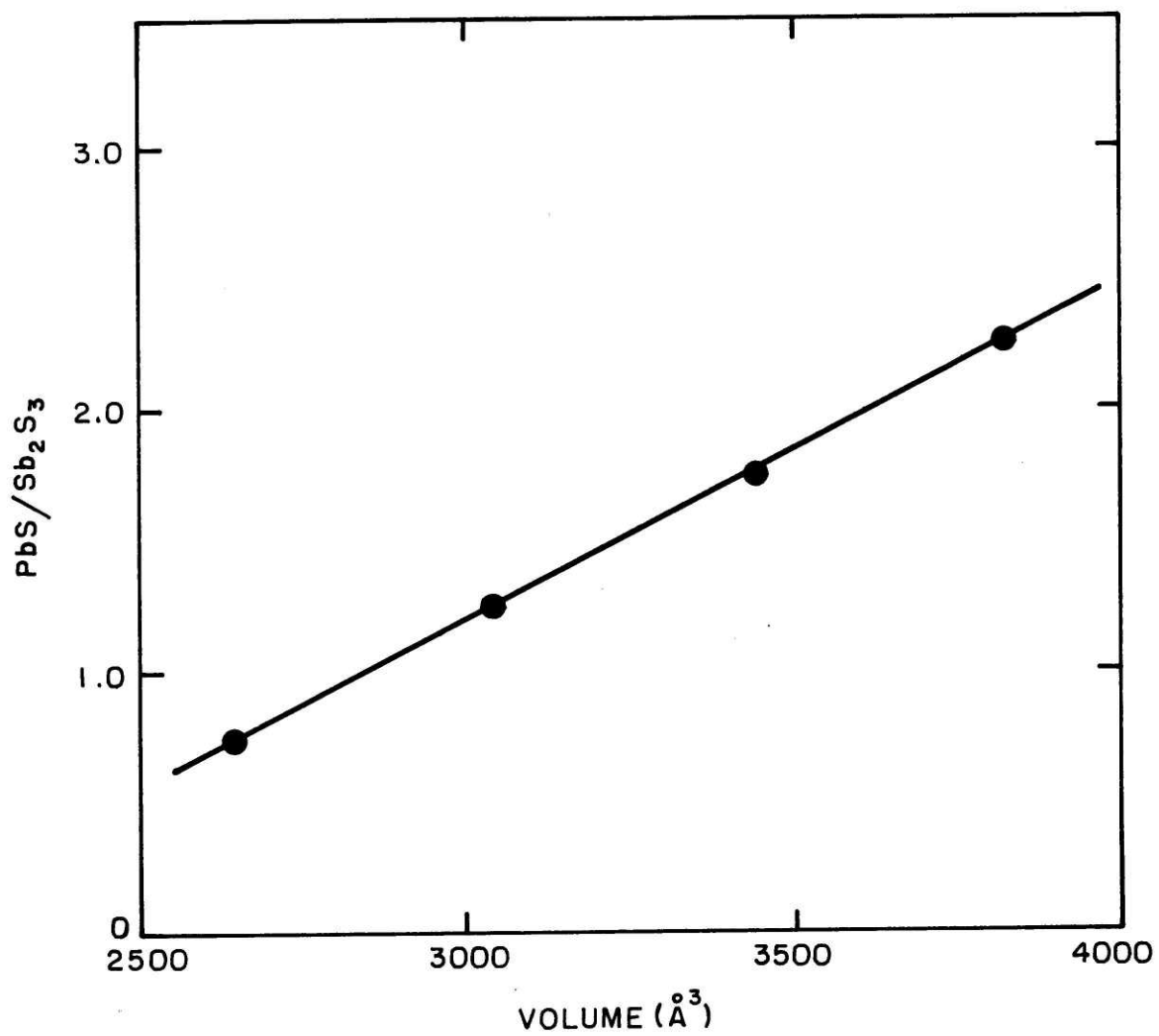


FIGURE 1

continued

Volume Variation of the Plagionite Group



basis of the homology can be established, then useful generalizations on structure may be made for the whole series, such as those made in the V_nO_{2n-1} ($3 < n < 8$) and Ti_nO_{2n-1} homologous series. (Horiuchi, 1972)

Chapter III

The Experimental Work

A. Preliminary X-ray Analysis

Semseyite, $Pb_9Sb_8S_{21}$, is the final and most complicated member of the plagionite group. Previously Peacock and Nuffield (1945) studied semseyite but they compiled mineralogical data but no structural data. They report that crystals of the material are somewhat lighter in color than plagionite with freshly broken surfaces showing nearly tin-white with a good metallic luster. The measured specific gravity for their crystals was 6.03.

The crystal used in this investigation was from Kisbanya, Roumania (Harvard Museum catalogue #99697). Due to the high x-ray absorptivity ($\mu_{\lambda}^0 = 1304.74 \text{ cm}^{-1}$ for $CuK\alpha$) an attempt was made to grind a sphere from the material following the method of Bond (1951). Difficulty was encountered as semseyite exhibits a perfect $\{112\}$ cleavage. A slightly ellipsoidal crystal was finally prepared for study. The average radius for the crystal was 0.00873 cm and $\mu_{\lambda} r = 11.391$ for $Cu K\alpha$.

Preliminary x-ray work indicated that semseyite was monoclinic with diffraction symmetry $2/m$. The second setting (b - axis unique) was selected for reference of the lattice constants. Systematic extinction, $h + k \neq 2n$ for $hk\ell$ and $\ell \neq 2n$ for 00ℓ , indicated that space groups $C 2/c$ and $C c$ were permitted. This is consistent with the diffraction symbol $2/mC_/c$. The centrosymmetric space group $C 2/c$ (C_{2h}^6) was chosen for subsequent study based on a previous morphological study. (Peacock and

Nuffield, 1945). This choice was subsequently confirmed by statistical tests on the set of diffracted intensities.

Precision lattice constants were measured with the aid of data collected with a back-reflection Weissenberg camera (diameter = 114.592 mm) and Cu radiation. With two settings of the crystal (b axis and c axis parallel to the spindle axis), 130 observations were indexed and film spacings measured. Precision lattice constants were obtained with a least-squares fit of the data by the use of Burnham's computer program LCLSQ (1961). Corrections were made for sample absorption, camera eccentricity, and film shrinkage. The lattice constants thus obtained were:

$$\begin{array}{ll} a = 13.603 \pm .003 \text{ \AA} & \alpha = 90.0^\circ \\ b = 11.935 \pm .007 & \beta = 106.046 \pm .010 \\ c = 24.452 \pm .007 & \gamma = 90.0 \end{array}$$

The resulting cell volume is 3815.7 \AA^3 with a calculated density of 6.12. This density assumes 4 formula weights per unit cell. Thus the cell contents are $\text{Pb}_{36}\text{Sb}_{32}\text{S}_{84}$, a total of 152 atoms. The calculated density of 6.12 compares favorably with the measured value of Peacock and Nuffield (1945) of 6.03. The lattice constants and the direct lattice correlation matrix as well as the constants of Peacock and Nuffield are presented in Table 3.

B. The Data Collection

During the determination of the space group with the precession camera and Mo radiation and the lattice constants determination, it was noted that the magnitude of the reflected inten-

TABLE 3

Semseyite Lattice Constants

	<u>Present Work</u>	<u>Peacock & Nuffield (1945)</u>
a	13.60 3 (3) Å	13.61 Å
b	11.93 6 (8)	11.99
c	24.45 3 (7)	24.52
α	90°	90°
β	106.047° (10)	105°49'
γ	90°	90°

Direct Lattice Correlation Matrix

	a	b	c	α	β	γ
a	1.0	.610	.567	0.0	-.238	0.0
b		1.0	.302	0.0	-.002	0.0
c			1.0	0.0	-.427	0.0
α				1.0	0.0	0.0
β					1.0	0.0
γ						1.0

sities was low. Peak to background ratios were also very small. Both of these problems were caused by the smallness of the crystal and the large x-ray absorptivity. Since neither predicament augered well for the planned data collection with Mo $K\alpha$ radiation by film methods, it was decided to attempt to use monochromated Ag radiation. The monochromation would improve the peak to background ratio and the absorptivity for Ag (252.1 cm^{-1}) was much lower than that for Cu (1304.74 cm^{-1}). A Supper monochromator was used with both the precession and equi-inclination Weissenberg cameras. Unfortunately scattering from the small crystal proved so weak that the data collection times would be prohibitive. Thus it was decided to utilize Cu $K\alpha$ radiation and the Weissenberg camera (to minimize the crystal to film distance). A highly accurate absorption correction was necessitated.

The initial data for semseyite were collected with a three-film pack on an equi-inclination Weissenberg camera. Eight levels, $h0\ell$ to $h7\ell$, were collected with exposure times ranging from 96 hours ($h0\ell$) to 225 hours ($h7\ell$). The films were then scanned by an autophotodensitometer unit at Boston University.* The optical density of the film was reported at 100μ intervals both horizontally and vertically. The data were stored on magnetic tapes by the Optronics unit.

C. Initial Data Analysis

The individual optical densities were reconstructed into

*PHOTOSCAN system P-1000 is manufactured by OPTRONICS INTERNATIONAL INC., Chelmsford, Massachusetts.

reflection intensities by the use of the computer program INTEN (initially written by R.Kadlec (Boston University) and subsequently modified by I. Kohatsu (1971)). Two major methods were utilized in a later version of the program modified by the author. (Appendix C) The first method involved extracting and assembling around each reflection a "window" sufficiently large to include the peak and ample background but small enough not to include any other reflection. The second alternative was to reconstruct the whole film by "dumping" the stored densities in the same order in which they were recorded. Then the whole digitized record of the film could be graphically indexed much as a normal x-ray film is indexed. Although the methods provided integrated intensities, both were tedious and neither completely satisfactory. (See Appendix A.) Reflections which were undiscernable to the eye on the x-ray film were marked unobservable and subsequently excluded from initial structure refinement.

Of the nearly 1500 integrated intensities measured, over one-third were marked unobservable. The remainder (approximately 1000) were corrected for Lorentz and polarization effects as well as absorption. The author followed the method of Prewitt and Wuensch (1965) and utilized the program ACAC which she extensively modified to permit the use of the Gaussian quadrature method. As mentioned in the Introduction, the absorption-effect correction is extremely critical for this material. Therefore, the crystal shape was carefully measured. The small crystal is an ellipsoid of circular cross-section described mathematically as

$\frac{x^2}{a^2} + \frac{y^2 + z^2}{b^2} = 1$ with $a = 0.00794 \pm .0003$ cm and $b = 0.00952 \pm .0003$ cm. The calculated volume of the sample, using 512 integration points, was 0.2516×10^{-5} cm³. The calculated geometrical volume was 0.3014×10^{-5} cm³. Three attempts at the absorption correction were made varying ellipsoid size and orientation. The best and final try yielded agreement of 14% between equivalent F_{hkl} 's. Much of the error was attributed to inaccuracies in the original measurement of the intensities.

Chapter IV

Initial Structure Determination

The essential job facing a crystallographer in analyzing a large structure is the determination of the phases of the structure factors. For a centrosymmetric structure this amounts to the assignment of positive or negative signs to the magnitude of the structure factors. The structure factor, which carries the atomic position information, is a complex quantity but only the magnitude (i.e. the reflection intensity) can be measured with current techniques. There are two main solutions to this dilemma - the Patterson method (Buerger, 1959) and Symbolic Addition (Karle and Hauptmann, 1953).

The Patterson method involves looking into atom-atom interactions in Patterson space. The Patterson function at the point (u,v,w) represents the average product of the electron density at points (X,Y,Z) and $(X+u,Y+v,Z+w)$. Therefore when atoms sit at the two points, the function will have maxima. Thus interatomic vectors may be obtained. It should be noted that since u,v,w cover all space, $n(n-1)$ peaks will result from the interactions of n atoms. Structures containing small numbers (1,2, or 3) of high atomic-number atoms and the rest electronically light atoms are particularly well suited to this method. Since the heavy atoms determine most of the phases, the positions of the lighter atoms can be determined with the regular electron density synthesis.

However, if the crystal structure contains large numbers of heavy and moderately heavy atoms and atomic arrangement is complicated, a Patterson map is nearly impossible to interpret. If the arrangement of atoms can be said to approach randomness, then the method of symbolic addition can be used. With this method only n peaks versus $n(n-1)$ peaks will appear in the same volume using electron density techniques. The symbolic addition method depends on inequalities that exist between structure factors with certain sets of hkl 's. (Karle and Hauptmann, 1953; Sayre, 1952) For a further discussion of the symbolic addition method, see Appendix B. Thus if enough data is examined, phases can be determined probabilistically.

Since the structure of semseyite contains five independent Pb's and four Sb's and is complicated, the Patterson method was discarded in favor of symbolic addition. The raw data (corrected for absorption, Lorentz, and polarization effects) were scaled so that all 'k' levels were on the same basis. The structure factors were multiplied by

$$\frac{\text{Exposure time of the } k^{\text{th}} \text{ level}}{\text{Exposure time of the } h0\ell \text{ level}}^{-0.5} .$$

This data was then processed by the program FAME (Fortran Automatic Manufacture of E's)(Dewar and Stone). The three hundred largest F_{hkl} 's which were measured were converted to E_{hkl} 's, the normalized structure factors - $F_{hkl} / \sum f_i$ where f_i are the atomic scattering factors. The best set of E_{hkl} 's selected on the

basis of absolute magnitude and number of interactions with other hkl 's were assigned symbolic signs A through H. The results of the Wilson calculation in FAME yielded an overall scale factor of 0.4954 (to convert from arbitrary to electron units) and a temperature factor (β) of 0.6813. The statistical distribution of E_{hkl} 's (derived from FAME) indicated a centric structure (Table 4). The symbolic signs assigned to the eight initial reflections are given in Table 5.

The normalized structure factors (E_{hkl} 's) were used as input to MAGIC (Multiphase Automatic Generation from Intensities in Centric Crystals)(Dewar and Stone). The eight reflections were used to initialize MAGIC. Through twenty successive iterations of MAGIC increasing numbers of real (+ or -) signs were acquired. Ultimately 249 E_{hkl} 's were signed, out of the possible 300 reflections. The sign combinations and the contradiction indices are given in Table 6. Of the four most probable sign combinations, two showed extremely low contradiction indices while the other two were slightly higher. All remaining sign combinations exhibited large contradiction indices.

The phased E_{hkl} 's (based on the four most probable sign combinations) were then used as input to an electron density synthesis program, FORDAP - 2 (Zalkin) to provide four E-maps. The Pb and Sb positions were readily located and used in an initial least-squares refinement using the program SFLS-5 (Prewitt, 1962). The first and third combinations yielded arrangements

TABLE 4

Statistical Distribution of E's Calculated from Wilson Plot

<u>Quantity</u>	<u>Calculated</u>	<u>Theoretical (Centric)</u>	<u>Theoretical (Acentric)</u>
Average Mag of E's	0.805	0.798	0.886
Average of E^2	1.023	1.000	1.000
Average of $ E^2-1 $	1.039	0.968	0.736
Percentage Greater Than One	27.94	32.00	37.00
Percentage Greater Than Two	6.16	5.00	1.80
Percentage Greater Than Three	0.33	0.30	0.01

TABLE 5

Assignment of Symbolic Signs

<u>h</u>	<u>k</u>	<u>l</u>	<u>E</u>	<u>Sign</u>
2	-5	2	2.6760	A
6	-6	1	3.0430	B
-5	-5	5	2.7280	C
-2	-6	2	2.6440	D
-4	-11	4	3.4800	E
-3	-6	1	2.4100	F
3	-5	5	2.8180	G
-8	-16	2	2.8090	H

TABLE 6

Sign Combinations and Contradiction Indices

Symbols								Contradiction
<u>A</u>	<u>B</u>	<u>C</u>	<u>D</u>	<u>E</u>	<u>F</u>	<u>G</u>	<u>H</u>	<u>Index</u>
+	+	0	+	0	+	+	-	63.1
-	+	0	-	0	+	+	+	72.9
+	-	0	-	0	-	+	-	108.0
-	-	0	+	0	-	+	+	127.6
+	-	0	-	0	+	+	-	1349.7
-	-	0	+	0	+	+	+	1357.3
+	+	0	+	0	-	+	-	1371.8
-	+	0	-	0	-	+	+	1396.1
-	-	0	+	0	-	+	-	1718.7
+	+	0	+	0	+	+	+	1752.7
+	-	0	-	0	-	+	+	1755.1
-	+	0	-	0	+	+	-	1764.4
-	+	0	-	0	-	+	-	1955.5
-	-	0	+	0	+	+	-	1963.5
+	+	0	+	0	-	+	+	1964.7
+	-	0	-	0	+	+	+	1994.4
+	+	0	+	0	+	-	+	2526.3
-	+	0	-	0	+	-	-	2539.0
+	-	0	-	0	-	-	+	2553.0
-	-	0	+	0	-	-	-	2577.3
+	-	0	-	0	+	-	+	2887.1
-	-	0	+	0	+	-	-	2892.2
+	+	0	+	0	-	-	+	2913.3
-	+	0	-	0	-	-	-	2933.1
+	+	0	+	0	-	-	-	3349.1
-	+	0	-	0	-	-	+	3349.1
-	-	0	+	0	+	-	+	3381.7
+	-	0	-	0	+	-	-	3392.0
-	-	0	+	0	-	-	+	3644.0
+	+	0	+	0	+	-	-	3678.0
-	+	0	-	0	+	-	+	3678.8
+	-	0	-	0	-	-	-	3679.8
+	+	0	-	0	-	+	+	8242.3
-	+	0	+	0	-	+	-	8246.8
+	-	0	+	0	+	+	+	8263.3
-	-	0	-	0	+	+	-	8285.6
+	-	0	+	0	-	+	+	8498.6
-	-	0	-	0	-	+	-	8530.3
-	+	0	+	0	+	+	-	8535.9
+	+	0	-	0	+	+	+	8538.9
-	+	0	+	0	+	+	+	8622.3
+	+	0	-	0	+	+	-	8646.8
+	-	0	+	0	-	+	-	8651.0

TABLE 6
(continued)

Sign Combinations and Contradiction Indices

<u>A</u>	<u>B</u>	<u>Symbols</u>						<u>Contradiction</u>
		<u>C</u>	<u>D</u>	<u>E</u>	<u>F</u>	<u>G</u>	<u>H</u>	<u>Index</u>
-	-	0	-	0	-	+	+	8653.0
+	-	0	+	0	+	+	-	8842.7
-	+	0	+	0	-	+	+	8849.9
-	-	0	-	0	+	+	+	8861.0
+	+	0	-	0	-	+	-	8874.7
+	+	0	-	0	-	-	-	9746.1
-	+	0	+	0	-	-	+	9759.7
+	-	0	+	0	+	-	-	9766.0
-	-	0	-	0	+	-	+	9795.5
+	-	0	+	0	-	-	-	10179.7
-	-	0	-	0	-	-	+	10198.7
-	+	0	+	0	+	-	+	10208.3
+	+	0	-	0	+	-	-	10222.1
-	+	0	+	0	-	-	-	10467.8
+	-	0	+	0	+	-	+	10468.5
-	-	0	-	0	+	-	-	10471.0
+	+	0	-	0	-	-	+	10497.2
-	+	0	+	0	+	-	-	10541.8
+	+	0	-	0	+	-	+	10563.4
-	-	0	-	0	-	-	-	10563.9
+	-	0	+	0	-	-	+	10570.5

which did not refine. The second combination initially refined to an R value of 29% without the sulfur atoms. However, upon addition of the sulfurs (located on a difference Fourier map), no atomic arrangement could be found that yielded believable (i.e. not too short) interatomic distances. The fourth sign group refined equally well and yielded nine good sulfur positions with reasonable interatomic distances. The E-map derived from this sign group is given in Figure 2 for the metal positions only.

Although initially there was some ambiguity as to the identification of some Sb and Pb, this was later resolved by difference-Fourier synthesis maps. The atomic configuration ultimately refined to a $R_{\text{reject}} = 18.9\%$ (omitting rejected reflections). This refinement included anomalous scattering, isotropic temperature factors, and rejection of all F_{hkl} 's with $(F_{\text{cal}} - F_{\text{obs}})/F_{\text{obs}}$ greater than 75%. The atomic parameters are given in Table 7.

On the whole, the atomic arrangement seemed reasonable, however, there were puzzling elements. Two of the eleven sulfurs were unlocatable - unusual for even a relatively light atom in a correct structure. With a very reasonable and loose rejection criteria ($\Delta F/F > 75\%$) over one-third of the data were rejected - unreasonable with a correct structure and a good set of data. These troublesome factors forced the author to conclude that collection of another set of data was in order. It was decided

FIGURE 2

Composite E-map

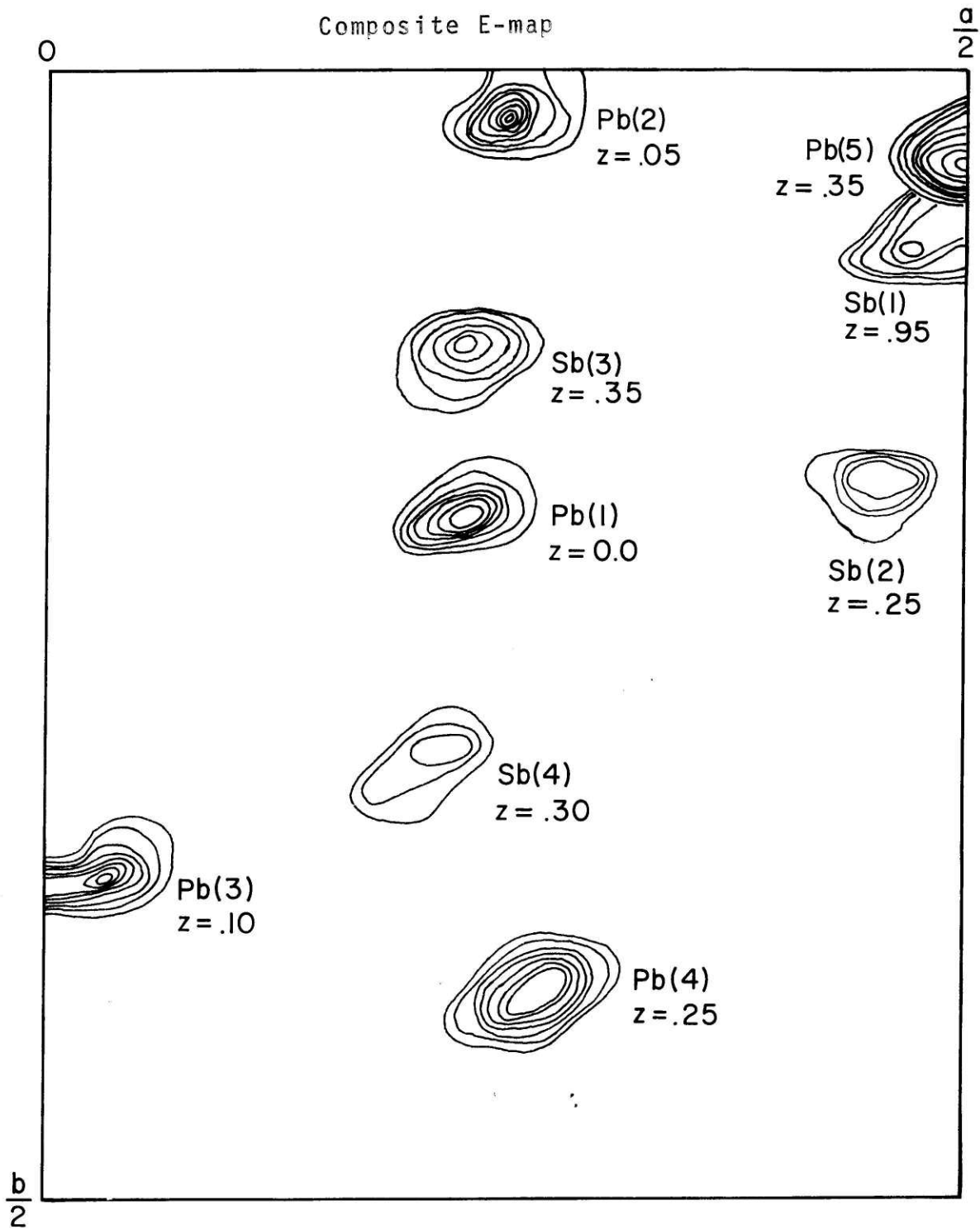


TABLE 7

Atomic Parameters Initial Refinement

	<u>Sb (1)</u>	<u>Sb (2)</u>	<u>Sb (3)</u>	<u>Sb (4)</u>	
x	.4825	.4528	.2248	.5069	
y	.9440	.2620	.3216	.3319	
z	.9257	.8157	.8779	.9742	
β	.8817	.9053	.7311	1.0578	
	<u>Pb (1)</u>	<u>Pb (2)</u>	<u>Pb (3)</u>	<u>Pb (4)</u>	<u>Pb (5)</u>
x	.2249	.2502	.0231	.2684	.50
y	.0130	.0547	.1141	.2256	.0404
z	.8076	.9826	.6426	.5935	.25
β	1.1372	1.5389	1.0207	1.1619	1.2639
	<u>S (1)</u>	<u>S (2)</u>	<u>S (3)</u>	<u>S (4)</u>	<u>S (5)</u>
x	.00	.3772	.3839	.3575	.3884
y	.0972	.1702	.0146	.1681	.2774
z	.25	.3492	.1307	.4988	.1932
β	.7432	1.1616	.0001	1.7254	2.4989
	<u>S (6)</u>	<u>S (7)</u>	<u>S (8)</u>	<u>S (9)</u>	
x	.1400	.1717	.3838	.1280	
y	.3519	.1048	.4430	.0686	
z	.2565	.1802	.4506	.3989	
β	.4129	2.9008	1.0911	.0001	

to collect this set with the same crystal on a four-circle automated diffractometer with monochromated Mo radiation. Thus absorption effects would be reduced and the inaccuracies of film scanning avoided.

Chapter V

Structure Refinement with new Data

New data was gathered for semseyite on a Picker-automated four-circle diffractometer in Dr. Charles T. Prewitt's laboratory at the State University of New York at Stony Brook. 2125 reflection intensities were collected in nearly four days using graphite-monochromated Mo $K\alpha$ radiation. This data set duplicated the one taken earlier with film methods and Cu $K\alpha$. The data was integrated and corrected for Lorentz and polarization effects during the collection process. The resulting structure factors were then corrected for absorption by the author in the manner previously described. (See Chapter III.) Agreement between 24 sets of equivalent structure factors was 6% compared with 14% for the first data set. Agreement was compared by calculating $(F_1 - F_2)/(.5(F_1+F_2))$ for each equivalent pair. Identical corrections were applied in each case.

Since the previous data set had refined to 18.9%, it was assumed that the metal positions were essentially correct. Thus these positions were used to initialize the refinement process. After one cycle of refining only the scale factor (initialized at 1,0) and two subsequent cycles of refining both atomic coordinates of the nine metals and the scale factor, the discrepancy index was 21.6%. This indicated that the hypothesis on the metal positions was correct. An electron difference Fourier synthesis was constructed. The positions of the eleven sulfur atoms were readily

located. Comparison with the original data set indicated that only six of the nine original sulfur positions agreed with the present data set. Table 8 compares the metal atomic positions of the two data sets.

Upon location of the sulfur atoms, they were included in the least-squares refinement and allowance was made for anomalous dispersion. Four cycles of refinement were performed in which the scale factor and atomic positions were varied. At this juncture the R value, defined as $(\sum ||F_{\text{obs}}| - |F_{\text{cal}}||) / \sum F_{\text{obs}}$, was 12.1% indicative of a correct structure. Another difference Fourier synthesis was performed, using the data phased on the current refinement. No large anomalous peaks were discovered. Anisotropic thermal motion was suggested, however, for the metal atoms.

At this point the isotropic temperature factors of all the metal and sulfur atoms were allowed to vary from their previously fixed values of 1.0 \AA^2 . After six cycles of refinement, the unweighted R value was 10.6% while the R weighted by sigma from counting statistics, $R = (\sum w(|F_{\text{obs}}| - |F_{\text{cal}}|)^2) / \sum w F_{\text{obs}}^2)^{0.5}$, was 9.3%.

The reflections whose integrated intensities were judged to be unobservable (i.e. either negative or values less than σ_{CS}) had previously been excluded from the refinement. These intensities, numbering nearly 300, constituted nearly one-seventh of the data set so it was decided to include them in the data. First, however, they were assigned minimum observable values. The minimum

TABLE 8

Shifts of Counter Metal
Positions From Film Data Positions

	<u>Sb(1)</u>	<u>Sb(2)</u>	<u>Sb(3)</u>	<u>Sb(4)</u>
Δx^*	.0016	-.0006	-.0016	.0002
Δy	-.0020	-.0034	.0014	.0009
Δz	-.0005	.0003	.0014	-.0002

	<u>Pb(1)</u>	<u>Pb(2)</u>	<u>Pb(3)</u>	<u>Pb(4)</u>	<u>Pb(5)</u>
Δx	.00	.0027	-.0001	-.0005	-.0004
Δy	-.0039	.0013	.0019	.0010	-.0020
Δz	.00	-.0008	-.0008	.0000	-.0005

* (counter positions - film positions) = Δ

TABLE 9

Atomic Parameters

Sb (1)	x	$=$	0.5067	\pm	$.0002$
	y	$=$	0.3328	\pm	$.0005$
	z	$=$	0.4740	\pm	$.0001$
	β_{11}	$=$	0.0017	\pm	$.00019$
	β_{22}	$=$	0.00030	\pm	$.00088$
	β_{33}	$=$	0.00063	\pm	$.00006$
	β_{12}	$=$	0.00018	\pm	$.00026$
	β_{13}	$=$	0.00033	\pm	$.00008$
	β_{23}	$=$	-0.00001	\pm	$.00016$
Sb (2)	x	$=$	0.4841	\pm	$.0002$
	y	$=$	0.9420	\pm	$.0005$
	z	$=$	0.4252	\pm	$.0001$
	β_{11}	$=$	0.00143	\pm	$.00018$
	β_{22}	$=$	0.00028	\pm	$.00090$
	β_{33}	$=$	0.00069	\pm	$.00006$
	β_{12}	$=$	-0.00010	\pm	$.00027$
	β_{13}	$=$	0.00038	\pm	$.00007$
	β_{23}	$=$	0.00003	\pm	$.00016$
Sb (3)	x	$=$	0.2232	\pm	$.0002$
	y	$=$	0.3230	\pm	$.0005$
	z	$=$	0.3793	\pm	$.0001$
	β_{11}	$=$	0.00176	\pm	$.00018$
	β_{22}	$=$	0.00021	\pm	$.00087$
	β_{33}	$=$	0.00052	\pm	$.00005$
	β_{12}	$=$	0.00022	\pm	$.00026$
	β_{13}	$=$	0.00037	\pm	$.00007$
	β_{23}	$=$	0.00029	\pm	$.00015$
Sb (4)	x	$=$	0.4522	\pm	$.0002$
	y	$=$	0.2586	\pm	$.0005$
	z	$=$	0.3160	\pm	$.0001$
	β_{11}	$=$	0.00170	\pm	$.00018$
	β_{22}	$=$	0.00163	\pm	$.00090$
	β_{33}	$=$	0.00057	\pm	$.000054$
	β_{12}	$=$	0.00011	\pm	$.00027$
	β_{13}	$=$	0.00041	\pm	$.00007$
	β_{23}	$=$	-0.00018	\pm	$.00015$

TABLE 9
(continued)

Atomic Parameters

Pb (1)	x	=	0.5000	±	.00
	y	=	0.9557	±	.0004
	z	=	0.2500	±	.00
	β_{11}	=	0.00292	±	.00018
	β_{22}	=	0.00121	±	.00082
	β_{33}	=	0.00081	±	.00005
	β_{12}	=	0.0		
	β_{13}	=	0.00020	±	.00080
	β_{23}	=	0.0		
Pb (2)	x	=	0.2276	±	.0001
	y	=	0.0143	±	.0003
	z	=	0.3068	±	.0001
	β_{11}	=	0.00185	±	.00011
	β_{22}	=	0.00110	±	.00052
	β_{33}	=	0.00060	±	.00003
	β_{12}	=	0.00027	±	.00016
	β_{13}	=	0.00020	±	.00004
	β_{23}	=	- .00007	±	.00009
Pb (3)	x	=	0.2683	±	.0001
	y	=	0.2275	±	.0003
	z	=	0.0927	±	.0001
	β_{11}	=	0.00184	±	.00011
	β_{22}	=	0.00106	±	.00054
	β_{33}	=	0.00064	±	.00003
	β_{12}	=	-0.00015	±	.00017
	β_{13}	=	0.00033	±	.00004
	β_{23}	=	0.00000	±	.00009
Pb (4)	x	=	0.0226	±	.0001
	y	=	0.1151	±	.0003
	z	=	0.1426	±	.0001
	β_{11}	=	0.00189	±	.00011
	β_{22}	=	0.00005	±	.00050
	β_{33}	=	0.00074	±	.00003
	β_{12}	=	0.00010	±	.00016
	β_{13}	=	0.00038	±	.00004
	β_{23}	=	0.00014	±	.00009

TABLE 9
(continued)

Atomic Parameters

Pb (5)	x	=	0.2498	±	.0002
	y	=	0.0527	±	.0003
	z	=	0.4821	±	.0001
	β_{11}	=	0.00252	±	.00012
	β_{22}	=	0.00227	±	.00054
	β_{33}	=	0.00070	±	.00003
	β_{12}	=	0.00022	±	.00018
	β_{13}	=	0.00036	±	.00005
	β_{23}	=	-0.00006	±	.00010
S (1)	x	=	0.0	±	0.0
	y	=	0.8955	±	.0024
	z	=	0.25	±	0.0
	β	=	1.4877	±	.3531
S (2)	x	=	0.3212	±	.0009
	y	=	0.4036	±	.0018
	z	=	0.3174	±	.0005
	β	=	1.2424	±	.2335
S (3)	x	=	0.1106	±	.0008
	y	=	0.4969	±	.0019
	z	=	0.3698	±	.0005
	β	=	0.9574	±	.2168
S (4)	x	=	0.3675	±	.0009
	y	=	0.1145	±	.0018
	z	=	0.4013	±	.0005
	β	=	1.1160	±	.2346
S (5)	x	=	0.3810	±	.0009
	y	=	0.5515	±	.0018
	z	=	0.4524	±	.0005
	β	=	1.1254	±	.2200
S (6)	x	=	0.3714	±	.0009
	y	=	0.4421	±	.0019
	z	=	0.1020	±	.0005
	β	=	1.3432	±	.2317
S (7)	x	=	0.1235	±	.0009
	y	=	0.3383	±	.0019
	z	=	0.1524	±	.0005
	β	=	1.2759	±	.2346

TABLE 9
(continued)

Atomic Parameters

S (8)	x =	0.1112 ±	.0008
	y =	0.2221 ±	.0019
	z =	0.3033 ±	.0005
	β =	1.1645 ±	.2268
S (9)	x =	0.3571 ±	.0010
	y =	0.1335 ±	.0019
	z =	0.2440 ±	.0005
	β =	1.5033 ±	.2345
S(10)	x =	0.0958 ±	.0009
	y =	0.2190 ±	.0019
	z =	0.4557 ±	.0005
	β =	1.3511 ±	.2345
S(11)	x =	0.3662 ±	.0009
	y =	0.1734 ±	.0018
	z =	0.0017 ±	.0005
	β =	1.1604 ±	.2232

recordable intensity (I_{\min}) that is statistically meaningful may be defined as

$$I_{\min} = E_{\min} - B,$$

where E_{\min} is the smallest meaningful peak expressed as

$$E_{\min} = PE(E) + B + PE(B),$$

where $PE(E)$ is the probable error in E (i.e. $0.6745 \sigma_E$) and $PE(B)$ is the probable error in the background B (i.e. $0.6745 \sigma_B$).

Finally the intensity of a statistically unobservable peak is for a centric structure

$$I_{\text{unobs}} = (1/3) I_{\min}.$$

Thus this procedure was followed for approximately 300 reflections. They were added to the data set but excluded from the refinement process.

In the last cycles of refinement the metal atoms and finally the sulfurs were allowed to vibrate anisotropically. This was meaningful for the metal atoms, but for the sulfur atoms such motion produced negative temperature factors so they were constrained to isotropic motion. Temperature factors, the scale factor and the atomic positions were all refined until convergence. The final discrepancy index was $R(\text{including unobs.})=11.3\%$, $R(\text{omitting unobs.})=10.0\%$, and $R_w = 8.3\%$. The final atomic parameters are given in Table 9. Ellipsoids of thermal vibration are given in Table 10 for the metal atoms. The structure factors are reported in Table 11.

As a side note, this data set was used as input to FAME. A

TABLE 10

Principal Axes and Orientations
Of Thermal-Vibration Ellipsoids

Atom	Principal Axes	RMS Amplitude	Orientation With Respect To		
			a	b	c
Sb(1)	1	0.044 (70) Å ^o	97°(10)	7°(11)	87°(9)
	2	0.120 (8)	9°(18)	83°(11)	112°(24)
	3	0.133 (6)	94°(24)	90°(9)	22°(24)
Sb(2)	1	0.043 (74)	96°(14)	174°(15)	87°(9)
	2	0.107 (8)	7°(13)	96°(15)	110°(9)
	3	0.140 (6)	86°(9)	89°(7)	20°(9)
Sb(3)	1	0.020 (150)	89°(10)	164°(9)	75°(11)
	2	0.113 (9)	34°(17)	98°(10)	138°(18)
	3	0.131 (5)	56°(17)	77°(8)	52°(16)
Sb(4)	1	0.096 (24)	120°(29)	42°(35)	56°(23)
	2	0.120 (14)	37°(26)	54°(28)	109°(42)
	3	0.132 (7)	70°(27)	108°(30)	40°(15)
Pb(1)	1	0.093 (32)	90°	0°	90°
	2	0.145 (31)	117°(32)	90°	136°(32)
	3	0.171 (48)	153°(32)	90°	47°(32)
Pb(2)	1	0.085 (21)	104°(9)	14°(8)	83°(7)
	2	0.124 (3)	130°(12)	97°(8)	124°(12)
	3	0.138 (5)	137°(10)	103°(8)	35°(12)
Pb(3)	1	0.086 (22)	81°(10)	8°(10)	93°(8)
	2	0.126 (5)	9°(13)	98°(10)	110°(21)
	3	0.134 (3)	86°(21)	90°(8)	20°(21)
Pb(4)	1	0.014 (130)	89°(5)	174°(4)	85°(4)
	2	0.126 (4)	3°(8)	89°(5)	109°(9)
	3	0.145 (3)	87°(9)	84°(4)	20°(8)
Pb(5)	1	0.124 (14)	108°(13)	22°(18)	73°(20)
	2	0.140 (4)	94°(21)	78°(17)	157°(23)
	3	0.150 (5)	18°(15)	72°(15)	105°(18)

TABLE 11
Comparison of F obs with F cal

k = 0		F obs		F cal		F obs		F cal		F obs		F cal		
-12	10	174.4	175.9	5	17	182.4	189.6	11	15	23.0	47.0	-2	23	
-12	12	78.6	79.2	5	18	95.4	98.7	11	16	27.5	53.7	-2	24	
-12	14	57.1	47.7	5	20	92.3	86.5	11	17	114.7	96.2	-2	25	
0	4	134.3	127.4	5	19	155.2	164.2	11	18	124.2	124.8	-2	26	
0	6	199.8	181.0	-12	20	314.3	321.1	5	22	190.6	172.6	-11	20	
0	8	151.0	145.2	-12	22	115.2	115.2	5	23	21.7	26.6	-11	21	
0	10	307.7	313.9	-12	24	45.4	27.6	5	24	256.8	249.5	-11	22	
0	12	156.3	157.3	-12	26	101.9	87.5	-11	5	151.1	132.5	-11	23	
0	14	248.1	253.4	-12	28	41.8	18.0	-11	6	59.3	36.6	-11	24	
0	16	212.8	207.2	-12	30	90.9	74.0	-11	7	21.8	21.1	-11	25	
0	18	711.0	715.2	-12	32	26.5	15.2	-11	8	175.5	156.0	-11	26	
0	20	112.3	109.8	-12	34	52.2	42.4	-11	9	46.8	43.9	-11	27	
0	22	226.6	215.0	-12	36	90.9	39.5	-11	10	125.2	102.9	-11	28	
0	24	218.0	256.8	-12	38	49.6	65.0	-11	11	48.3	37.0	-11	29	
0	26	86.8	78.3	-12	40	301.9	326.7	-11	12	147.9	149.1	-11	30	
0	28	154.9	146.9	-12	42	123.5	125.9	-11	13	17.6	33.2	-11	31	
0	30	219.8	214.8	-12	44	231.3	226.6	-11	14	118.5	139.7	-11	32	
0	32	59.2	43.5	-12	46	92.8	106.1	-11	15	159.6	129.9	-11	33	
0	34	145.1	140.9	-12	48	360.3	385.5	-11	16	125.2	102.9	-11	34	
0	36	676.0	686.5	-12	50	182.1	194.3	-11	17	94.4	79.0	-11	35	
0	38	252.8	231.3	-12	52	21.7	46.5	-11	18	179.9	138.2	-11	36	
0	40	115.0	116.3	-12	54	382.6	392.8	-11	19	627.5	501.0	-11	37	
0	42	216.4	207.3	-12	56	73.7	63.5	-11	20	540.6	501.0	-11	38	
0	44	134.8	154.5	-12	58	211.4	218.6	-11	21	35.4	35.4	-11	39	
0	46	41.8	36.9	-12	60	69.5	29.4	-11	22	65.6	36.8	-11	40	
0	48	34.5	31.6	-12	62	22.7	22.7	-11	23	286.4	286.4	-11	41	
0	50	22.2	24.8	-12	64	22.7	22.7	-11	24	520.2	520.2	-11	42	
0	52	28.6	39.2	-12	66	140.2	189.3	-11	25	476.8	405.1	-11	43	
0	54	228.5	220.8	-12	68	174.1	174.1	-11	26	21.8	13.8	-11	44	
0	56	34.5	41.1	-12	70	1.1	1.1	-11	27	51.9	16.8	-11	45	
0	58	19.9	38.4	-12	72	20.5	35.8	-11	28	20.5	35.8	-11	46	
0	60	274.6	232.1	-12	74	177.0	178.4	-11	29	117.9	106.5	-11	47	
0	62	1189.7	1172.0	-12	76	168.1	168.1	-11	30	147.8	115.5	-11	48	
0	64	35.8	30.7	-12	78	175.1	194.6	-11	31	64.2	32.3	-11	49	
0	66	306.0	292.5	-12	80	264.3	264.3	-11	32	76.4	76.4	-11	50	
0	68	42.6	49.5	-12	82	44.7	47.4	-11	33	275.2	286.9	-11	51	
0	70	136.8	150.1	-12	84	351.4	351.4	-11	34	181.0	173.1	-11	52	
0	72	85.7	10.8	-12	86	79.5	67.4	-11	35	311.8	315.6	-11	53	
0	74	60.2	47.2	-12	88	188.5	191.0	-11	36	40.4	40.4	-11	54	
0	76	127.5	158.4	-12	90	44.6	12.5	-11	37	62.6	106.1	-11	55	
0	78	58.1	58.1	-12	92	188.5	188.5	-11	38	40.4	40.4	-11	56	
0	80	415.5	376.4	-12	94	83.2	119.3	-11	39	145.1	117.5	-11	57	
0	82	201.5	202.2	-12	96	61.1	67.3	-11	40	43.4	32.3	-11	58	
0	84	114.0	114.0	-12	98	130.2	109.3	-11	41	15.1	12.7	-11	59	
0	86	225.9	232.9	-12	100	57.4	45.1	-11	42	159.9	110.7	-11	60	
0	88	102.6	96.2	-12	102	116.0	116.0	-11	43	206.3	157.7	-11	61	
0	90	296.2	296.2	-12	104	237.6	237.6	-11	44	103.6	97.2	-11	62	
0	92	53.1	44.7	-12	106	20.5	20.5	-11	45	244.4	263.4	-11	63	
0	94	204.4	286.3	-12	108	122.8	108.8	-11	46	400.9	454.4	-11	64	
0	96	97.2	72.5	-12	110	291.2	309.2	-11	47	95.6	91.0	-11	65	
0	98	634.8	631.1	-12	112	383.9	386.3	-11	48	133.7	140.0	-11	66	
0	100	76.6	77.1	-12	114	22.2	19.9	-11	49	44.0	41.3	-11	67	
0	102	241.2	241.2	-12	116	95.4	79.4	-11	50	240.2	187.7	-11	68	
0	104	174.4	190.0	-12	118	265.8	270.5	-11	51	398.7	385.2	-11	69	
0	106	229.2	202.6	-12	120	21.9	21.0	-11	52	125.6	103.9	-11	70	
0	108	178.4	183.0	-12	122	43.8	43.8	-11	53	149.4	149.4	-11	71	
0	110	491.1	491.1	-12	124	21.6	36.8	-11	54	169.4	169.4	-11	72	
0	112	174.5	174.5	-12	126	191.6	191.6	-11	55	22.6	34.3	-11	73	
0	114	69.0	21.5	-12	128	159.3	136.1	-11	56	138.9	150.8	-11	74	
0	116	43.1	47.7	-12	130	47.7	47.7	-11	57	199.2	199.2	-11	75	
0	118	105.9	71.4	-12	132	64.7	54.3	-11	58	97.9	86.4	-11	76	
0	120	293.8	289.1	-12	134	136.4	141.1	-11	59	23.0	18.0	-11	77	
0	122	185.5	156.1	-12	136	24.8	24.8	-11	60	98.4	75.6	-11	78	
0	124	176.6	187.2	-12	138	19.7	34.3	-11	61	56.1	63.6	-11	79	
0	126	591.2	591.2	-12	140	78.0	78.0	-11	62	62.1	62.1	-11	80	
0	128	383.6	397.4	-12	142	177.0	160.0	-11	63	175.2	175.2	-11	81	
0	130	141.5	141.5	-12	144	51.4	51.4	-11	64	159.4	181.5	-11	82	
0	132	241.2	221.1	-12	146	76.8	64.9	-11	65	36.3	38.7	-11	83	
0	134	148.7	162.8	-12	148	76.8	71.8	-11	66	109.6	131.2	-11	84	
0	136	46.2	46.2	-12	150	116.0	116.0	-11	67	166.2	166.2	-11	85	
0	138	161.0	145.1	-12	152	81.3	83.2	-11	68	120.7	124.4	-11	86	
0	140	228.7	228.7	-12	154	48.5	48.5	-11	69	48.5	48.5	-11	87	
0	142	141.5	143.3	-12	156	488.7	468.1	-11	70	253.3	253.1	-11	88	
0	144	59.1	60.3	-12	158	241.2	235.4	-11	71	374.3	374.3	-11	89	
0	146	112.0	109.7	-12	160	135.1	136.5	-11	72	48.5	48.5	-11	90	
0	148	76.4	76.4	-12	162	209.2	209.2	-11	73	22.8	22.8	-11	91	
0	150	196.0	208.5	-12	164	134.5	121.7	-11	74	146.0	128.9	-11	92	
0	152	76.4	76.4	-12	166	111.5	111.5	-11	75	71.8	71.8	-11	93	
0	154	103.9	103.0	-12	168	20.5	36.2	-11	76	20.5	36.2	-11	94	
0	156	41.1	26.0	-12	170	195.8	199.4	-11	77	187.5	162.8	-11	95	
0	158	161.5	151.5	-12	172	181.5	181.5	-11	78	149.3	149.3	-11	96	
0	160	203.4	195.3	-12	174	21.7	7.8	-11	79	189.8	206.8	-11	97	
0	162	103.9	103.9	-12	176	181.5	181.5	-11	80	133.7	133.7	-11	98	
0	164	224.8	202.7	-12	178	45.3	43.1	-11	81	93.2	109.7	-11	99	
0	166	460.2	410.0	-12	180	336.6	336.6	-11	82	381.3	381.3	-11	100	
0	168	80.7	726.0	-12	182	0	87.8	39.2	-11	83	0	87.8	-11	101
0	170	142.1	138.2	-12	184	81.6	78.0	-11	84	110.3	102.2	-11	102	
0	172	149.3	146.2	-12	186	136.5	136.5	-11	85	218.5	202.2	-11	103	
0	174	155.7	136.6	-12	188	191.1	198.0	-11	86	202.7	202.2	-11	104	
0	176	34.9	34.9	-12	190	31.0	31.0	-11	87	32.8	32.8	-11	105	
0	178	95.6	131.8	-12	192	51.2	53.5	-11	88	77.7	29.2	-11	106	
0	180	22.9	112.6	-12	194	17.9	50.6	-11	89	84.4	37.3	-11	107	
0	182	222.9	252.2	-12	196	101.3	79.3	-11	90	199.3	180.0	-11	108	
0	184	109.6	461.9	-12	198	64.6	64.6	-11	91	19.7	76.9	-11	109	
0	186	440.7	420.0	-12	200	285.3	277.8	-11	92	218.5	277.8	-11	110	
0	188	276.8	296.6	-12	202	617.5	615.6	-11	93	617.5	615.6	-11	111	
0	190	8.8	47.8	-12	204	352.1	352.1	-11	94	352.1	352.1	-11	112	
0	192	8.8	418.9	-12	206	53.7	90.7	-11	95	45.9	465.9	-11	113	
0	194	136.6	136.6	-12	208	187.8	187.8	-11	96	187.8	187.8	-11	114	
0	196	27.4	10.2	-12	210	345.7	346.2	-11	97	229.0	225.7	-11	115	
0	198	167.8	167.8	-12	212	11.9	11.9	-11	98	11.9	11.9	-11	116	
0	200	20.4	268.0	-12	214	31.5	64.7	-11	99	111.9	111.9	-11	117	
0	202	118.5	302.2	-12	216	144.1	124.0							

Table 11 (cont.)

7 0	570.5	525.6	13 9	189.7	193.3	-4 11	816.3	755.3	-10 17	119.7	130.7	3 4	327.7	349.1	9 1*	21.0	35.1
7 1	399.0	383.3	13 10	156.3	151.0	-12 12	800.5	732.3	-10 18	282.5	303.4	3 5	591.8	637.3	9 2	4	2.2
7 2	72.7	75.9	13 11	88.1	120.3	-13 13	292.4	256.5	-10 19	221.0	231.3	3 6	299.3	338.2	9 3	23.5	27.9
7 3	81.1	85.8	13 12	144.0	168.3	-14 14	311.8	339.9	-10 20	293.8	339.9	3 7	162.8	168.1	9 4	83.4	7.0
7 4	34.3	34.4	13 13	201.4	212.1	-15 15	146.4	162.3	-10 21	102.4	109.7	3 8	37.7	37.7	9 5	37.7	15.4
7 5	37.7	34.0	13 14	81.3	100.0	-16 16	20.9	20.9	-10 22	307.6	347.3	3 9	87.9	82.9	9 6	161.9	137.4
7 6	144.4	140.0	13 15	132.1	147.6	-17 17	94.8	73.1	-10 23	89.5	100.6	3 10	303.9	330.9	9 7	20.9	22.8
7 7	88.8	96.1	13 16	187.6	201.1	-18 18	242.0	263.9	-10 24	83.7	109.4	3 11	21.1	70.1	9 8	12.0	13.0
7 8	323.8	348.9	13 17	82.7	69.7	-19 19	245.6	255.9	-10 25	95.1	114.5	3 12	50.6	85.8	9 9	67.1	52.7
7 9	146.6	154.4	13 18	137.3	169.4	-20 20	141.3	156.6	-10 26	107.6	126.6	3 13	109.4	208.9	9 10	174.7	120.7
7 10	146.6	154.4	13 19	80.7	179.4	-21 21	21.3	35.1	-10 27	22.6	23.4	3 14	17.7	61.7	9 11	73.8	27.9
7 11	146.6	154.4	13 20	105.8	212.2	-22 22	109.4	109.4	-10 28	18.6	36.2	3 15	172.3	178.5	9 12	11.4	11.4
7 12	196.2	205.3	13 21	283.8	299.3	-23 23	113.3	109.7	-10 29	151.8	170.5	3 16	84.1	53.9	9 13	203.2	198.9
7 13	71.8	71.8	13 22	68.3	71.8	-24 24	22.3	23.9	-10 30	20.5	19.2	3 17	41.9	25.7	9 14	86.5	98.0
7 14	20.7	27.2	13 23	121.8	127.4	-25 25	115.5	136.0	-10 31	174.8	191.3	3 18	40.3	29.4	9 15	91.8	74.6
7 15	43.0	51.7	13 24	131.6	152.1	-26 26	32.6	54.2	-10 32	58.2	76.1	3 19	32.7	51.9	9 16	158.2	152.1
7 16	118.9	112.8	13 25	210.1	191.7	-27 27	21.7	7.3	-10 33	40.5	92.0	3 20	162.0	181.3	9 17	183.2	178.3
7 17	46.0	55.6	13 26	267.1	268.7	-28 28	93.4	83.9	-10 34	101.1	112.7	3 21	103.0	123.7	9 18	110.0	92.9
7 18	158.9	183.0	13 27	118.1	141.7	-29 29	78.9	39.1	-10 35	102.4	114.7	3 22	105.6	105.6	9 19	23.0	27.0
7 19	113.1	105.7	13 28	53.8	15.4	-30 30	64.0	64.0	-10 36	130.5	12.6	3 23	378.6	409.8	9 20	23.0	49.6
7 20	21.8	31.7	13 29	22.1	30.0	-31 31	42.5	41.0	-10 37	42.5	41.0	3 24	124.8	163.6	9 21	23.0	24.3
7 21	77.0	84.4	13 30	141.3	131.5	-32 32	136.9	12.6	-10 38	419.0	12.7	3 25	124.8	163.6	9 22	23.0	24.3
7 22	74.2	59.6	13 31	21.4	11.9	-33 33	90.2	83.9	-10 39	102.5	100.5	3 26	55.9	83.4	9 23	23.0	24.3
7 23	201.0	181.1	13 32	60.5	85.2	-34 34	46.0	46.0	-10 40	102.5	100.5	3 27	112.5	121.1	9 24	23.0	24.3
7 24	64.2	59.6	13 33	21.4	11.9	-35 35	90.2	83.9	-10 41	102.5	100.5	3 28	55.9	83.4	9 25	23.0	24.3
7 25	175.2	179.9	13 34	21.6	40.7	-36 36	55.2	46.0	-10 42	102.5	100.5	3 29	187.2	178.2	9 26	23.0	24.3
7 26	109.5	81.9	13 35	157.4	189.6	-37 37	188.4	198.9	-10 43	102.5	100.5	3 30	55.9	83.4	9 27	23.0	24.3
7 27	44.4	44.4	13 36	21.6	40.7	-38 38	21.1	22.2	-10 44	102.5	100.5	3 31	119.3	114.9	9 28	23.0	24.3
7 28	24.8	46.8	13 37	21.9	27.0	-39 39	77.3	102.4	-10 45	102.5	100.5	3 32	197.2	178.2	9 29	23.0	24.3
7 29	100.4	80.8	13 38	61.8	42.9	-40 40	122.7	137.6	-10 46	102.5	100.5	3 33	267.3	231.1	9 30	23.0	24.3
7 30	127.2	117.8	13 39	57.2	96.5	-41 41	55.3	45.8	-10 47	102.5	100.5	3 34	58.9	59.9	9 31	23.0	24.3
7 31	53.5	29.6	13 40	13.4	67.9	-42 42	92.7	63.3	-10 48	102.5	100.5	3 35	236.2	215.2	9 32	23.0	24.3
7 32	193.2	173.3	13 41	67.7	28.3	-43 43	21.1	15.2	-10 49	102.5	100.5	3 36	209.6	271.2	9 33	23.0	24.3
7 33	120.5	105.0	13 42	165.5	201.3	-44 44	48.6	48.6	-10 50	102.5	100.5	3 37	89.6	74.4	9 34	23.0	24.3
7 34	108.8	97.3	13 43	27.4	26.4	-45 45	27.8	26.1	-10 51	102.5	100.5	3 38	76.6	61.3	9 35	23.0	24.3
7 35	272.2	235.0	13 44	21.9	27.0	-46 46	22.3	23.0	-10 52	102.5	100.5	3 39	47.1	13.9	9 36	23.0	24.3
7 36	41.0	14.3	13 45	224.2	285.8	-47 47	367.8	366.1	-10 53	102.5	100.5	3 40	119.8	20.7	9 37	23.0	24.3
7 37	44.1	44.1	13 46	1.4	1.4	-48 48	136.7	108.6	-10 54	102.5	100.5	3 41	202.9	188.5	9 38	23.0	24.3
7 38	362.8	326.3	13 47	332.3	334.9	-49 49	221.3	198.4	-10 55	102.5	100.5	3 42	336.2	329.0	9 39	23.0	24.3
7 39	217.4	217.4	13 48	18.3	51.9	-50 50	146.4	146.4	-10 56	102.5	100.5	3 43	187.0	174.6	9 40	23.0	24.3
7 40	60.6	13.5	13 49	137.0	137.9	-51 51	22.0	9.0	-10 57	102.5	100.5	3 44	21.6	17.6	9 41	23.0	24.3
7 41	16.4	16.4	13 50	90.6	90.6	-52 52	113.3	113.3	-10 58	102.5	100.5	3 45	112.0	126.1	9 42	23.0	24.3
7 42	342.7	328.9	13 51	130.0	145.4	-53 53	113.4	129.4	-10 59	102.5	100.5	3 46	249.7	244.2	9 43	23.0	24.3
7 43	430.7	418.9	13 52	276.0	236.1	-54 54	116.8	136.3	-10 60	102.5	100.5	3 47	10.6	76.1	9 44	23.0	24.3
7 44	191.2	178.9	13 53	408.3	513.2	-55 55	88.4	50.7	-10 61	102.5	100.5	3 48	193.3	219.3	9 45	23.0	24.3
7 45	775.9	775.9	13 54	951.9	951.9	-56 56	111.1	111.1	-10 62	102.5	100.5	3 49	171.7	171.7	9 46	23.0	24.3
7 46	175.8	181.1	13 55	509.3	508.5	-57 57	73.3	58.5	-10 63	102.5	100.5	3 50	23.6	75.2	9 47	23.0	24.3
7 47	175.8	181.1	13 56	509.3	508.5	-58 58	152.0	143.7	-10 64	102.5	100.5	3 51	17.6	46.7	9 48	23.0	24.3
7 48	46.7	10.4	13 57	563.9	564.8	-59 59	123.4	132.7	-10 65	102.5	100.5	3 52	69.9	60.0	9 49	23.0	24.3
7 49	175.8	181.1	13 58	40.9	93.8	-60 60	125.4	117.2	-10 66	102.5	100.5	3 53	22.6	43.6	9 50	23.0	24.3
7 50	46.7	10.4	13 59	563.9	564.8	-61 61	92.9	42.9	-10 67	102.5	100.5	3 54	42.9	42.9	9 51	23.0	24.3
7 51	21.3	9.3	13 60	313.4	319.2	-62 62	132.8	119.3	-10 68	102.5	100.5	3 55	94.7	20.8	9 52	23.0	24.3
7 52	173.2	205.9	13 61	185.5	201.6	-63 63	107.8	173.8	-10 69	102.5	100.5	3 56	143.7	151.2	9 53	23.0	24.3
7 53	140.2	136.5	13 62	127.2	147.3	-64 64	52.5	21.1	-10 70	102.5	100.5	3 57	57.0	126.5	9 54	23.0	24.3
7 54	79.0	76.5	13 63	105.0	144.9	-65 65	143.1	144.9	-10 71	102.5	100.5	3 58	171.4	174.3	9 55	23.0	24.3
7 55	126.7	130.5	13 64	19.9	238.6	-66 66	225.9	221.3	-10 72	102.5	100.5	3 59	73.7	108.0	9 56	23.0	24.3
7 56	225.3	217.8	13 65	51.2	47.3	-67 67	181.6	181.1	-10 73	102.5	100.5	3 60	192.4	215.0	9 57	23.0	24.3
7 57	46.7	10.4	13 66	563.9	564.8	-68 68	137.8	137.8	-10 74	102.5	100.5	3 61	140.3	146.3	9 58	23.0	24.3
7 58	175.8	181.1	13 67	23.0	90.0	-69 69	234.9	244.0	-10 75	102.5	100.5	3 62	89.9	190.5	9 59	23.0	24.3
7 59	115.6	139.4	13 68	211.0	211.0	-70 70	488.1	496.2	-10 76	102.5	100.5	3 63	20.0	57.9	9 60	23.0	24.3
7 60	206.1	195.0	13 69	50.3	52.6	-71 71	212.2	213.3	-10 77	102.5	100.5	3 64	169.2	178.9	9 61	23.0	24.3
7 61	239.0	231.4	13 70	598.4	595.4	-72 72	243.6	243.6	-10 78	102.5	100.5	3 65	113.0	128.1	9 62	23.0	24.3
7 62	239.0	231.4	13 71	214.3	215.7	-73 73	319.2	336.1	-10 79	102.5	100.5	3 66	93.7	96.8	9 63	23.0	24.3
7 63	136.6	120.3	13 72	63.8	87.8	-74 74	22.2	29.4	-10 80	102.5	100.5	3 67	60.8	59.0	9 64	23.0	24.3
7 64	217.7	217.7	13 73	598.4	595.4	-75 75	159.7	172.9	-10 81	102.5	100.5	3 68	162.7	152.0	9 65	23.0	24.3
7 65	242.7	256.8	13 74	96.0	85.8	-76 76	122.9	142.9	-10 82	102.5	100.5	3 69	21.4	55.7	9 66	23.0	24.3
7 66	224.6	227.1	13 75	76.8	82.1	-77 77	76.1	32.9	-10 83	102.5	100.5	3 70	185.2	183.6	9 67	23.0	24.3
7 67	46.7	10.4	13 76	563.9	564.8	-78 78	181.7	182.3	-10 84	102.5	100.5	3 71	145.0	145.0	9 68	23.0	24.3
7 68	175.8	181.1	13 77	165.2	184.7	-79 79	159.7	170.9	-1								

Wilson calculation was made yielding an overall scale factor of 0.5100 and an overall temperature factor of 1.3825. This compares with the final scale factor from the refinement process of 0.4772. The statistics indicate a centric structure and are given in Table 12.

TABLE 12

Statistical Distribution of E's Calculated
From Wilson Plot
(Counter Data)

<u>Quantity</u>	<u>Calculated</u>	<u>Theoretical (Centric)</u>	<u>Theoretical (Acentric)</u>
Average Mag of E's	0.810	0.798	0.886
Average of E^2	0.994	1.000	.1000
Average of $ E^2 - 1 $	0.976	0.968	0.736
Percentage Greater Than One	28.68	32.00	37.00
Percentage Greater Than Two	5.47	5.00	1.80
Percentage Greater Than Three	0.33	0.30	0.01

Chapter VI

Description of the Structure

Semseyite is a complicated structure which may be best understood by viewing it in two different projections. The first is the standard (010) projection. The second is a projection onto (112). Before discussing the total structure, the individual polyhedra will be examined. There are twenty atoms in the asymmetric unit: five Pb, four Sb, and eleven S. All the antimony atoms occupy the general position as do four of the lead atoms and ten of the sulfur. The remaining lead and sulfur atoms occupy equi-point (4e) at (0,y,0.25).

A. The Polyhedra

The lead coordination polyhedra are basically of three types: an eight-coordinate Pb, a seven coordinate and three of either five or six coordination. The eight-fold coordinated lead atom, Pb(1), is the one that occupies the special position with two-fold symmetry. It can be described as a square-antiprism with top and bottom of the antiprism related by the two-fold axis. The lead atom has four close sulfur neighbors, S(9¹), S(9³) at 2.85 Å and S(3⁵), S(3⁷) at 2.94 Å. A third pair of sulfur atoms, S(8⁵) and S(8⁷), occur at a distance of 3.27 Å; while the fourth pair, S(7⁵) and S(7⁷), is at a distant 3.56 Å.

The remaining lead coordination polyhedra are characterized by a "split-vertex" which is simply the vertex below the equatorial plane being occupied by two atoms - splitting the vertex into two parts. Pb(2), the seven-coordinated lead atom, occupies the

general position. The general form of the polyhedron is an octahedron with a 'split' sixth vertex. S(4¹) occupies an apex at a distance of 2.82 Å above an equatorial plane comprised of four sulfur atoms, S(7⁷), S(8¹), S(9¹), and S(6⁷) at distances of 2.90, 2.93, 3.00, and 3.03 Å respectively. The 'split' vertex is composed of S(2⁷) and S(1¹) at distances of 3.21 and 3.34 Å.

Of the three remaining lead atoms two, Pb(3) and Pb(4), are quite simply described as six-coordinated by sulfur. The third lead, Pb(5), is predominately five-coordinated with a longer distance to a sixth sulfur. All of these polyhedra are octahedra with the vertex below the equatorial plane displaced. Pb(3) has an apical sulfur, S(11⁶) at 2.78 Å and four sulfur atoms in the equatorial plane, S(6¹), S(5⁷), S(11¹) and S(7¹) at distances of 2.90, 2.92, 2.96, and 3.06 Å respectively. The displaced vertex sulfur is S(3⁷) at 3.21 Å. Pb(4) has similar octahedral coordination with one vertex displaced. The apical sulfur, S(10²), is located at 2.79 Å while the equatorial sulfurs, S(8³), S(6⁵), S(7¹), and S(5⁷) are at distances of 2.83, 2.89, 2.98 and 3.06 Å respectively. The sixth, displaced, vertex sulfur, S(2⁷), is located at 3.27 Å. The final lead Pb(5) is really best described as five-coordinated; the sixth sulfur is at a much larger distance. The apex of the 'octahedron' is S(6⁷) at a distance of 2.61 Å from Pb(5). The equatorial plane contains sulfurs, S(10¹), S(4¹), S(5⁶) and S(11⁴) at 2.83, 2.96, 2.98, and 3.10 Å respectively. The almost missing displaced vertex sulfur, S(10⁶) occurs at 3.52 Å

completing the six sulfur coordination scheme.

With each of these three Pb-polyhedra it is possible to locate a seventh sulfur neighbor which would change the 'displaced-vertex' scheme to a 'split-vertex' octahedron. This polyhedral description would then resemble the coordination of Pb(2). For Pb(3) the seventh neighbor, S(9¹), occurs at 3.73 Å, for Pb(4), S(1¹) comes at 3.78 Å and for Pb(5), S(3⁶) comes at 3.64 Å. Thus all the lead atoms occupying the general position have very similar polyhedral configuration, seven-coordinate; although the seventh neighbors occur at distances ranging from 3.34 Å to 3.78 Å. Considering the sulfurs in the equatorial plane of these three Pb-polyhedron, the average Pb-S bond distance for the four Pb-S bonds in the plane is 2.96, 2.93, and 2.96 Å for Pb(3), Pb(4), and Pb(5) polyhedra respectively. The equatorial average for the seven-coordinate Pb(2) is 3.04 Å. Thus these four polyhedra can be seen to resemble closely each other. The bond distances, bond angles, and errors for the five Pb-polyhedra are given in Table 13. The polyhedra themselves are presented in Figure 3.

The four antimony atoms in the asymmetric unit all occupy the general position. They are basically of two types: five-coordinated by sulfur and three-coordinated. Sb(1), Sb(2), Sb(3) have the first coordination while Sb(4) has the latter scheme. Sb(1) has a square pyramid of sulfurs surrounding it. The apical sulfur, S(5²) occurs at a distance of 2.44 Å. The basal plane has four sulfurs, S(11³), S(10⁶), S(5¹), and S(6³), at distances of 2.53, 2.57, 3.08, and 3.10 Å respectively. Sb(2) has a similar square

Figure 3

Pb-Coordination Polyhedron - Semseyite

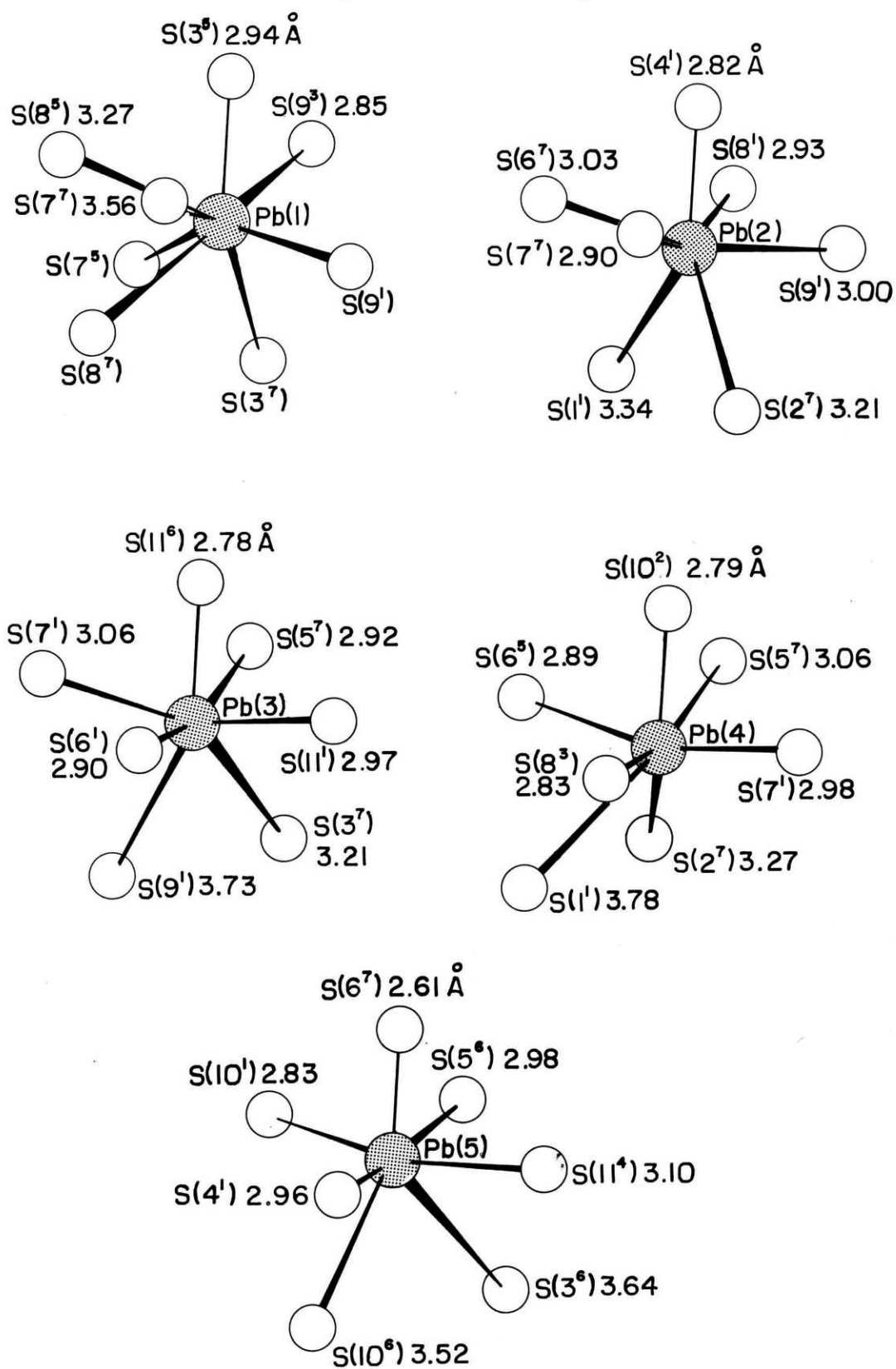


TABLE 13

Pb-S Bond Distances and Angles

A. Bond Distances

Pb (1)			Pb (2)		
S (9 ¹)	2.854	(20) Å ^o	S (4 ¹)	2.820	(13) Å ^o
S (9 ³)	2.854	(20)	S (7 ⁷)	2.897	(18)
S (3 ⁵)	2.942	(11)	S (8 ¹)	2.931	(20)
S (3 ⁷)	2.942	(11)	S (6 ⁷)	3.031	(15)
S (8 ⁵)	3.267	(20)	S (9 ¹)	2.998	(17)
S (8 ⁷)	3.267	(20)	S (2 ⁷)	3.211	(14)
S (7 ⁵)	3.564	(16)	S (1 ¹)	3.339	(12)
S (7 ⁷)	3.564	(16)			
Pb (3)			Pb (4)		
S (11 ⁶)	2.782	(13) Å ^o	S (10 ²)	2.789	(14) Å ^o
S (6 ¹)	2.899	(21)	S (8 ³)	2.833	(16)
S (5 ⁷)	2.918	(17)	S (6 ⁵)	2.890	(18)
S (11 ¹)	2.965	(14)			
S (7 ¹)	3.057	(16)	S (7 ¹)	2.976	(21)
S (3 ⁷)	3.208	(20)	S (5 ⁷)	3.061	(14)
S (9 ¹)	3.731	(14)	S (2 ⁷)	3.270	(19)
			S (1 ¹)	3.782	(20)
Pb (5)					
	S (6 ⁷)	2.610	(15) Å ^o		
	S (10 ¹)	2.829	(18)		
	S (4 ¹)	2.959	(14)		
	S (5 ⁶)	2.978	(15)		
	S (11 ⁴)	3.098	(20)		
	S (10 ⁶)	3.518	(19)		
	S (3 ⁶)	3.642	(11)		

TABLE 13
(continued)

Pb-S Bond Distances and Angles

B. Bond Angles

Pb(1)

S(9 ¹) - Pb - S(9 ³)	83.93(75)	degrees
S(9 ¹) - Pb - S(3 ⁷)	70.75(44)	2x
S(9 ¹) - Pb - S(3 ⁵)	94.65(46)	2x
S(9 ¹) - Pb - S(7 ⁷)	83.49(46)	2x
S(9 ¹) - Pb - S(7 ⁵)	134.27(39)	2x
S(9 ¹) - Pb - S(8 ⁵)	152.75(40)	2x
S(9 ¹) - Pb - S(8 ⁷)	112.34(42)	2x
S(3 ⁵) - Pb - S(3 ⁷)	160.75(89)	
S(3 ⁵) - Pb - S(7 ⁷)	66.72(37)	2x
S(3 ⁵) - Pb - S(7 ⁵)	121.78(33)	2x
S(3 ⁵) - Pb - S(8 ⁷)	126.38(50)	2x
S(3 ⁵) - Pb - S(8 ⁵)	72.07(49)	2x
S(7 ⁵) - Pb - S(7 ⁷)	133.70(71)	
S(7 ⁵) - Pb - S(8 ⁷)	69.47(39)	2x
S(7 ⁵) - Pb - S(8 ⁵)	71.31(39)	2x
S(8 ⁵) - Pb - S(8 ⁷)	62.82(51)	

Pb(2)

S(4 ¹) - Pb - S(6 ⁷)	81.65(41)	degrees
S(4 ¹) - Pb - S(7 ⁷)	77.08(51)	
S(4 ¹) - Pb - S(8 ¹)	84.38(46)	
S(4 ¹) - Pb - S(9 ¹)	81.93(41)	
S(4 ¹) - Pb - S(1 ¹)	149.22(29)	
S(4 ¹) - Pb - S(2 ⁷)	149.95(37)	
S(6 ⁷) - Pb - S(7 ⁷)	87.21(45)	
S(6 ⁷) - Pb - S(8 ¹)	85.18(49)	
S(7 ⁷) - Pb - S(9 ¹)	93.82(47)	
S(9 ¹) - Pb - S(8 ¹)	88.42(51)	
S(7 ⁷) - Pb - S(8 ¹)	160.80(38)	
S(6 ⁷) - Pb - S(9 ¹)	162.88(47)	
S(1 ¹) - Pb - S(2 ⁷)	60.40(27)	
S(1 ¹) - Pb - S(6 ⁷)	68.67(25)	
S(1 ¹) - Pb - S(7 ⁷)	108.37(57)	
S(1 ¹) - Pb - S(8 ¹)	85.17(52)	
S(1 ¹) - Pb - S(9 ¹)	126.61(27)	
S(2 ⁷) - Pb - S(6 ⁷)	124.19(46)	
S(2 ⁷) - Pb - S(7 ⁷)	88.24(43)	
S(2 ⁷) - Pb - S(8 ¹)	110.59(39)	
S(2 ⁷) - Pb - S(9 ¹)	72.93(44)	

TABLE 13
(continued)

Pb-S Bond Distances and Angles

B. Bond Angles

			Pb(3)	
S(11 ⁶)	- Pb -	S(7 ¹)	81.33(40)	degrees
S(11 ⁶)	- Pb -	S(6 ¹)	83.23(48)	
S(11 ⁶)	- Pb -	S(11 ¹)	78.37(47)	
S(11 ⁶)	- Pb -	S(5 ⁷)	76.30(50)	
S(11 ⁶)	- Pb -	S(9 ¹)	155.31(38)	
S(11 ⁶)	- Pb -	S(3 ⁷)	140.31(47)	
S(5 ⁷)	- Pb -	S(11 ¹)	88.27(44)	
S(5 ⁷)	- Pb -	S(7 ¹)	91.08(45)	
S(7 ¹)	- Pb -	S(6 ¹)	86.68(50)	
S(6 ¹)	- Pb -	S(11 ¹)	86.72(50)	
S(5 ⁷)	- Pb -	S(6 ¹)	159.51(40)	
S(11 ¹)	- Pb -	S(7 ¹)	159.25(43)	
S(9 ¹)	- Pb -	S(3 ⁷)	57.26(39)	
S(9 ¹)	- Pb -	S(7 ¹)	74.45(37)	
S(9 ¹)	- Pb -	S(6 ¹)	99.87(40)	
S(9 ¹)	- Pb -	S(11 ¹)	126.11(39)	
S(9 ¹)	- Pb -	S(5 ⁷)	99.13(41)	
S(3 ⁷)	- Pb -	S(7 ¹)	125.63(43)	
S(3 ⁷)	- Pb -	S(6 ¹)	122.47(40)	
S(3 ⁷)	- Pb -	S(11 ¹)	74.09(44)	
S(3 ⁷)	- Pb -	S(5 ⁷)	74.86(43)	
			Pb(4)	
S(10 ²)	- Pb -	S(6 ⁵)	80.47(51)	degrees
S(10 ²)	- Pb -	S(5 ⁷)	73.90(42)	
S(10 ²)	- Pb -	S(8 ³)	84.78(42)	
S(10 ²)	- Pb -	S(7 ¹)	79.31(47)	
S(10 ²)	- Pb -	S(2 ⁷)	140.69(45)	
S(10 ²)	- Pb -	S(1 ¹)	140.21(35)	
S(7 ¹)	- Pb -	S(5 ⁷)	89.90(47)	
S(7 ¹)	- Pb -	S(8 ³)	84.31(51)	
S(8 ³)	- Pb -	S(6 ⁵)	89.66(48)	
S(6 ⁵)	- Pb -	S(5 ⁷)	88.58(44)	
S(2 ⁷)	- Pb -	S(1 ¹)	55.17(33)	
S(2 ⁷)	- Pb -	S(6 ⁵)	83.88(47)	
S(2 ⁷)	- Pb -	S(5 ⁷)	69.87(40)	
S(2 ⁷)	- Pb -	S(8 ³)	131.09(41)	
S(2 ⁷)	- Pb -	S(7 ¹)	114.83(40)	
S(1 ¹)	- Pb -	S(6 ⁵)	63.71(35)	
S(1 ¹)	- Pb -	S(5 ⁷)	119.27(49)	
S(1 ¹)	- Pb -	S(8 ³)	78.59(47)	
S(1 ¹)	- Pb -	S(7 ¹)	133.55(34)	

TABLE 13
(continued)

Pb-S Bond Distances and Angles

B. Bond Angles

			Pb(5)	
S(6 ⁷)	- Pb -	S(10 ¹)	84.74(52)	degrees
S(6 ⁷)	- Pb -	S(4 ¹)	86.62(43)	
S(6 ⁷)	- Pb -	S(11 ⁴)	82.29(50)	
S(6 ⁷)	- Pb -	S(5 ⁶)	82.59(43)	
S(6 ⁷)	- Pb -	S(10 ⁶)	154.66(49)	
S(6 ⁷)	- Pb -	S(3 ⁶)	137.98(56)	
S(10 ¹)	- Pb -	S(4 ¹)	100.15(47)	
S(4 ¹)	- Pb -	S(11 ⁴)	88.45(47)	
S(11 ⁴)	- Pb -	S(5 ⁶)	84.77(46)	
S(5 ⁶)	- Pb -	S(10 ¹)	84.27(48)	
S(10 ⁶)	- Pb -	S(3 ⁶)	67.12(42)	
S(3 ⁶)	- Pb -	S(10 ¹)	119.34(40)	
S(3 ⁶)	- Pb -	S(4 ¹)	118.37(29)	
S(3 ⁶)	- Pb -	S(11 ⁴)	66.51(40)	
S(3 ⁶)	- Pb -	S(5 ⁶)	67.75(30)	
S(10 ⁶)	- Pb -	S(10 ¹)	82.58(33)	
S(10 ⁶)	- Pb -	S(4 ¹)	74.20(41)	
S(10 ⁶)	- Pb -	S(11 ⁴)	112.93(38)	
S(10 ⁶)	- Pb -	S(5 ⁶)	117.68(39)	
S(4 ¹)	- Pb -	S(5 ⁶)	167.93(52)	
S(10 ¹)	- Pb -	S(11 ⁴)	163.98(47)	

pyramidal coordination. S(7⁷) is the apical sulfur at a distance of 2.40 Å while the basal plane is composed of S(3⁵), S(4¹), S(10⁵), and S(11⁴) at distances of 2.55, 2.57, 3.05, 3.10 Å respectively. Sb(3) again has the square-pyramidal coordination by sulfur. The apex sulfur, S(8¹) is located 2.38 Å from the antimony atom. The basal plane sulfur atoms are S(2¹), S(3¹), S(4¹), and S(10¹), at distances of 2.47, 2.55, 3.12, and 3.13 Å respectively. The final antimony atom, Sb(4), is primarily three-coordinated. The shortest distance in the trigonal pyramid (considering the antimony atom as a vertex) is S(9¹) which is at 2.40 Å. The other vertices S(2¹) and S(1³) occur at 2.49 and 2.51 Å respectively shorter than second and third neighbors in the other polyhedra. It should be noticed that fourth and fifth neighbors can be found for Sb(4) but at much larger distances, S(4¹) at 3.16 and S(9³) at 3.63 Å. This generates a polyhedron similar to those of Sb(1), Sb(2), and Sb(3).

Interestingly, an additional neighbor for each antimony can be found resulting in a polyhedron resembling that of the 'split-vertex' octahedron for Pb. To do this requires consideration of sulfurs at non-bonding distances. For Sb(1), S(4¹) at 3.42 Å and S(2²) at 4.05 Å complete the 'split-vertex' octahedron, for Sb(2) S(11³) at 3.60 Å and S(4²) at 4.22 Å, for Sb(3) S(5¹) at 3.62 Å and S(10⁶) at 4.13 Å, and for Sb(4) in addition to the two sulfurs already added S(6³) at 3.45 Å and S(3⁵) at 3.82 Å complete the coordination. The bond distances, bond angles, and errors are presented in Table 14. The Sb polyhedra are shown in Figure 4.

FIGURE 4

Sb Coordination Polyhedra - Semseyite

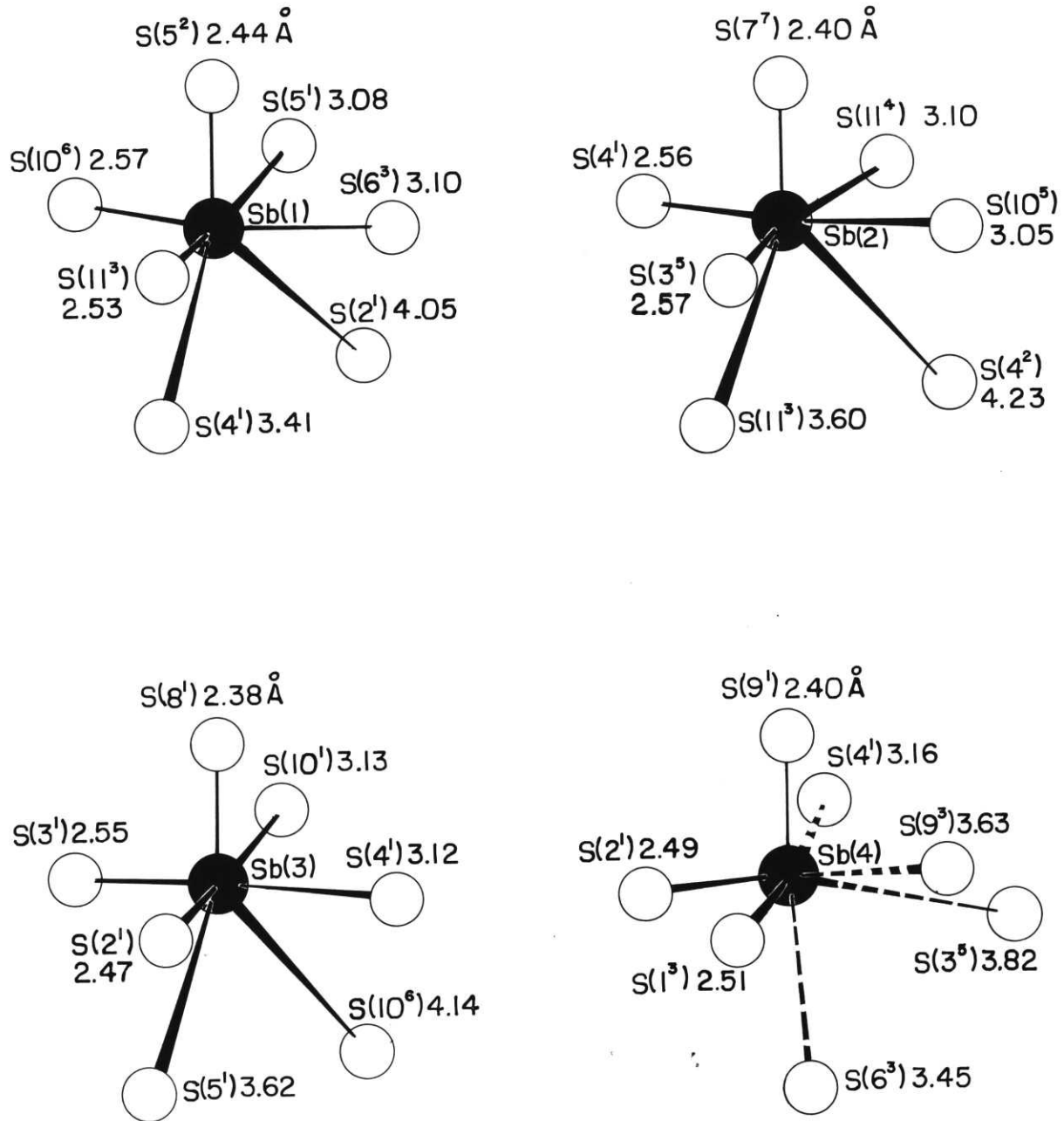


TABLE 14

Sb-S Bond Distances and Angles

A. Bond Distances

Sb(1)			Sb(2)		
S(5 ²)	2.441(15)	°	S(7 ⁷)	2.395(15)	°
S(11 ³)	2.528(19)	Å	S(3 ⁵)	2.553(14)	
S(10 ⁶)	2.570(15)		S(4 ¹)	2.566(19)	
S(5 ¹)	3.085(20)		S(10 ⁵)	3.053(21)	
S(6 ³)	3.100(16)		S(11 ⁴)	3.102(16)	
[S(4 ¹)	3.418(18)]		[S(11 ³)	3.601(19)]	
[S(2 ¹)	4.050(12)]		[S(4 ²)	4.219(12)]	
Sb(3)			Sb(4)		
S(8 ¹)	2.378(14)	°	S(9 ¹)	2.398(17)	°
S(2 ¹)	2.470(16)	Å	S(2 ¹)	2.492(18)	
S(3 ¹)	2.552(20)		S(1 ³)	2.506(19)	
S(4 ¹)	3.123(20)		[S(4 ¹)	3.157(17)]	
S(10 ¹)	3.134(16)		[S(6 ³)	3.453(17)]	
[S(5 ¹)	3.622(18)]		[S(9 ³)	3.635(19)]	
[S(10 ⁶)	4.136(12)]		[S(3 ⁵)	3.817(20)]	

B. Bond Angles

Sb(1)			
S(5 ²) - Sb - S(10 ⁶)	89.30(49)		degrees
S(5 ²) - Sb - S(11 ³)	90.27(54)		
S(5 ²) - Sb - S(5 ¹)	81.50(41)		
S(5 ²) - Sb - S(6 ³)	82.81(46)		
S(10 ⁶) - Sb - S(11 ³)	97.10(56)		
S(11 ³) - Sb - S(6 ³)	90.77(50)		
S(6 ³) - Sb - S(5 ¹)	84.49(47)		
S(11 ³) - Sb - S(5 ¹)	170.94(49)		
S(10 ⁶) - Sb - S(6 ³)	168.89(66)		
S(5 ¹) - Sb - S(10 ⁶)	86.63(54)		

TABLE 14
(continued)

Sb-S Bond Distances and Angles

B. Bond Angles

Sb(2)

S(7 ⁷) - Sb - S(4 ¹)	91.74(56)	degrees
S(7 ⁷) - Sb - S(3 ⁵)	93.81(48)	
S(7 ⁷) - Sb - S(11 ⁴)	86.77(48)	
S(7 ⁷) - Sb - S(10 ⁵)	84.09(56)	
S(4 ¹) - Sb - S(3 ⁵)	97.93(58)	
S(3 ⁵) - Sb - S(10 ⁵)	89.43(55)	
S(10 ⁵) - Sb - S(11 ⁴)	76.77(46)	
S(11 ⁴) - Sb - S(4 ¹)	116.82(28)	
S(11 ⁴) - Sb - S(3 ⁵)	166.06(57)	
S(4 ¹) - Sb - S(10 ⁵)	171.79(48)	

Sb(3)

S(8 ¹) - Sb - S(3 ¹)	95.87(54)	degrees
S(8 ¹) - Sb - S(2 ¹)	93.25(49)	
S(8 ¹) - Sb - S(10 ¹)	85.70(46)	
S(8 ¹) - Sb - S(4 ¹)	88.14(54)	
S(2 ¹) - Sb - S(4 ¹)	89.79(53)	
S(4 ¹) - Sb - S(10 ¹)	90.40(47)	
S(10 ¹) - Sb - S(3 ¹)	87.65(51)	
S(3 ¹) - Sb - S(2 ¹)	92.24(59)	
S(2 ¹) - Sb - S(10 ¹)	178.92(38)	
S(4 ¹) - Sb - S(3 ¹)	175.39(36)	

Sb(4)

S(9 ¹) - Sb - S(2 ¹)	101.55(53)	degrees
S(9 ¹) - Sb - S(1 ³)	96.70(56)	
S(9 ¹) - Sb - S(9 ³)	75.42(55)	
S(9 ¹) - Sb - S(4 ¹)	85.67(51)	
S(2 ¹) - Sb - S(1 ³)	82.54(58)	
S(1 ³) - Sb - S(9 ³)	70.56(55)	
S(9 ³) - Sb - S(4 ¹)	118.29(50)	
S(4 ¹) - Sb - S(2 ¹)	88.61(51)	
S(1 ³) - Sb - S(4 ¹)	171.13(57)	
S(2 ¹) - Sb - S(9 ³)	152.18(48)	

There are eleven sulfur atoms in the asymmetric unit - ten in the general position and one in the special position $4e$, S(1). Basically there are two types of sulfur coordination polyhedra - four coordinate and either five or six coordinate. Five of the sulfur atoms fall in the first category and six in the latter.

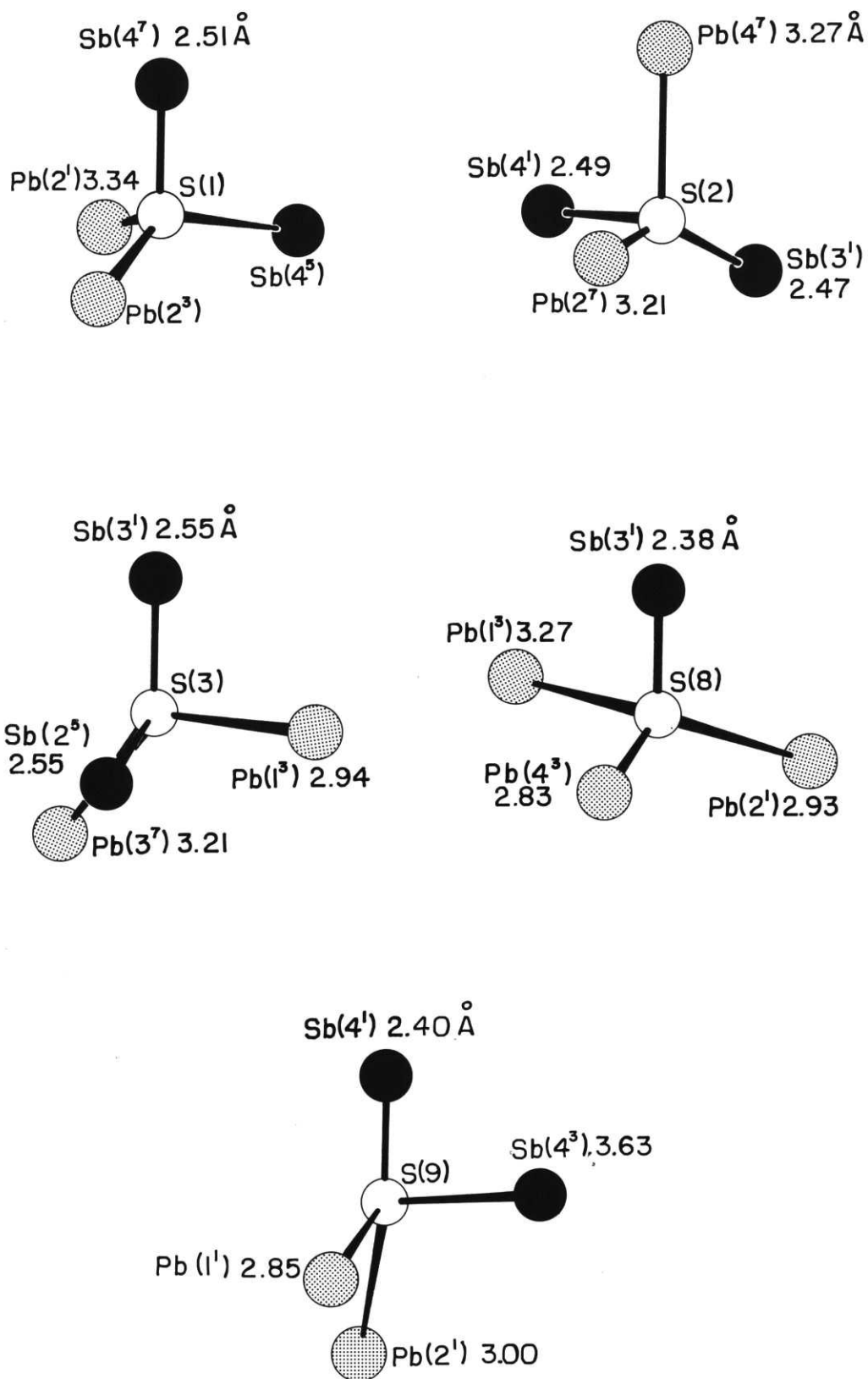
The four-coordinated sulfur atoms all have distorted tetrahedra of metals. These sulfurs are S(1), S(2), S(3), S(8), and S(9). The remaining sulfur atoms are all six-coordinated with the exception of S(7) which is five-coordinated. In some cases the sixth neighbor is at large distances. The six-coordinated sulfur atoms are S(4), S(5), S(6), S(10), and S(11). All the sulfur coordination polyhedra are shown in Figure 5. Bond distances and angles and the associated errors are given in Table 15. The sulfur-sulfur contact distances in the metal polyhedra are reported in Table 16.

B. Projections of the Structure

Semseyite may be understood by studying it in two projections, (010) and (112). These projections are presented as Figures 6 and 7 respectively.

The (010) projection (Figure 6) looks like a complete jumble on first glance. However, study reveals that the lead atom on the two-fold special position, Pb(1), acts as a pivot point for what appears to be chains of lead and antimony atoms. These 'chains' run parallel to the c axis and occur at $x = 0, .25, .5, \text{ and } .75$. Basically there are two types of 'chains'. Those occurring at $x = 0, 0.5$ are antimony 'chains' with a few lead atoms. They contain

S - Coordination Polyhedra - Semseyite



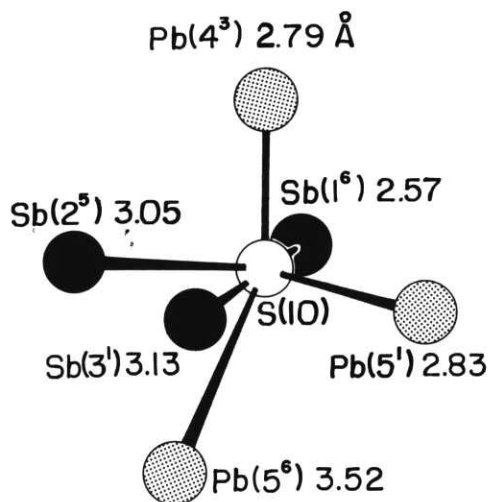
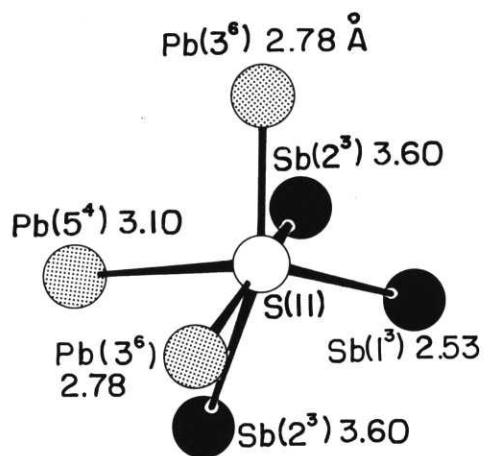
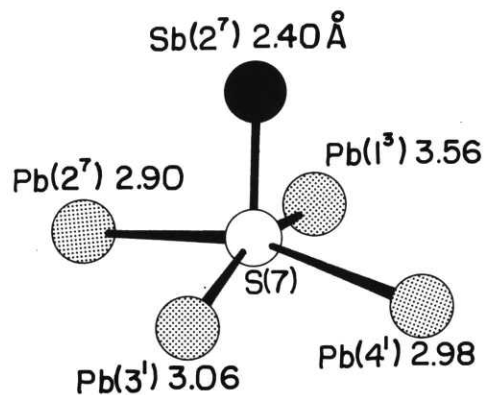
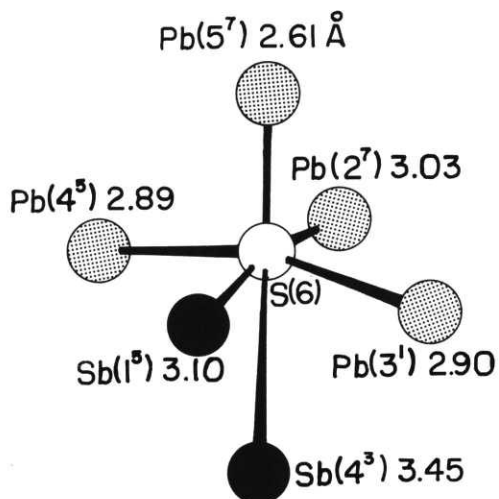
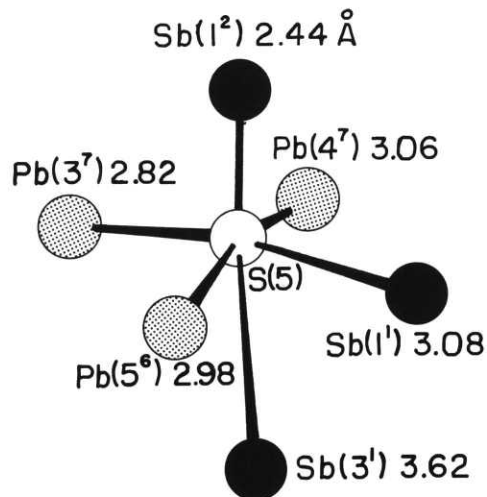
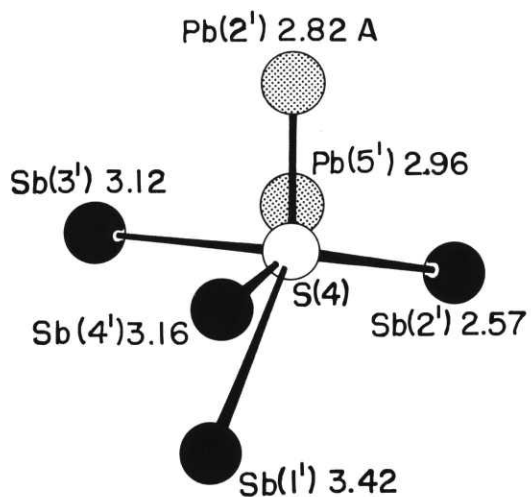


TABLE 15

Sulfur-Metal Bond Distances and Angles

A. Bond Distances

S (1)		S (2)	
Sb (4 ⁷)	2.506 (19) Å	Sb (3 ¹)	2.470 (16) Å
Sb (4 ⁵)	2.506 (19)	Sb (4 ¹)	2.492 (18)
Pb (2 ³)	3.339 (12)	Pb (2 ⁷)	3.211 (14)
Pb (2 ¹)	3.339 (12)	Pb (4 ⁷)	3.270 (19)
S (3)		S (4)	
Sb (3 ¹)	2.552 (20) Å	Sb (2 ¹)	2.566 (19) Å
Sb (2 ⁵)	2.553 (14)	Pb (2 ¹)	2.820 (13)
Pb (1 ³)	2.942 (11)	Pb (5 ¹)	2.959 (14)
Pb (3 ⁷)	3.208 (20)	Sb (3 ¹)	3.123 (19)
		Sb (4 ¹)	3.157 (17)
		Sb (1 ¹)	3.418 (18)
S (5)		S (6)	
Sb (1 ²)	2.441 (15) Å	Pb (5 ⁷)	2.610 (15) Å
Pb (3 ⁷)	2.918 (17)	Pb (4 ⁵)	2.890 (18)
Pb (5 ⁶)	2.978 (15)	Pb (3 ¹)	2.899 (21)
Pb (4 ⁷)	3.061 (14)	Pb (2 ⁷)	3.031 (15)
Sb (1 ¹)	3.085 (20)	Sb (1 ³)	3.100 (16)
Sb (3 ¹)	3.622 (18)	Sb (4 ³)	3.453 (17)
S (7)		S (8)	
Sb (2 ⁷)	2.395 (15) Å	Sb (3 ¹)	2.378 (15) Å
Pb (2 ⁷)	2.897 (18)	Pb (4 ³)	2.833 (16)
Pb (4 ¹)	2.976 (21)	Pb (2 ¹)	2.931 (20)
Pb (3 ¹)	3.057 (16)	Pb (1 ³)	3.267 (20)
Pb (1 ³)	3.564 (16)		

TABLE 15
(continued)

Sulfur-Metal Bond Distances and Angles

A. Bond Distances

S(9)		S(10)	
Sb(4 ¹)	2.398(17) Å	Sb(1 ⁶)	2.570(15) Å
Pb(1 ¹)	2.854(20)	Pb(4 ³)	2.789(14)
Pb(2 ¹)	2.998(17)	Pb(5 ¹)	2.859(18)
Sb(4 ³)	3.635(17)	Sb(2 ⁵)	3.053(21)
		Sb(3 ¹)	3.134(16)
		Pb(5 ⁶)	3.518(19)

S(11)

Sb(1 ³)	2.528(19) Å
Pb(3 ⁶)	2.782(13)
Pb(3 ¹)	2.965(14)
Pb(5 ⁴)	3.098(20)
Sb(2 ⁴)	3.102(16)
Sb(2 ³)	3.601(19)

B. Bond Angles

S(1)

Sb(4 ⁵) - S - Sb(4 ⁷)	98.56(1.01) degrees
Sb(4 ⁷) - S - Pb(2 ³)	112.62(16) 2x
Sb(4 ⁷) - S - Pb(2 ¹)	99.74(12) 2x
Pb(2 ³) - S - Pb(2 ¹)	129.77(89)

S(2)

Pb(4 ⁷) - S - Sb(4 ¹)	97.59(39) degrees
Pb(4 ⁷) - S - Pb(2 ⁷)	84.96(47)
Pb(4 ⁷) - S - Sb(3 ¹)	122.29(53)
Sb(4 ¹) - S - Pb(2 ⁷)	103.50(45)
Pb(2 ⁷) - S - Sb(3 ¹)	137.27(43)
Sb(3 ¹) - S - Sb(4 ¹)	104.31(75)

TABLE 15
(continued)

Sulfur-Metal Bond Distances and Angles

B. Bond Angles

S(3)

Sb(3 ¹) - S - Pb(1 ³)	94.77(56)	degrees
Sb(3 ¹) - S - Sb(2 ⁵)	102.65(73)	
Sb(3 ¹) - S - Pb(3 ⁷)	115.10(39)	
Pb(1 ³) - S - Sb(2 ⁵)	104.53(42)	
Sb(2 ⁵) - S - Pb(3 ⁷)	115.92(59)	
Pb(3 ⁷) - S - Pb(1 ³)	120.57(59)	

S(4)

Pb(2 ¹) - S - Pb(5 ¹)	94.24(44)	degrees
Pb(2 ¹) - S - Sb(3 ¹)	86.97(33)	
Pb(2 ¹) - S - Sb(4 ¹)	88.69(34)	
Pb(2 ¹) - S - Sb(2 ¹)	94.65(64)	
Pb(2 ¹) - S - Sb(1 ¹)	154.28(66)	
Pb(5 ¹) - S - Sb(3 ¹)	83.30(38)	
Sb(3 ¹) - S - Sb(4 ¹)	77.22(46)	
Sb(2 ¹) - S - Sb(4 ¹)	105.82(46)	
Sb(2 ¹) - S - Pb(5 ¹)	93.55(56)	
Sb(4 ¹) - S - Pb(5 ¹)	160.13(73)	
Sb(3 ¹) - S - Sb(2 ¹)	176.57(54)	
Sb(1 ¹) - S - Sb(4 ¹)	71.18(40)	
Sb(1 ¹) - S - Sb(3 ¹)	73.35(46)	
Sb(1 ¹) - S - Pb(5 ¹)	99.58(41)	
Sb(1 ¹) - S - Sb(2 ¹)	105.94(35)	

S(5)

Sb(1 ²) - S - Pb(3 ⁷)	95.71(68)	degrees
Sb(1 ²) - S - Pb(5 ⁶)	100.63(42)	
Sb(1 ²) - S - Sb(1 ¹)	98.50(41)	
Sb(1 ²) - S - Pb(4 ⁷)	96.17(52)	
Sb(1 ²) - S - Sb(3 ¹)	162.62(65)	
Pb(3 ⁷) - S - Pb(5 ⁶)	92.68(38)	
Pb(5 ⁶) - S - Sb(1 ¹)	86.55(52)	
Sb(1 ¹) - S - Pb(4 ⁷)	90.40(41)	
Pb(4 ⁷) - S - Pb(3 ⁷)	86.22(44)	
Sb(3 ¹) - S - Pb(3 ⁷)	95.75(29)	
Sb(3 ¹) - S - Pb(5 ⁶)	92.68(38)	
Sb(3 ¹) - S - Sb(1 ¹)	95.75(29)	
Sb(3 ¹) - S - Pb(4 ⁷)	97.59(37)	
Pb(4 ⁷) - S - Pb(5 ⁶)	163.20(56)	
Pb(3 ⁷) - S - Sb(1 ¹)	165.67(54)	

TABLE 15
(continued)

Sulfur-Metal Bond Distances and Angles

B. Bond Angles

S(6)

Pb(5 ⁷) - S - Pb(4 ⁵)	98.31(70)	degrees
Pb(5 ⁷) - S - Sb(1 ³)	93.85(39)	
Pb(5 ⁷) - S - Pb(3 ¹)	101.46(42)	
Pb(5 ⁷) - S - Pb(2 ⁷)	97.06(53)	
Pb(5 ⁷) - S - Sb(4 ³)	164.76(63)	
Pb(4 ⁵) - S - Sb(1 ³)	93.37(40)	
Sb(1 ³) - S - Pb(3 ¹)	84.77(55)	
Pb(3 ¹) - S - Pb(2 ⁷)	90.27(44)	
Pb(2 ⁷) - S - Pb(4 ⁵)	87.86(49)	
Sb(1 ³) - S - Pb(2 ⁷)	168.72(66)	
Pb(3 ¹) - S - Pb(4 ⁵)	160.22(57)	
Sb(4 ³) - S - Pb(4 ⁵)	86.49(29)	
Sb(4 ³) - S - Sb(1 ³)	71.35(38)	
Sb(4 ³) - S - Pb(3 ¹)	74.23(48)	
Sb(4 ³) - S - Pb(2 ⁷)	97.57(36)	

S(7)

Sb(2 ⁷) - S - Pb(1 ³)	91.69(52)	degrees
Sb(2 ⁷) - S - Pb(2 ⁷)	96.53(72)	
Sb(2 ⁷) - S - Pb(3 ¹)	100.29(44)	
Sb(2 ⁷) - S - Pb(4 ¹)	103.41(46)	
Pb(1 ³) - S - Pb(2 ⁷)	84.18(45)	
Pb(2 ⁷) - S - Pb(3 ¹)	96.53(72)	
Pb(3 ¹) - S - Pb(4 ¹)	85.30(55)	
Pb(4 ¹) - S - Pb(1 ³)	96.51(40)	
Pb(3 ¹) - S - Pb(1 ³)	167.15(38)	
Pb(2 ⁷) - S - Pb(4 ¹)	160.01(56)	

S(8)

Sb(3 ¹) - S - Pb(1 ³)	90.32(67)	degrees
Sb(3 ¹) - S - Pb(4 ³)	102.67(44)	
Sb(3 ¹) - S - Pb(2 ¹)	100.44(43)	
Pb(1 ³) - S - Pb(4 ³)	106.51(43)	
Pb(4 ³) - S - Pb(2 ¹)	90.94(61)	
Pb(2 ¹) - S - Pb(1 ³)	157.06(46)	

TABLE 15
(continued)

Sulfur-Metal Bond Distances and Angles

B. Bond Angles

S(9)

Sb(4 ¹) - S - Pb(1 ¹)	101.74 (42)	degrees
Sb(4 ¹) - S - Sb(4 ³)	74.92 (46)	
Sb(4 ¹) - S - Pb(2 ¹)	101.12 (47)	
Pb(1 ¹) - S - Pb(2 ¹)	96.25 (64)	
Pb(2 ¹) - S - Sb(4 ³)	171.04 (48)	
Sb(4 ³) - S - Pb(1 ¹)	76.97 (34)	

S(10)

Pb(4 ³) - S - Sb(3 ¹)	86.84 (36)	degrees
Pb(4 ³) - S - Pb(5 ¹)	95.70 (63)	
Pb(4 ³) - S - Sb(1 ⁶)	100.27 (53)	
Pb(4 ³) - S - Sb(2 ⁵)	92.70 (37)	
Pb(4 ³) - S - Pb(5 ⁶)	148.32 (62)	
Sb(3 ¹) - S - Sb(1 ⁶)	170.25 (87)	
Pb(5 ¹) - S - Sb(2 ⁵)	162.72 (65)	
Sb(3 ¹) - S - Pb(5 ¹)	85.22 (38)	
Pb(5 ¹) - S - Sb(1 ⁶)	100.56 (62)	
Sb(1 ⁶) - S - Sb(2 ⁵)	92.73 (51)	
Sb(2 ⁵) - S - Sb(3 ¹)	80.19 (49)	
Pb(5 ⁶) - S - Sb(3 ¹)	65.76 (36)	
Pb(5 ⁶) - S - Pb(5 ¹)	97.42 (33)	
Pb(5 ⁶) - S - Sb(1 ⁶)	105.46 (50)	
Pb(5 ⁶) - S - Sb(2 ⁵)	68.16 (45)	

S(11)

Pb(3 ⁶) - S - Sb(2 ⁴)	91.13 (35)	degrees
Pb(3 ⁶) - S - Pb(5 ⁴)	92.94 (36)	
Pb(3 ⁶) - S - Pb(3 ¹)	101.63 (47)	
Pb(3 ⁶) - S - Sb(1 ³)	97.20 (66)	
Pb(3 ⁶) - S - Sb(2 ³)	152.91 (65)	
Sb(2 ⁴) - S - Pb(5 ⁴)	81.20 (49)	
Pb(5 ⁴) - S - Pb(3 ¹)	89.39 (42)	
Pb(3 ¹) - S - Sb(1 ³)	94.56 (55)	
Sb(1 ³) - S - Sb(2 ⁴)	92.42 (42)	
Sb(2 ³) - S - Sb(2 ⁴)	69.09 (46)	
Sb(2 ³) - S - Pb(5 ⁴)	66.61 (41)	
Sb(2 ³) - S - Pb(3 ¹)	95.96 (40)	
Sb(2 ³) - S - Sb(1 ³)	101.80 (35)	
Pb(3 ¹) - S - Sb(2 ⁴)	164.55 (73)	
Pb(5 ⁴) - S - Sb(1 ³)	168.13 (64)	

TABLE 16

Sulfur-Sulfur Contact Distances

Pb (1)		
S (7 ⁷) - S (9 ³)	4.306 (28)	^o A 2x
S (9 ³) - S (3 ⁵)	3.356 (22)	2x
S (3 ⁵) - S (8 ⁵)	3.662 (29)	2x
S (8 ⁵) - S (7 ⁷)	3.900 (21)	2x
S (7 ⁷) - S (8 ⁷)	3.989 (20)	2x
S (7 ⁷) - S (3 ⁷)	3.615 (20)	2x
S (9 ³) - S (3 ⁷)	4.262 (18)	2x
S (9 ³) - S (9 ¹)	3.817 (27)	
S (8 ⁵) - S (8 ⁷)	3.405 (19)	
Pb (2)		
S (4 ¹) - S (6 ⁷)	3.828 (23)	^o A
S (4 ¹) - S (7 ⁷)	3.563 (30)	
S (4 ¹) - S (9 ¹)	3.817 (18)	
S (4 ¹) - S (8 ¹)	3.863 (17)	
S (6 ⁷) - S (7 ⁷)	4.089 (21)	
S (7 ⁷) - S (9 ¹)	4.301 (28)	
S (9 ¹) - S (8 ¹)	4.134 (20)	
S (8 ¹) - S (6 ⁷)	4.035 (28)	
S (1 ¹) - S (2 ⁷)	3.297 (14)	
S (2 ⁷) - S (7 ⁷)	4.258 (16)	
S (2 ⁷) - S (9 ¹)	3.694 (26)	
S (1 ¹) - S (8 ¹)	4.253 (33)	
S (1 ¹) - S (6 ⁷)	3.602 (12)	
Pb (3)		
S (11 ⁶) - S (7 ¹)	3.810 (18)	^o A
S (11 ⁶) - S (6 ¹)	3.774 (18)	
S (11 ⁶) - S (11 ¹)	3.634 (31)	
S (11 ⁶) - S (5 ⁷)	3.523 (29)	
S (7 ¹) - S (6 ¹)	4.089 (21)	
S (6 ¹) - S (11 ¹)	4.027 (27)	
S (11 ¹) - S (5 ⁷)	4.097 (20)	
S (5 ⁷) - S (7 ¹)	4.266 (27)	
S (3 ⁷) - S (9 ¹)	3.356 (22)	
S (7 ¹) - S (9 ¹)	4.141 (23)	
S (11 ¹) - S (3 ⁷)	3.724 (23)	
S (3 ⁷) - S (5 ⁷)	3.731 (16)	

TABLE 16
(continued)

Sulfur-Sulfur Contact Distances

Pb(4)

S(10 ²) - S(6 ⁵)	3.669(30)	° Å
S(10 ²) - S(8 ³)	3.790(18)	
S(10 ²) - S(5 ⁷)	3.523(23)	
S(10 ²) - S(7 ¹)	3.681(18)	
S(6 ⁵) - S(8 ³)	4.035(28)	
S(8 ³) - S(7 ¹)	3.900(21)	
S(7 ¹) - S(5 ⁷)	4.266(27)	
S(5 ⁷) - S(6 ⁵)	4.158(21)	
S(6 ⁵) - S(1 ¹)	3.602(12)	
S(5 ⁷) - S(2 ⁷)	3.630(21)	
S(7 ¹) - S(2 ⁷)		
S(1 ¹) - S(2 ⁷)	3.297(14)	

Pb(5)

S(6 ⁷) - S(10 ¹)	3.669(30)	° Å
S(6 ⁷) - S(4 ¹)	3.828(22)	
S(6 ⁷) - S(11 ⁴)	3.774(18)	
S(6 ⁷) - S(5 ⁶)	3.698(18)	
S(10 ¹) - S(4 ¹)	4.440(20)	
S(4 ¹) - S(11 ⁴)	4.226(27)	
S(11 ⁴) - S(5 ⁶)	4.097(20)	
S(5 ⁶) - S(10 ¹)	3.897(28)	
S(10 ⁶) - S(3 ⁶)	3.950(21)	
S(10 ⁶) - S(4 ¹)	3.933(22)	
S(10 ⁶) - S(10 ¹)	4.221(23)	
S(3 ⁶) - S(11 ⁴)	3.724(23)	
S(5 ⁶) - S(3 ⁶)	3.731(15)	

Sb(1)

S(5 ²) - S(10 ⁶)	3.523(23)
S(5 ²) - S(11 ³)	3.523(29)
S(5 ²) - S(6 ³)	3.698(18)
S(5 ²) - S(5 ¹)	3.640(24)
S(10 ⁶) - S(11 ³)	3.823(21)
S(11 ³) - S(6 ³)	4.027(27)
S(6 ³) - S(5 ¹)	4.158(21)
S(5 ¹) - S(10 ⁶)	3.897(28)
S(4 ¹) - S(2 ¹)	3.974(28)
S(2 ¹) - S(5 ¹)	3.630(21)
S(2 ¹) - S(6 ³)	4.127(16)
S(4 ¹) - S(10 ⁶)	3.933(22)
S(4 ¹) - S(11 ³)	3.807(16)

TABLE 16
(continued)

Sulfur-Sulfur Contact Distances

Sb(2)

S(7 ⁷) - S(4 ¹)	3.563(30)
S(7 ⁷) - S(3 ⁵)	3.615(22)
S(7 ⁷) - S(10 ⁵)	3.681(18)
S(7 ⁷) - S(11 ⁴)	3.810(18)
S(4 ¹) - S(3 ⁵)	3.861(20)
S(3 ⁵) - S(10 ⁵)	3.960(29)
S(10 ⁵) - S(11 ⁴)	3.822(21)
S(11 ⁴) - S(4 ¹)	3.807(16)
S(11 ³) - S(4 ²)	4.226(27)
S(11 ³) - S(4 ¹)	3.807(16)
S(11 ³) - S(3 ⁵)	3.724(23)
S(4 ²) - S(10 ⁵)	3.933(22)
S(4 ²) - S(11 ⁴)	3.807(16)

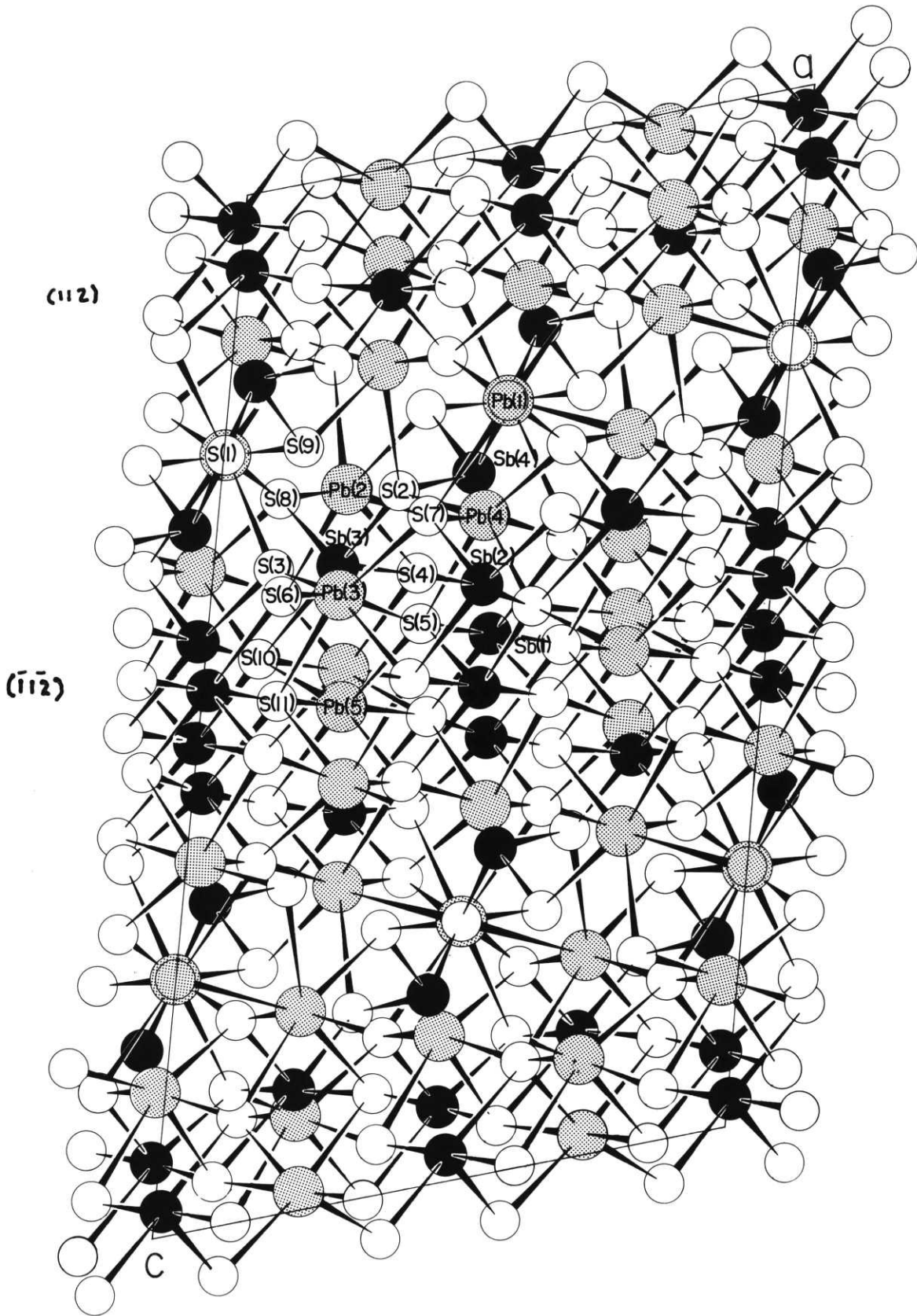
Sb(3)

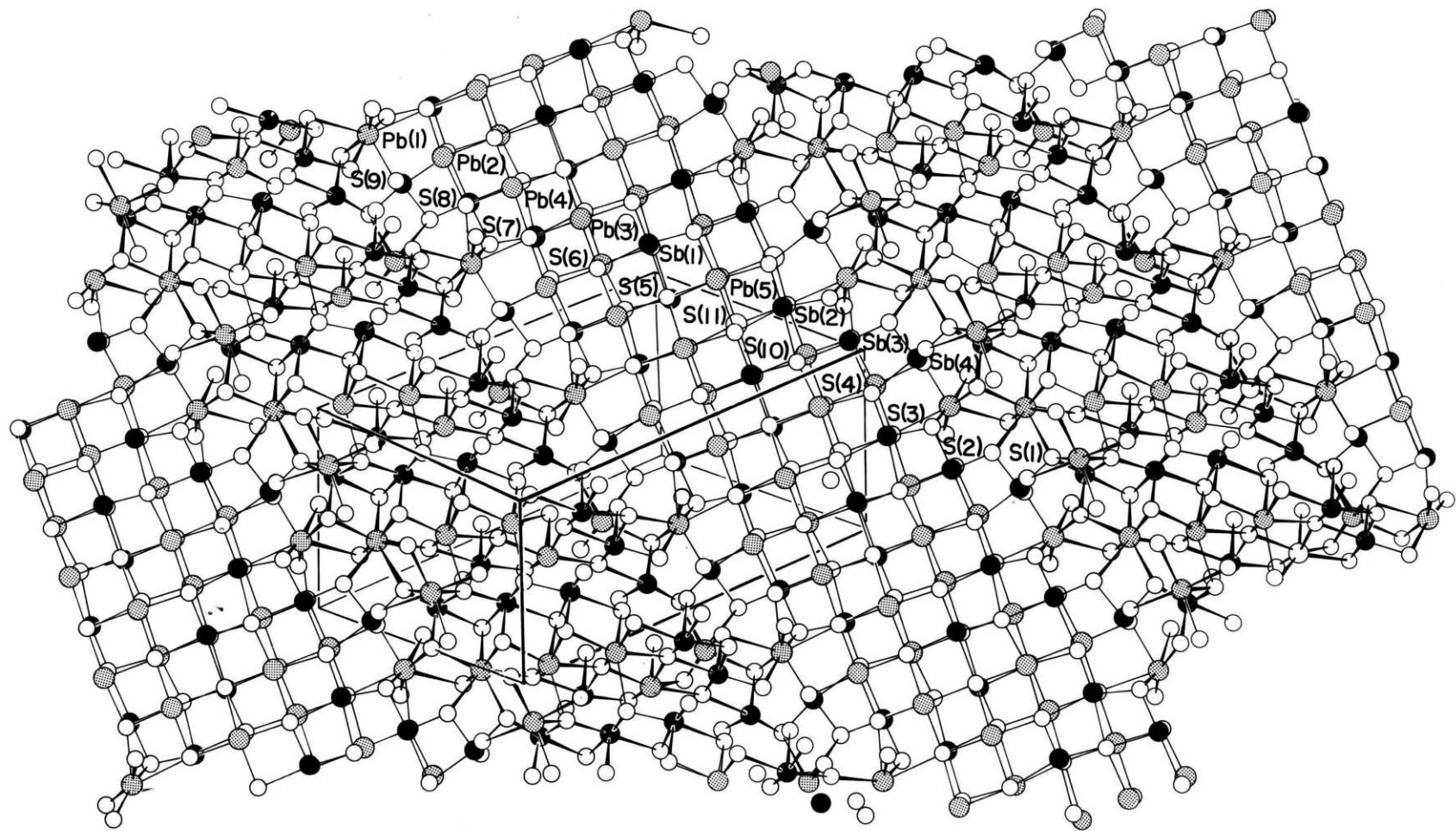
S(8 ¹) - S(3 ¹)	3.662(30)
S(8 ¹) - S(2 ¹)	3.525(23)
S(8 ¹) - S(4 ¹)	3.863(17)
S(8 ¹) - S(10 ¹)	3.790(18)
S(3 ¹) - S(2 ¹)	3.620(20)
S(2 ¹) - S(4 ¹)	3.974(28)
S(4 ¹) - S(10 ¹)	4.440(20)
S(10 ¹) - S(3 ¹)	3.960(28)
S(5 ¹) - S(10 ⁶)	3.897(28)
S(5 ¹) - S(3 ¹)	3.731(16)
S(5 ¹) - S(2 ¹)	3.630(21)
S(10 ⁶) - S(4 ¹)	3.933(22)
S(10 ⁶) - S(10 ¹)	4.221(23)

Sb(4)

S(9 ¹) - S(2 ¹)	3.789(29)
S(9 ¹) - S(1 ³)	3.664(32)
S(9 ¹) - S(9 ³)	3.817(27)
S(9 ¹) - S(4 ¹)	3.817(18)
S(2 ¹) - S(1 ³)	3.297(14)
S(1 ³) - S(9 ³)	3.664(14)
S(4 ¹) - S(2 ¹)	3.974(28)
S(6 ³) - S(2 ¹)	4.127(16)
S(6 ³) - S(1 ³)	3.602(12)
S(3 ⁵) - S(9 ³)	3.356(22)
S(3 ⁵) - S(4 ¹)	3.861(20)

(010) Projection Semseyite





(112) Projection Semseyite

FIGURE 17.

Pb(1), Pb(4), Sb(4), Sb(2), and Sb(1). The chains at $x = .25$ and $.75$ are predominately lead 'chains' with Pb(2), Pb(3), Pb(5) and Sb(3). The sulfur atoms provide a chain-like formation that joins the lead and antimony 'chains'. Between the Pb(1)'s, on the two-fold positions, the density of bonds can be seen to be quite thick. However, in the immediate vicinity of $z = .25, 0.75$ ($x=0$ to 1) the density of bonds appears to be quite sparse. This combination of an area of thick bonding with a region of thin bonding suggests that the structure might be described as sheets or slabs joined to one another at points of relatively sparse bonding. The (010) projection has indicated upon it (Figure 6) regions designated as (112) and ($\bar{1}\bar{1}\bar{2}$). This designates the plane to which the slab-like unit is parallel. The slabs in the two orientations are related by the two-fold rotation axis (at Pb(1)) parallel to b .

For further study, the structure was projected onto (112), the plane of one of the two slabs). (Figure 7) Here there is a region which resembles a rock-salt type configuration bordered by what seems to be a jumbled mess. This confusion is merely the projection of the second slab parallel to ($\bar{1}\bar{1}\bar{2}$). Notice that the rock-salt-like area is terminated by the lead atoms (Pb(1)) and the sulfur atoms (S(1)) in the position of two-fold symmetry. The slab is composed of two levels which are related by a center of inversion. A diagonal line of metal atoms will be noticed running along [110] of the PbS-like cells on either level. The line starts with Pb(1) and is terminated by Sb(4). Running from Pb(1) to Sb(4) the atoms are Pb(1), Pb(2), Pb(4), Pb(3), Sb(1), Pb(5), Sb(2), Sb(3),

and Sb(4). Parallel to this diagonal line of metals is a line of sulfur atoms again running along the [110] of a PbS cell. Starting with the sulfur on the two-fold special position, the line is S(1), S(2), S(3), S(4), S(10), S(11), S(5), S(6), S(7), S(8), and S(9). These two chains, all on one level of the slab, are the complete asymmetric unit of the structure. The rest of the slab may be generated by the center of inversion and the C centering translation. The C centering translation appears on the (112) projections as the distance and direction between equivalent Pb(1) atoms on the same level (i.e. top or bottom of the slab, not mixed).

The coordination polyhedra can be visualized very easily in the (112) projection. (It should be noted that atoms not lying in the PbS-like slab but rather in an adjacent one are not shown for the rock-salt portion. Therefore, with the exception of Pb(1) and Sb(4), the polyhedra will not be complete. Thus the sixth and seventh neighbors for all the other atoms represent bonding between the adjacent (112) slabs.) It can be seen that three of the four lead atoms in the general position, Pb(3), Pb(4), and Pb(5), share the four equatorial edges with polyhedra in the same level. The exception Pb(2), which is near the edge of the slab, shares only three of these edges. Likewise all four general position lead atoms share all four of their nearest apex edges with polyhedra in the adjacent level. Similarly the antimony polyhedra can be understood. Sb(1) shares four basal edges and four apical edges; Sb(2) shares three basal and four apical edges. Sb(3) and Sb(4)

which are near the edge of the slab, share fewer elements with the other polyhedra. Sb(3) shares two basal and three apical edges and one corner while Sb(4) shares only corners.

Visualization of the structure in three dimensions is not difficult if one abandons the traditional 'ball and stick' approach to adopt the slab, or as it is known locally, the 'kite' method. Take one 'rock-salt-like slab' parallel to (112) and imagine it as a unit which is two atoms thick. This slab is mounted in the cell by anchoring it at the two-fold axes. The slab itself extends indefinitely along $[1\bar{1}0]$. It is repeated by the b-axis translation and rotated by the two-fold axes to form $(\bar{1}1\bar{2})$ slabs which are equivalent. Thus semseyite is a stack of (112) slabs joined to and alternating with $(\bar{1}1\bar{2})$ slabs at the lead and sulfur atoms, Pb(1) and S(1). The observed perfect (112) cleavage is explained by the fact that only a few long weak bonds bind the stack of (112) slabs together. Bonding within a single (112) slab is much stronger. Also it should be noted that the sulfurs with tetrahedral coordination all occur along the edges of the slab, while the higher coordinated sulfurs occur in the center of the slab.

Thus semseyite, the end member of the plagionite group, is seen to be a series of 'rock-salt-like' slabs two atoms thick connected in the c direction by a lead and sulfur atom at the special two-fold positions. The slabs are extended indefinitely along $[1\bar{1}0]$ and are 'stacked' by the b translation.

Chapter VII

Semseyite, Stibnite, Galena, and Plagionite

Since only one other lead-antimony sulfosalt structure, plagionite, has been solved, the number of other related minerals available for comparison to the structure of semseyite is somewhat limited. However, the coordination geometry of the metals in semseyite can be compared with that in stibnite, Sb_2S_3 , and galena, PbS .

Recently Nowacki and Bayliss (1971) refined the structure of stibnite and calculated more precise bond distances. They found that antimony is both five-coordinated and three-coordinated. The former scheme is similar to that known for the bismuth sulfosalts while the latter is characteristic of arsenic sulfosalts. The five-coordinated Sb atom has one near sulfur neighbor at $2.455(3)\text{Å}$, four intermediate at $2.678(2)\text{Å}$ and 2.854Å . The three-coordinated antimony atom has a very near sulfur neighbor at $2.521(3)\text{Å}$ then two at a distance of $2.539(2)\text{Å}$. In semseyite three of the antimony atoms, Sb(1), Sb(2), and Sb(3), are decidedly five-coordinated. The fourth, Sb(4), is three-coordinated. Considering the five-coordinated antimony atoms, the average equatorial bond distances are 2.766Å for stibnite but slightly larger values of 2.821Å (Sb(1)), 2.818Å (Sb(2)) and 2.819Å (Sb(3)) in semseyite. The distances to the apical sulfur are slightly shorter for two of the antimony atoms. Sb(2) and Sb(3) have apical distances of 2.395Å and 2.378Å respectively. This is nearly 0.05Å shorter than the similar stibnite distance, 2.455Å or the apical distance

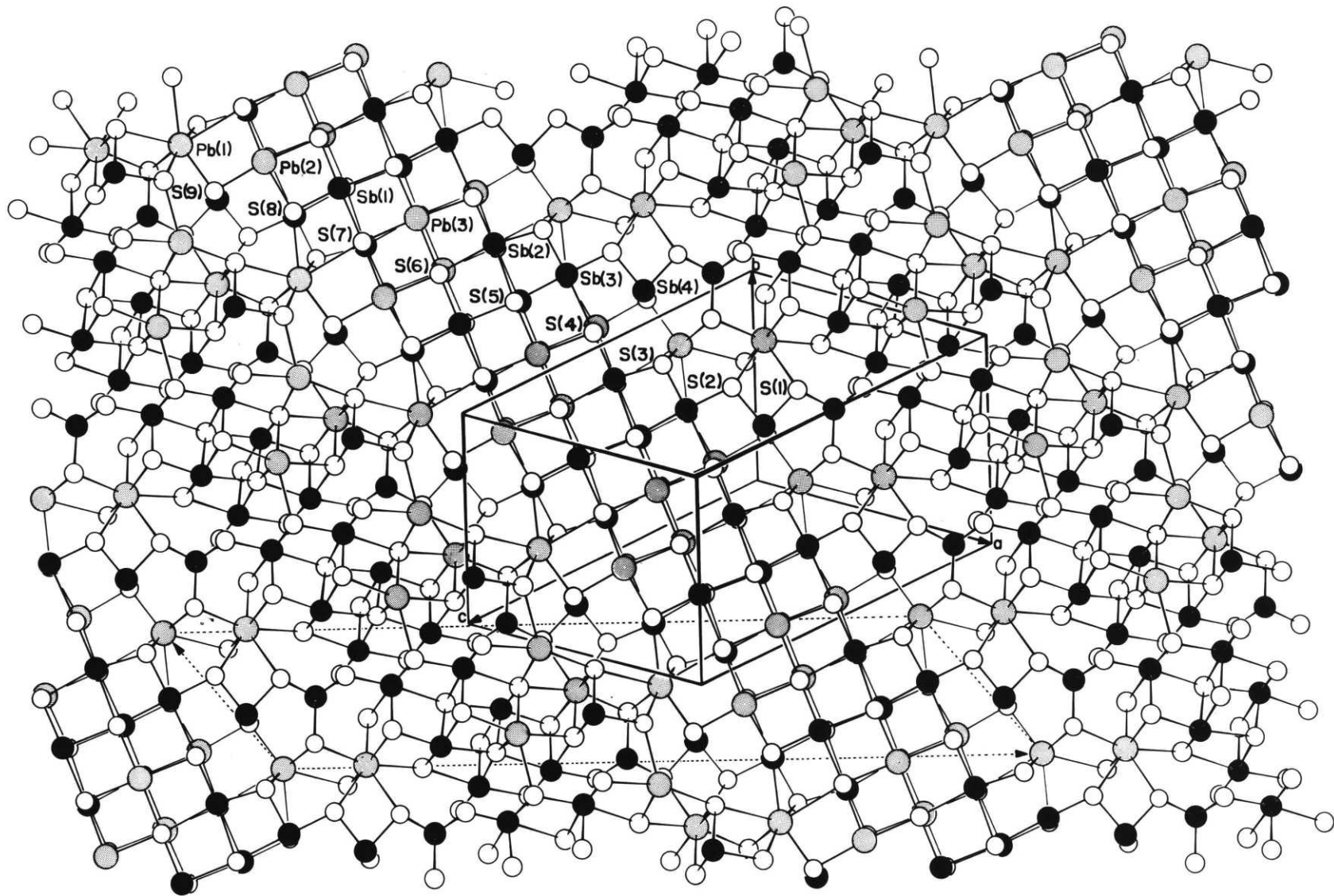
for Sb(1), 2.441 Å. It should be noted that although these antimony atoms in semseyite are not located on a mirror plane as they are in stibnite, their equatorial sulfur neighbors come in distinct, nearly equal, pairs, i.e. the coordination is [1+2+2]. For Sb(1) the first pair is 2.528 and 2.570 Å, and the second pair 3.085 and 3.100 Å. For Sb(2) the pairs are 2.553 - 2.556 Å and 3.053 - 3.102 Å and for Sb(3) 2.470 - 2.552 Å and 3.123 - 3.134 Å. The fourth antimony atom, Sb(4), is three-coordinated. The average bond distance is 2.465 Å, nearly 0.1 Å shorter than the average 2.533 Å value of stibnite. Although five neighbors can be located for Sb(4), they do not conform to the 'pair-arrangement' described for the other three Sb atoms and stibnite. Sb(4) can have one pair of equatorial sulfur atoms at 2.492 - 2.506 Å but the second 'pair' is a 3.157 - 3.454 Å. Therefore it must be concluded that Sb(4) has a decidedly different configuration from the other three.

The obvious comparison to make is that of the lead polyhedra in semseyite with galena, PbS. For galena the Pb-S distance for six-coordinate lead is 2.965 Å. Two of the semseyite lead polyhedra Pb(3) and Pb(4) have average six-coordinated distances of 2.971 and 2.970 Å. The five-coordinated Pb(5) has a shorter average distance - 2.895 Å while the seven and eight coordinated lead atoms, Pb(2) and Pb(1), have average distances of 3.023 and 3.021 Å respectively. Thus to within 0.06 Å, the average Pb-S distance in semseyite agrees with that in galena. However, it should be noticed that within each coordination polyhedra bond distances

range from 2.854 to 3.564 Å for Pb(1), 2.820 to 3.339 Å, Pb(2), 2.782 to 3.208 Å, Pb(3), 2.789 to 3.270 Å, Pb(4), and 2.610 to 3.098 Å, Pb(5). Thus while the overall view of the structure reveals galena-like coordination for the lead atoms (see (112) projection, Figure 7), the details of the coordination are different.

Comparison can also be made of the structure of semseyite to that of her sister mineral plagionite. In both minerals there are four independent antimony atoms. Three Sb atoms in each structure are five-coordinated and one, Sb(4), is three-coordinated. The two sets of polyhedra (i.e. plagionite and semseyite) are remarkably similar. Small differences arise in apical bond distances - semseyite is generally slightly shorter (~ 0.04 Å) - and the second 'pair' of equatorial sulfurs - semseyite is generally equal or longer (~ 0.10 Å). This may be rationalized as the effect of the addition of two lead atoms and two sulfur atoms. Considering the (112) projection, the apical bond distance measures the thickness of the 'slab', while the equatorial distances represent distances within one level of the slab. Thus comparing the (112) projections of semseyite (Figure 7) and plagionite (Figure 8) it can be seen that while the thickness of the 'slab' does not change the width does - thereby slightly distorting the equatorial distances.

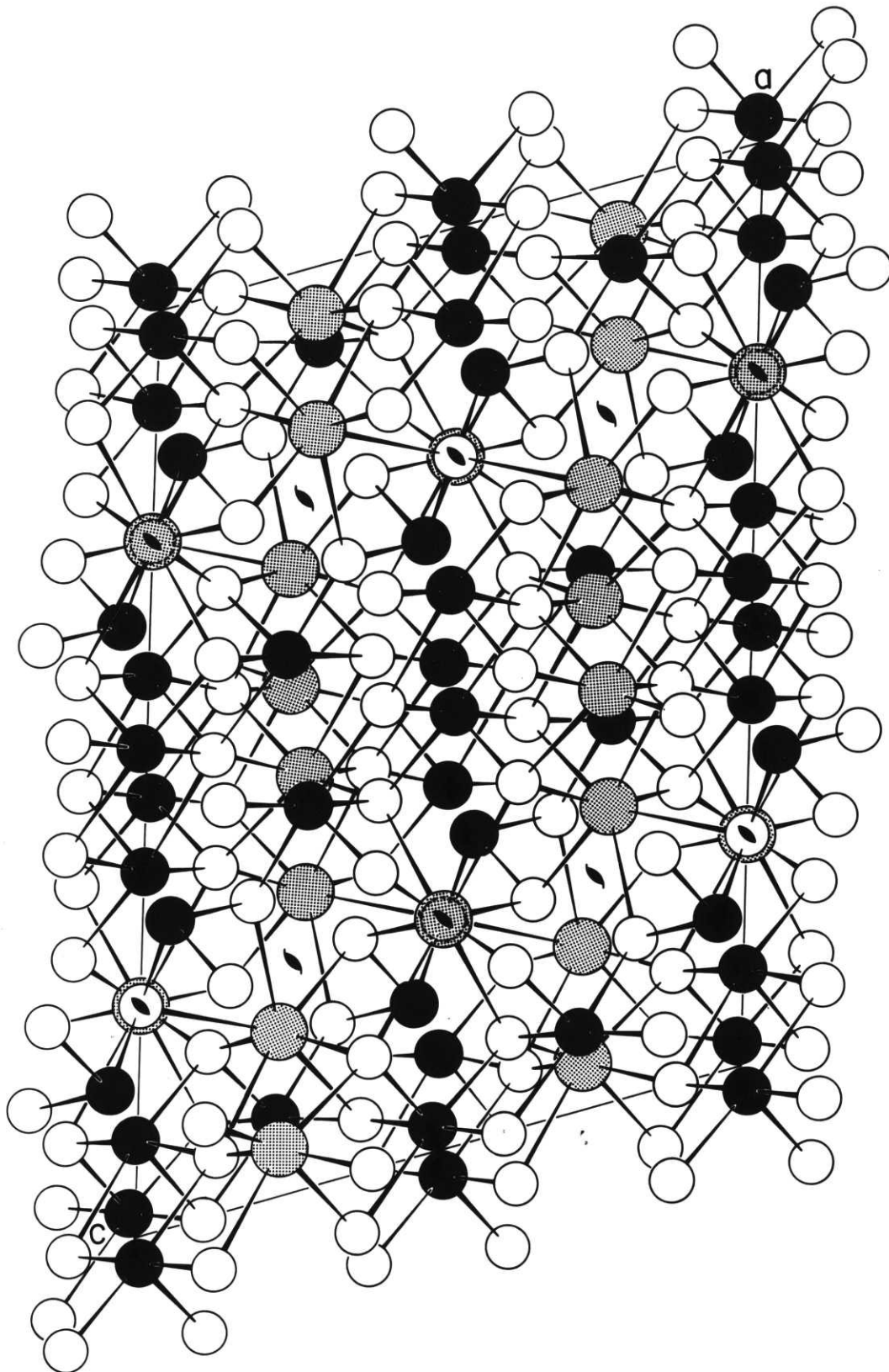
Before comparing the lead polyhedra, it is necessary to decide which two lead atoms have been added to plagionite to form semseyite. Close scrutiny of the (010) projections of semseyite and plagionite (Figure 6 and Figure 9) revealed that Pb(1), Pb(2),



(112) Projection Plagionite

FIGURE 8

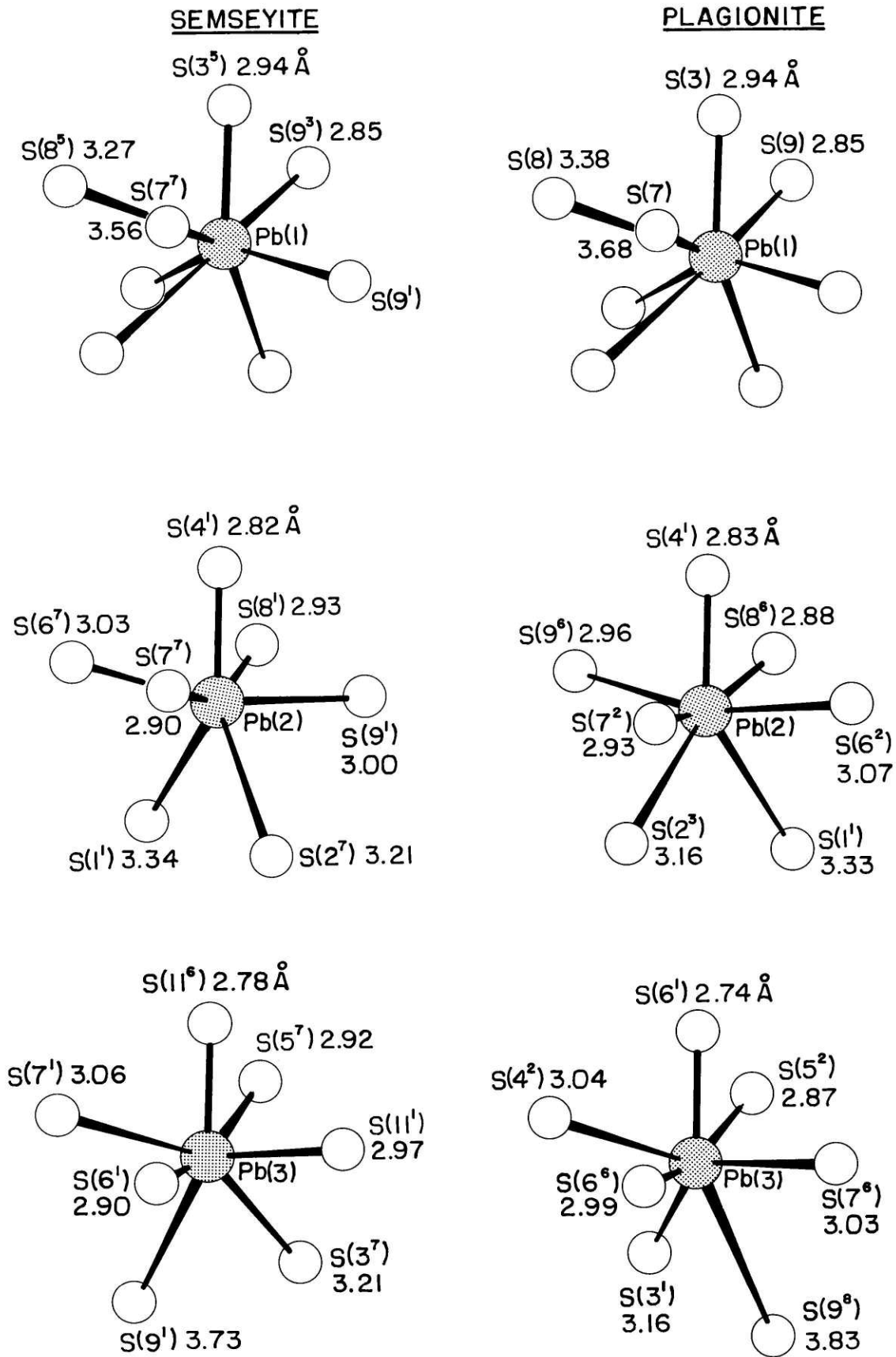
(010) Projection Plagioclase



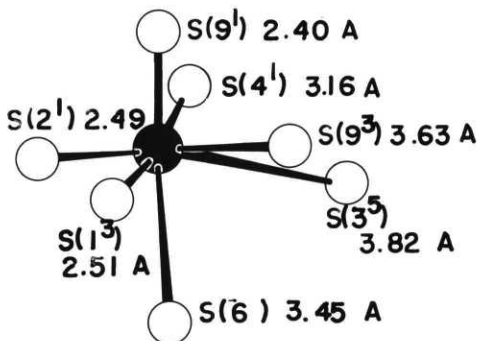
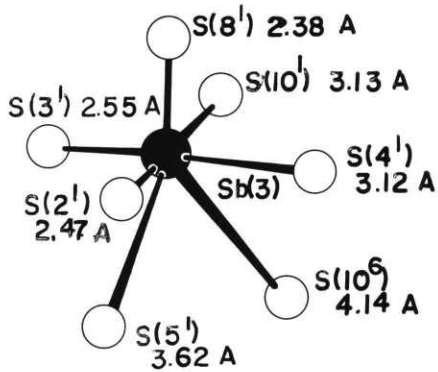
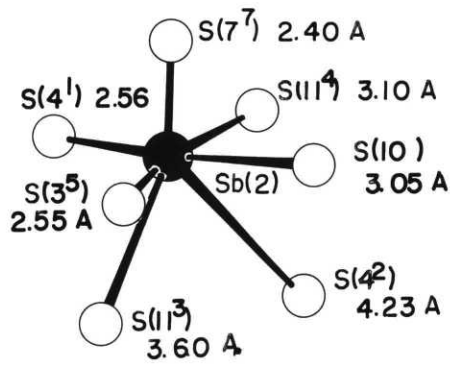
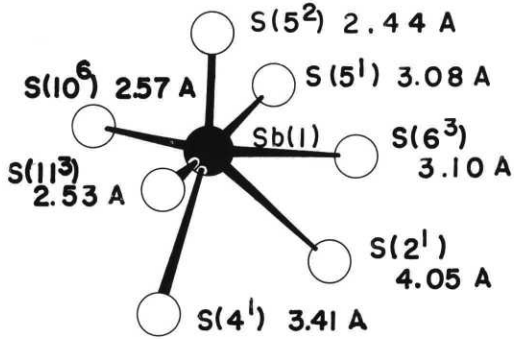
and Pb(3) were virtually identical. However, Pb(4) and S(10) and Pb(5) and S(11) have no counterparts in plagionite. The variations in bond distances are, as a rule, within the error of the measurements for the lead polyhedra occurring in both structures. However, Pb(1) in semseyite, the lead atom in equipoint 4e, is more closely coordinated by its fifth and sixth and seventh and eighth neighbors by nearly 0.1 \AA than Pb(1) in plagionite. A visual comparison of the antimony polyhedra and three lead polyhedra of both semseyite and plagionite is presented in Figure 10.

Comparing the (112) slabs of both plagionite and semseyite, one finds that plagionite has nearly flat levels of the slabs. The maximum variation is only 0.6 \AA . In semseyite, however, the levels of the slab approximate hills and valleys with a difference within one line of the level being as much as 2.0 \AA . The thickness of the two slabs is very similar as it represents Sb-S and Pb-S apical bonding.

It is most interesting to consider how plagionite can be "made" from semseyite. The clearest way to see this is to study the (010) projections. Consider Figure 11, the (010) projection of semseyite. The halftone region represents the portion of the structure that is similar to plagionite. The white area represents the 'new' region. If the 's-shaped' region is removed, and the bonds broken along the dashed lines, the two portions will collapse together removing the void. This is plagionite. The direction of the collapse is not exactly [001] but rather the direction of



SEMSEYITE



PLAGIONITE

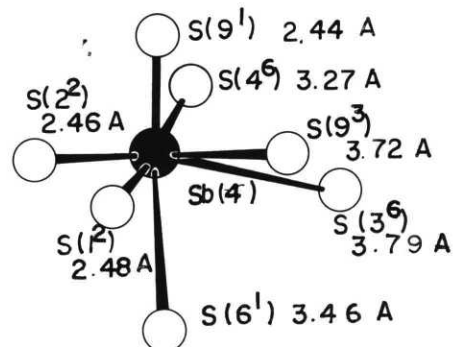
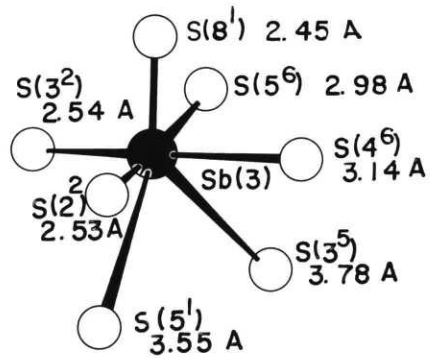
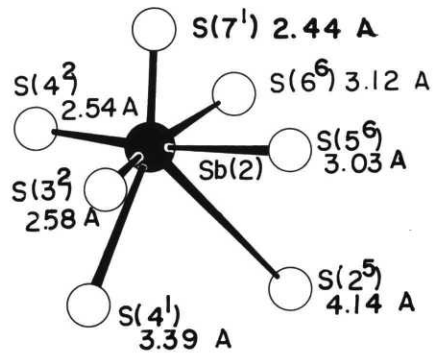
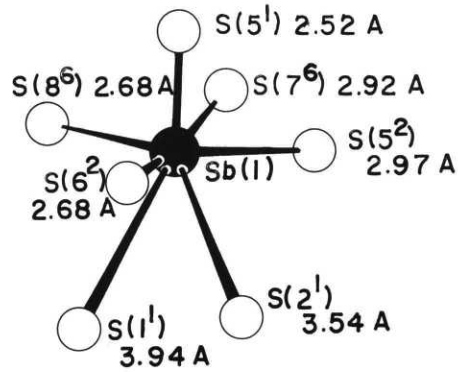
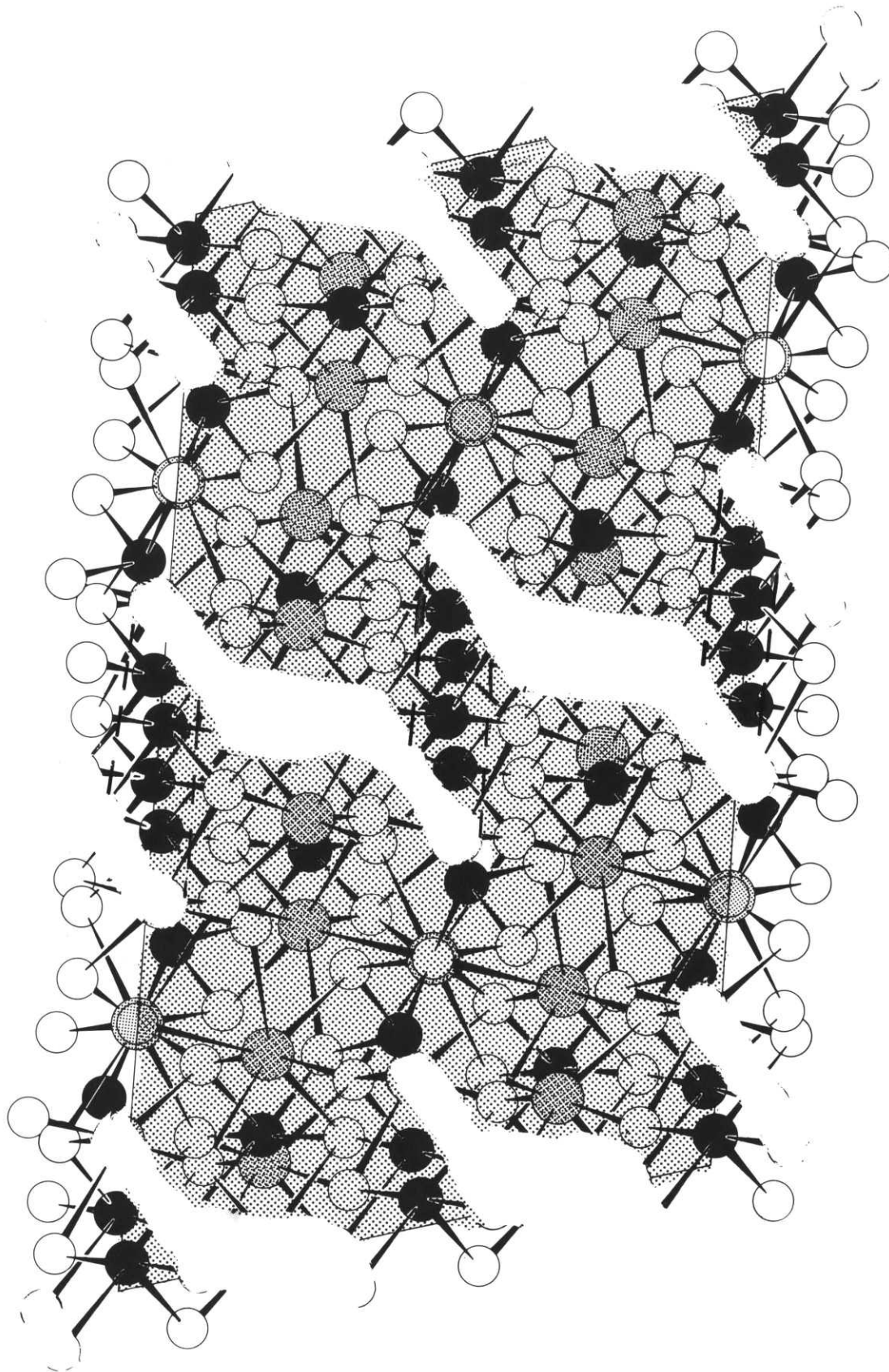


FIGURE 11
"Making" Plagionite from Semseyite



$c \sin \beta$. Thus as Jambor (1969) predicted $c \sin \beta$ rather than c shows a linear increase as one goes from plagiomite to semseyite.

Chapter VIII

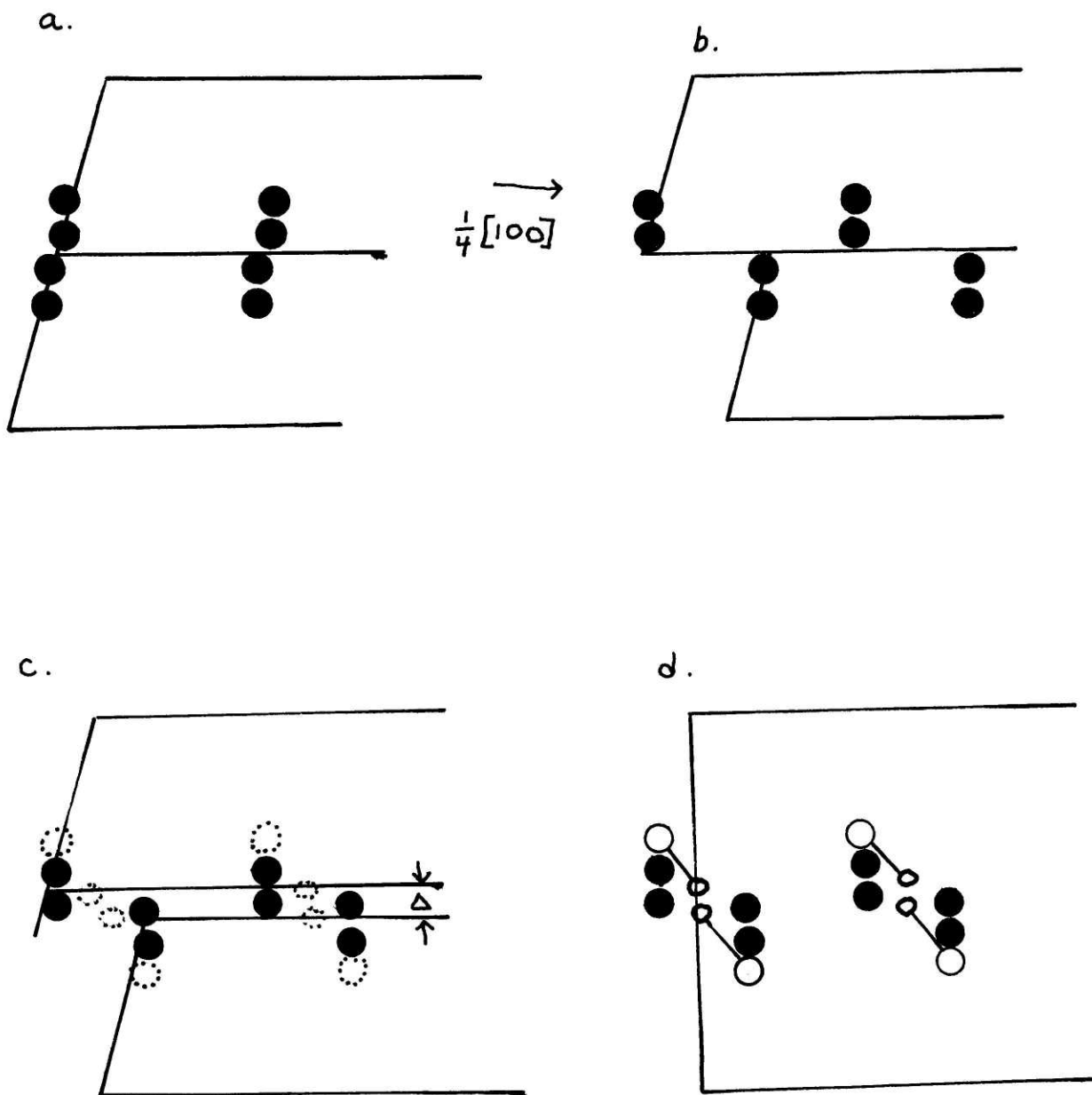
The Homologous Series $Pb_{3+2n}Sb_8S_{15+2n}$

It is believed that the plagionite group - fülöppite, plagionite, heteromorphite, and semseyite - forms an homologous series. The series is represented by the general equation - $Pb_{3+2n}Sb_8S_{15+2n}$ - as proposed by Peacock and Nuffield (1945) and Jambor (1969). From the results of the previous chapter, this formulization may be rewritten as $(2n+1)PbS \cdot 4Sb_2S_3$. Alternatively this is better understood when written



where the portion enclosed in brackets is invariant throughout the series. Jambor has shown (Figure 1 and Table 2) that the density of the minerals increases linearly with n as does $c \sin \beta$. Table 17 presents the density figures and $\Delta(c \sin \beta)$ for the series. Thus in constructing the series we must look for a method that provides a density increase as well as the 2.3 \AA° increase in $c \sin \beta$.

From the previous chapter we saw that plagionite could be 'made' from semseyite by removal of a s-shaped region in a compound type operation. Breaking this operation down into its two components, we find that we can remove Pb(4) and S(10) to get a thin sausage shaped region or remove Pb(5) and S(11) to obtain a fatter and shorter sausage. The first process is shown schematically in Figure 12. For addition - first you must cut the structure at $z=.50$ parallel to $[100]$. Then separate the

FIGURE 12
Addition Process 1

halves an Sb-Sb separation in the direction of $c \sin \beta$ (i.e. perpendicular to [100]). Then move the top half $0.25[100]$ relative to the bottom half. Thus you have created a void into which you can put a Pb and S. Note that you have disturbed only the interior region - not the area of the Pb(1), the lead on the 2-fold position, and Sb(4), the trigonal Sb. If you connect the regions of undisturbed area, you find you have a nearly orthogonal cell characteristic of fülöppite and heteromorphite.

Similarly if you now take this structure as your starting point, you can begin addition process 2 which is shown schematically in Figure 13. Keeping the two Sb atoms together and repeating the cutting, separating, and sliding processes of Process 1, we arrive at an elliptical-type void into each two PbS can go. If the edges of the undisturbed region are connected $\beta \sim 106^\circ$ which is typical of plagionite and semseyite.

Now if you calculate a typical Sb-Sb separation along c in the a - c plane, you find that you must separate the two halves approximately 1.15 \AA (data from the Sb(1) - Sb(2) separation in semseyite). This separation occurs twice in the length of c - so the increase in $c \sin \beta$ is about 2.3 \AA . This is exactly what Jambor found. (Table 17)

The next item which requires explanation is the density increase. It would appear that since we are increasing c that addition of another atom or atoms would not produce a significant density change. However, one must remember that we have moved as Sb-Sb separation and therefore left what might be called

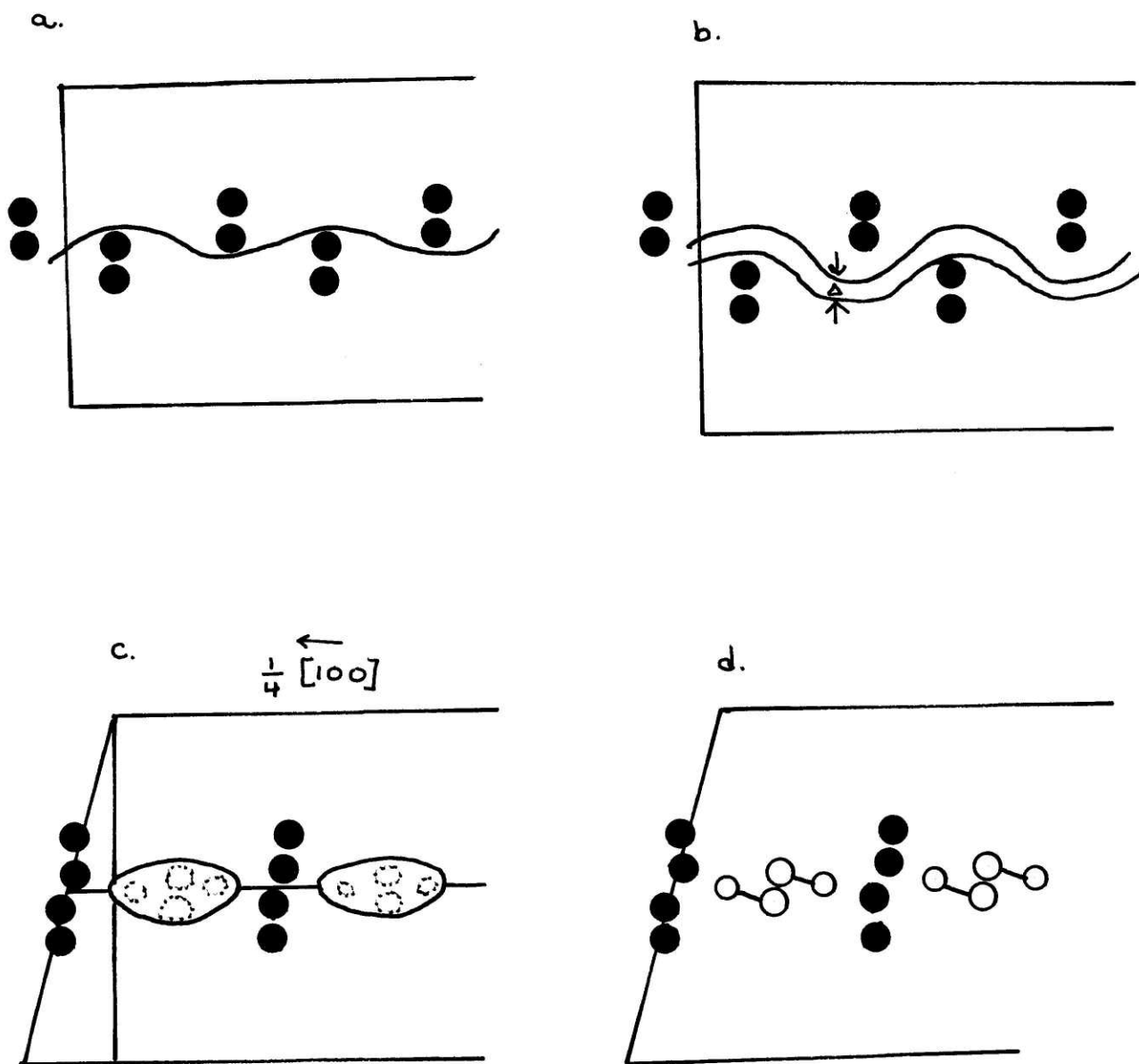
FIGURE 13
Addition Process 2

TABLE 17

Densities of the Plagionite Group and Changes of $c \sin \beta$

	ρ_{meas}	ρ_{calc}	$c \sin \beta$
fulloppite	5.21	5.22	
			2.3 A°
plagionite	5.58	5.54	
			2.3
hetero- morphite	5.86	5.73	
			2.3
semseyite	6.03	6.12	

a Sb hole. Into this vacant area we have put a lead. Therefore into an area (or better volume) expecting a Sb we have placed a Pb. Thus the progressive density increase arises.

Finally we must be concerned with how a Pb atom can occupy a site previously occupied by Sb. In Figure 4 the polyhedra for Sb were shown. If these are compared with those for Pb (Figure 3) one can see the great similarity of the seven-coordinated atoms. Thus while Sb only uses five neighboring S atoms as bonding partners two other S atoms are in the near neighborhood to complete a coordination polyhedra similar to that of seven coordinate Pb. It is well to note that seven-coordinated bismuth in gladiolite undergoes similar substitution by Pb in that lead-bismuth sulfosalt. (Kohatsu, I 1971)

Now that there is a predicted means of addition of PbS, it is well to attempt to construct, at least in projection, the members of the plagioclase group. The subtraction process is easier to show graphically so we shall first attempt to form heteromorphite from semseyite. Studying the unit cell constants we see this involves moving from a cell with $\beta \sim 106^\circ$ to $\beta \sim 90^\circ$. Therefore the subtraction process must be accomplished by the reverse of the second addition process (Figure 13). Pb(5) and S(11) are the atoms which are removed. The initial portion of the transformation is shown in Figure 14. The predicted structure of heteromorphite is shown in (010) projection in Figure 15.

Next plagioclase can be formed from heteromorphite by the reverse of the first addition process. Pb(4) and S(10) are removed

FIGURE 14
"Making" Heteromorphite from Semseyite

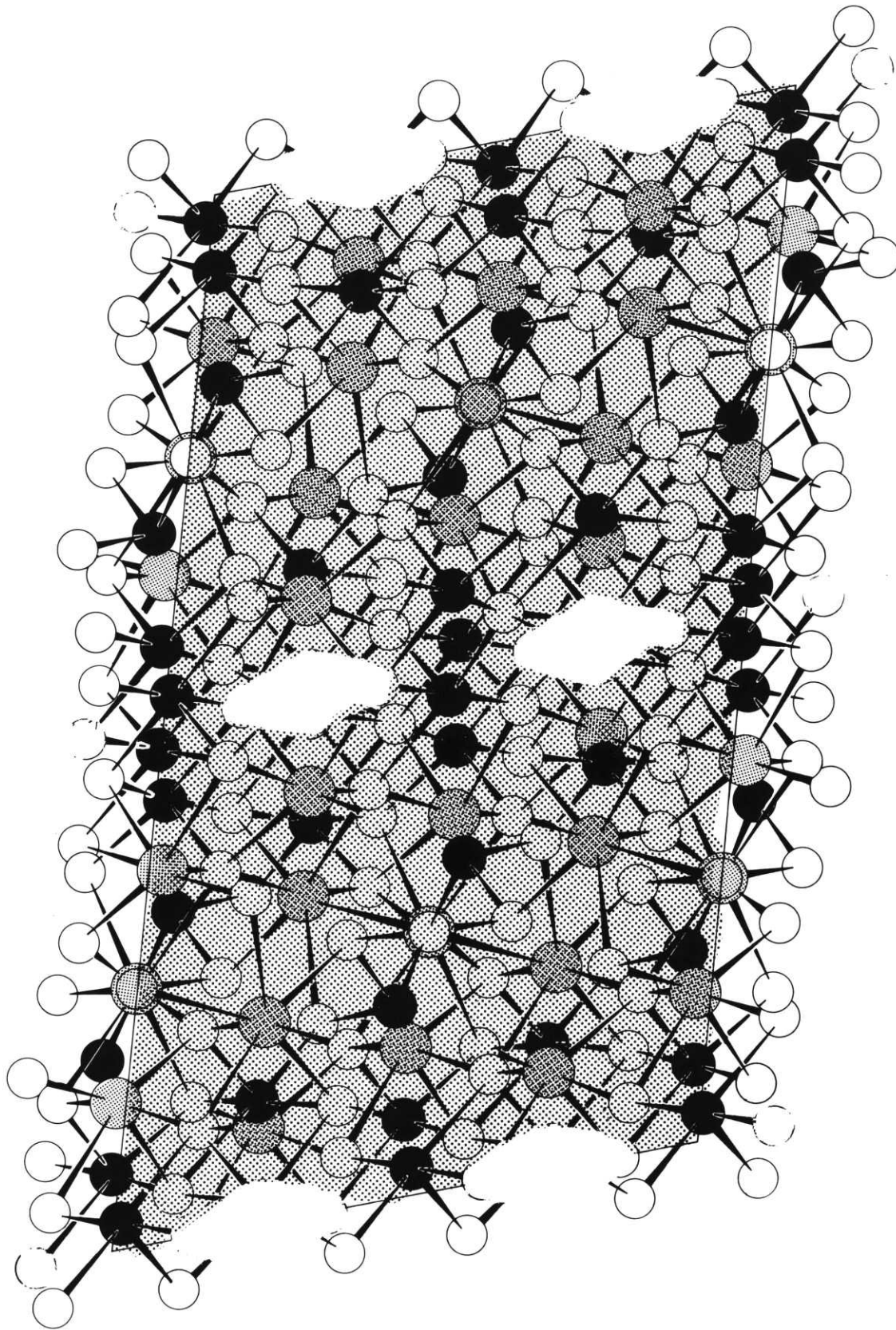
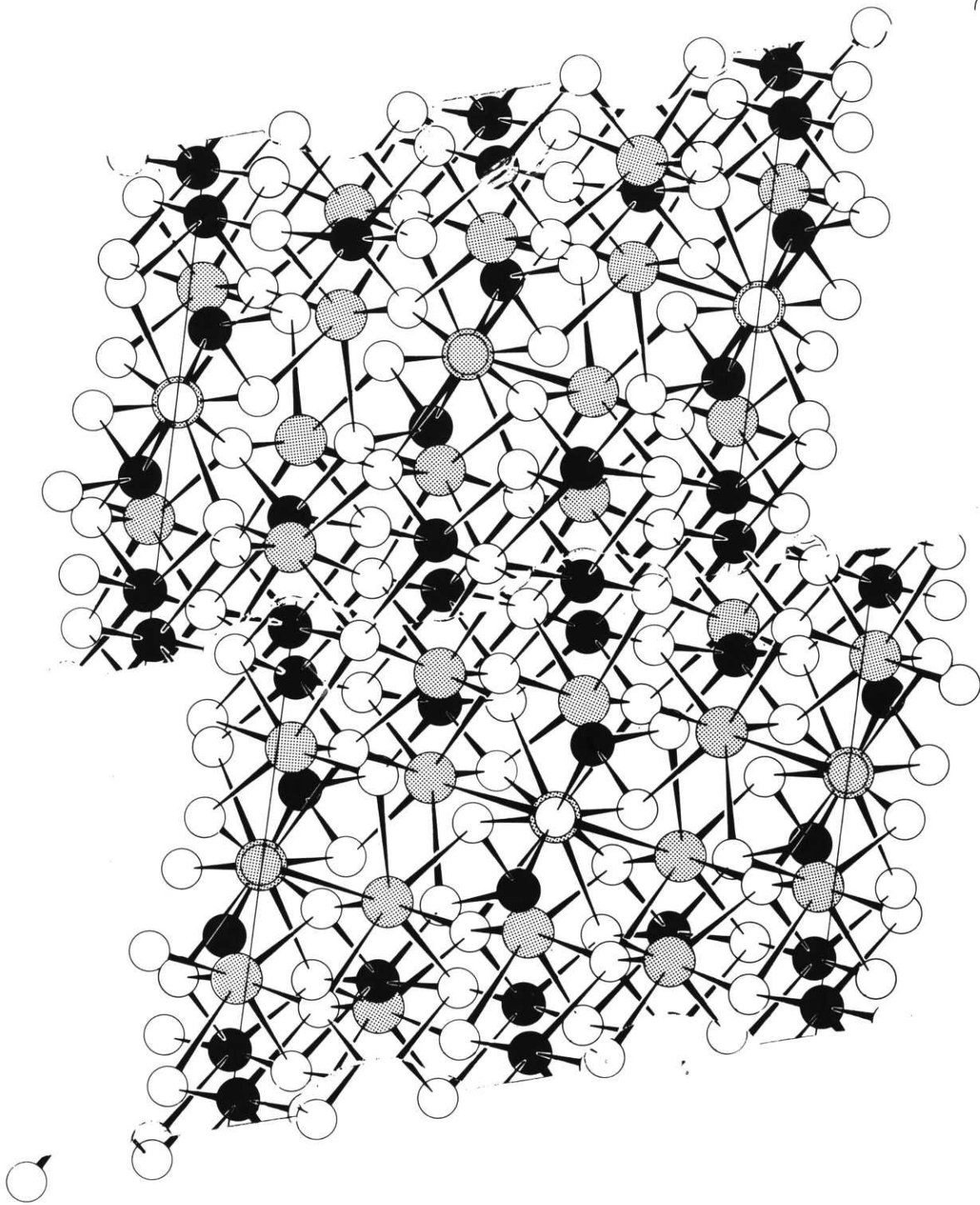


FIGURE 15
Predicted (010) Projection-Heteromorphite



this time. The initial step of the process is shown in Figure 16. The (010) projection of plagionite was presented in Figure 9.

Finally fülöppite can be made from plagionite. This requires the removal of Pb(3) and S(5) and the reverse of the second addition process. The dissection of plagionite is shown in Figure 17 and the predicted structure in projection of fülöppite is shown in Figure 18.

Looking back at the four structures, fuloppite, plagionite, heteromorphite, and semseyite, we find that although the space group has remained the same, the position of the lines of lead, antimony and sulfur atoms has shifted relative to the inversion centers. In the 90° compounds, fuloppite and heteromorphite, the sulfur lines (or chains) pass through the inversion centers at $x=0, .25, .5, .75$. The two lead and antimony 'chains' are now quite similar and occur at $x=.125, .375, .625, .875$. In the 106° compounds, semseyite and plagionite, the lead and the antimony 'chains' pass through the inversion centers. Now, however, there are two distinct types of 'chains' - the predominately antimony chains at $x=0, .5$ and the lead ones at $x=.25, .75$. The sulfur line now occupies the intermediate positions.

The structures as viewed on (112) appear relatively similar. They are sketched schematically in Figure 19. Essentially a PbS is removed from the interior region and the slab is collapsed to fill the void along the [110] of the PbS-like cell.

The next question that arises is can more Pb-S be added to continue the group from semseyite to form para-heteromorphite and para-semseyite. Adding PbS to semseyite requires the first type

FIGURE 16
"Making" Plagionite from Heteromorphite

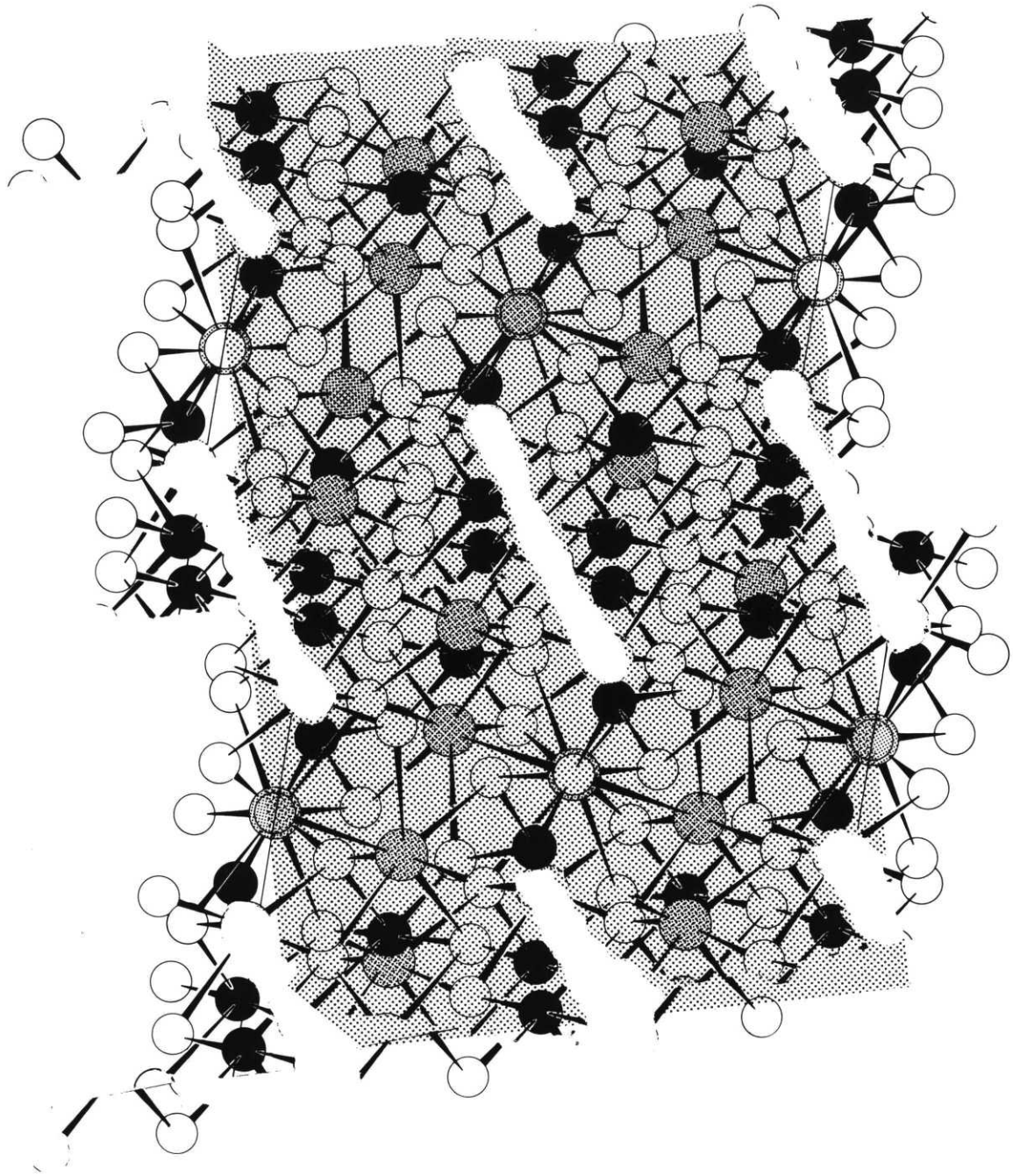


FIGURE 17
"Making" Fulloppite from Plagionite

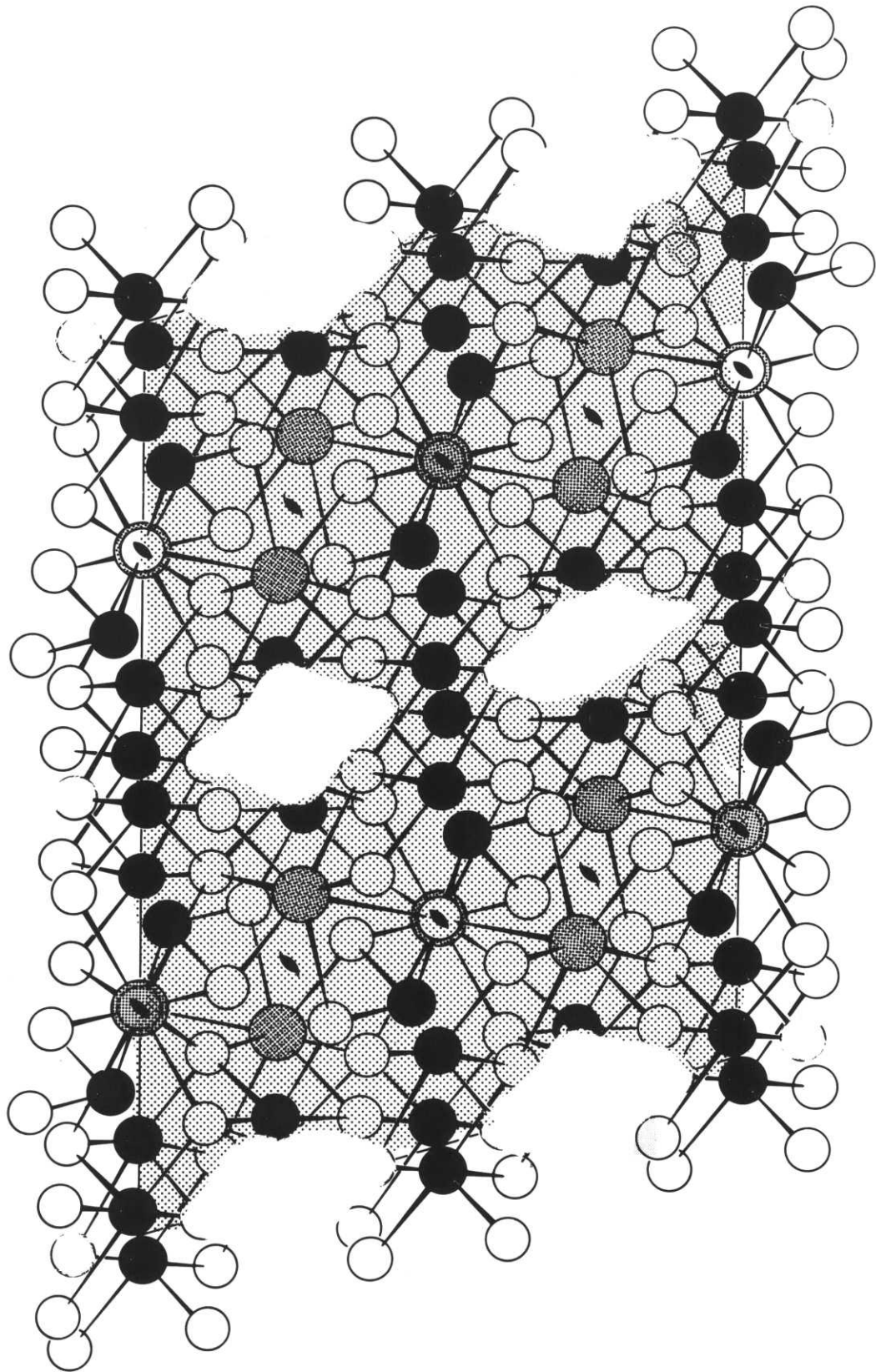


FIGURE 18
Predicted (010) Projection-Fuloppite

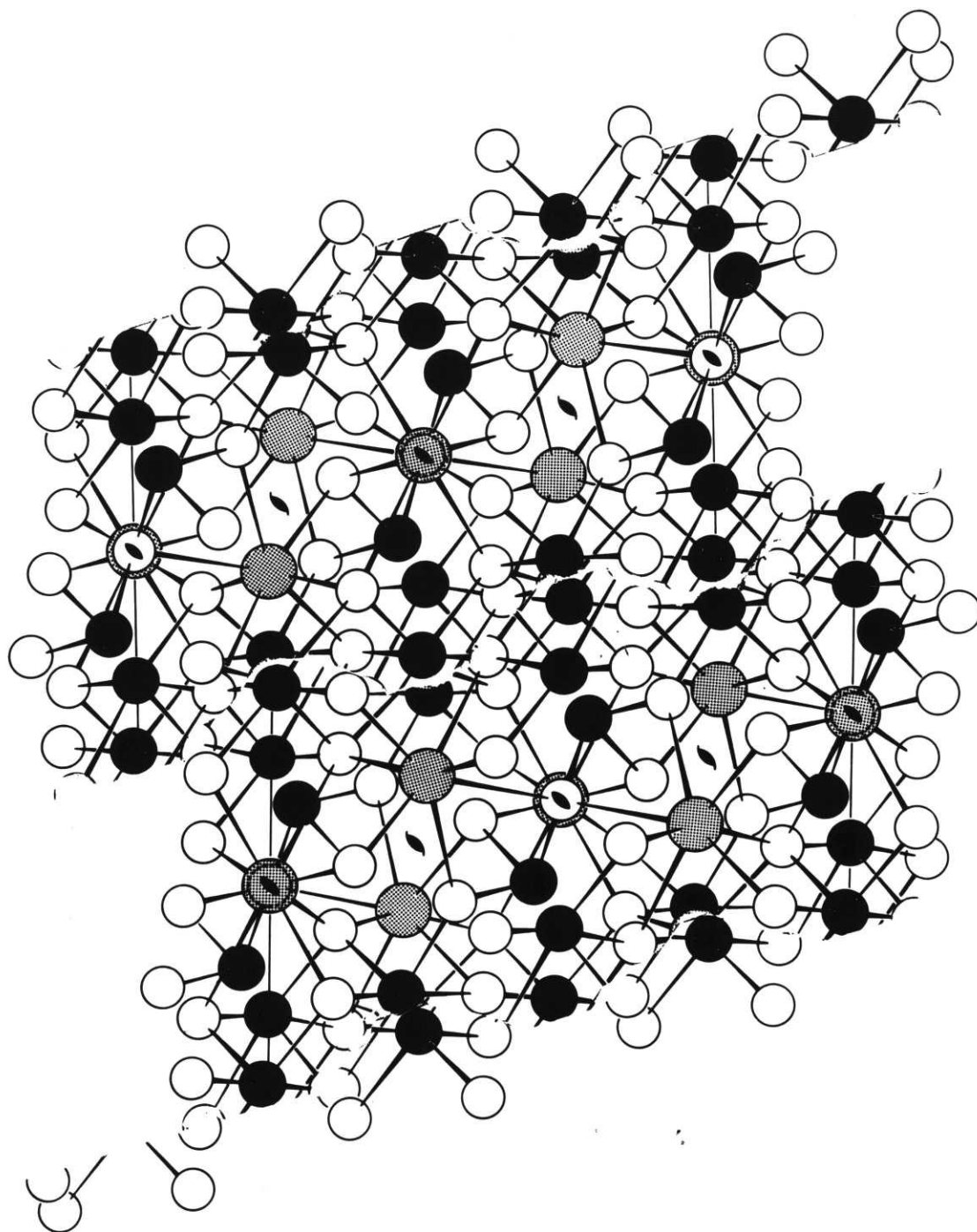
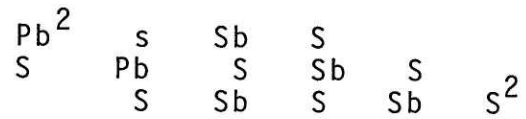


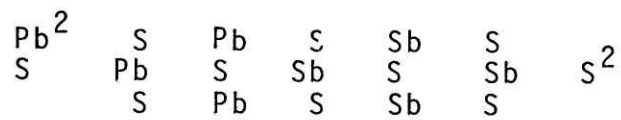
FIGURE 19

Schematic (112) Projections for the Plagionite Group

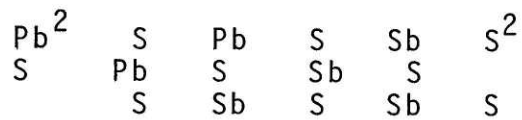
Fuloppite



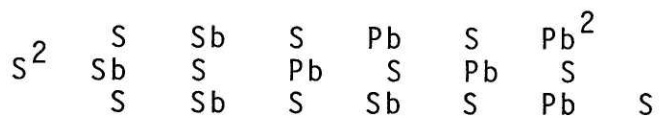
Heteromorphite



Plagionite



Semseyite



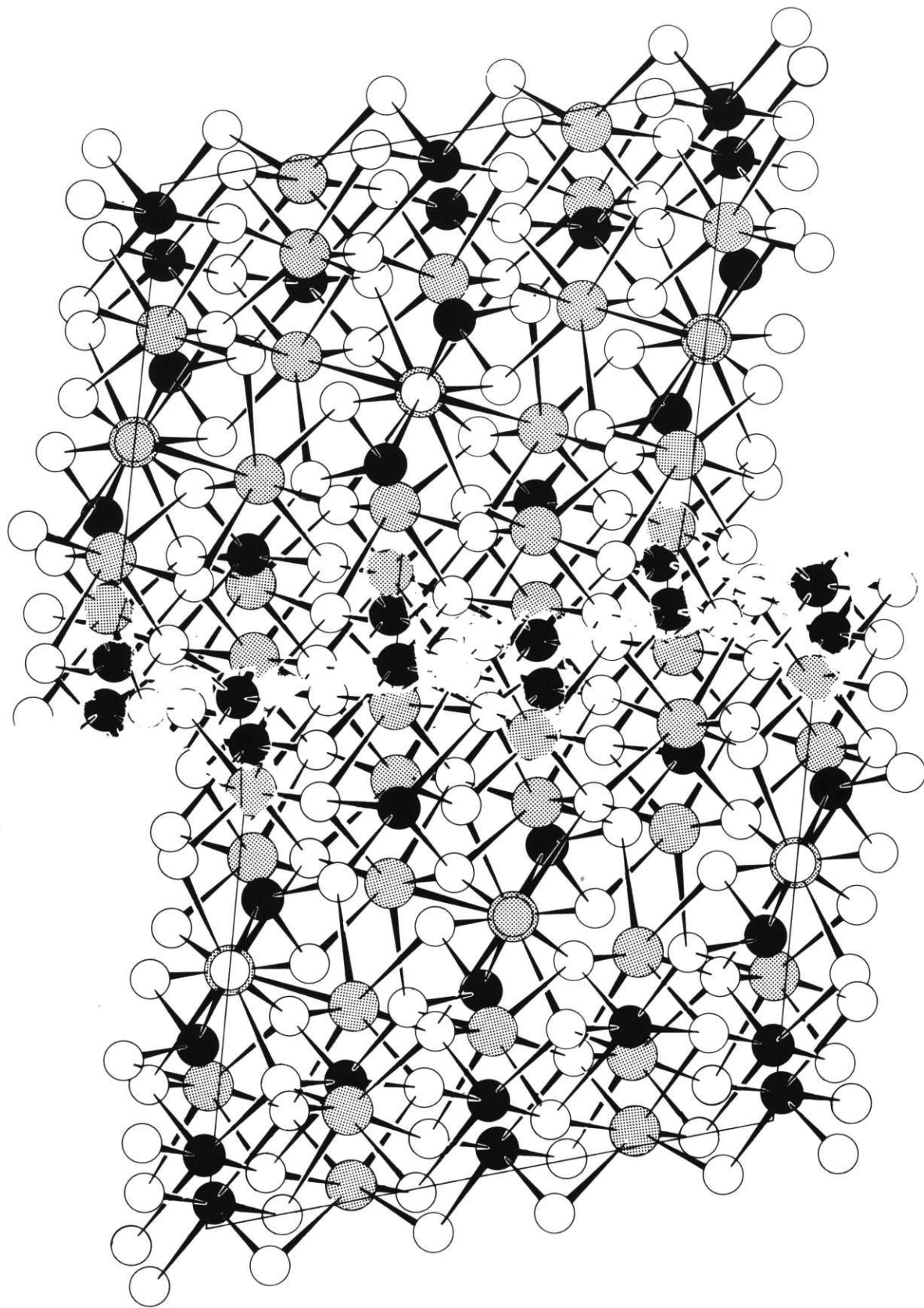
Superscript 2 denotes atom located in 2-fold position

addition process (Figure 11). This should yield a cell with $\beta \sim 90^\circ$, $c \sin \beta \sim 25.8 \text{ \AA}$, $a = a_s, b = b_s$. This process is shown in Figure 20. It would also appear that an additional PbS could be added, the second addition process, to form para-semseyite. There seems to be no reason why this process can not be repeated again and again, leaving the Pb(1) and Sb(4) region undisturbed with alternating type 1 and type 2 additions. Although these additional compounds are not known to be naturally occurring, their appearance may be hindered only by kinetics in nature and they perhaps may be synthetically prepared.

Thus the plagionite group is indeed a homologous series. It might be better expressed as $2n\text{PbS}[\text{PbSb}_8\text{S}_{13}]$ with $n=1$ fülöppite, $n=2$ plagionite, $n=3$ heteromorphite, $n=4$ semseyite... The space group $C 2/c$ characterizes the series and a and b remain relatively invariant as $c \sin \beta$ increases with n . The odd-numbered compounds ($n=1,3,5,\dots$) have the fülöppite structure with $\beta \sim 90^\circ$. The even-numbered ones ($n=2,4,6,\dots$) have the plagionite configuration with $\beta \sim 107^\circ$.

The basis of the homology is the addition of PbS to the interior, not the edge, of the rock-salt like slab. The region at the edges of the slab remains invariant throughout the series. There are two types of addition - 1) the fülöppite-plagionite addition, and 2) the plagionite-heteromorphite addition. The linear increase of $c \sin \beta$, β , and the increase in density as n increases are all predicted by these models.

FIGURE 20
"Making" Para-Heteromorphite from Semseyite



Appendix A

Film Methods versus Counter Techniques

In the course of this work two methods were used to acquire two data sets, both of which were subsequently used for structure determination and refinement. The first method involved recording the reflection intensities on film and then scanning the film with a photodensitometer. The second method utilized an automated four-circle diffractometer with monochromated radiation.

With the film technique, all the data from one hkl level was recorded simultaneously. A pack of three films was used for each level so that the intensity of both the strongest and weakest reflections might be recorded within the linear region of the film's recording range. The stability of the x-ray intensity within one level was not a problem as it would be if the data were recorded sequentially. The whole process to record eight levels took nearly seven weeks - a time comparable with that required to collect the data with a manual diffractometer. It must be confessed that the film method required far less effort on the experimenter's part than a manual diffractometer method would have. In addition the problem of the counter stability was eliminated and that of generator stability minimized.

On the other hand the collection of an equivalent data set with a computer-controlled automated four-circle diffractometer was even more efficient. To collect some 2200 intensities only

four days were required. The problems of generator and counter stability although present were reduced by the rapid collection process. The main drawback of such a process is that - while every laboratory has the equipment to record film data - many laboratories do not possess such expensive instrumentation as the automated four-circle diffractometer.

The advantages of the diffractometer data become immediately evident when data reduction begins. With the second method one is presented for each $hk\ell$ reflection a peak intensity, background counts on either side of the peak, a background counting time and a peak counting time. This data may be easily manipulated to provide an integrated intensity plus a standard deviation well documented by counting statistics. With film methods, the experimenter is faced with a stack of films whose photodensity he must evaluate. There are basically three approaches:

- a) the strong, medium, weak visual estimations,
- b) manual scanning and strip chart recording of densities,
- or c) scanning with an autophotodensitometer and receiving a digitized density. The first alternative is not consistent in accuracy with that of the rest of the structure determination procedure. The second is painstaking and tedious but possible; although stability questions arise about the light source. The last of the three is, at least theoretically, the most accurate and efficient. Even with this alternative the experimenter is left with a digitized record of his film which still must be indexed and then integrated. Various techniques can be employed to

interpret the film. If the locations of two points on the film are known, the digital record may be indexed and with suitable computer programs a "window" around each hkl reflection may be examined, the peak integrated and a background correction made. This method requires great faith in (1) the exact orientation of the film relative to the scanner (i.e. the film's horizontal axis must exactly correspond with the scanner's horizontal travel) and (2) the ability of the computer program to separate peak from background and not to include an adjacent peak in the computation. Instead of trusting the computer program to be so discriminating one could just request that each hkl window be 'dumped', allowing him to integrate manually each reflection. Still the computer has indexed the film so that the orientation must still be exact. This is an especially critical assumption if reflections are closely spaced - as will happen with cell dimensions as small as 20 \AA . The last resort is to reconstruct the film by merely 'dumping' the complete digitized record of the film just as it was recorded. Then the output can be graphically indexed much as a regular film would be. This alternative presents two problems. Indexing can be a non-trivial matter with moderately large or large lattice constants when Weissenberg films are used. Secondly the amount of output generated is gigantic. For the top half of a Weissenberg film with $\text{Cu K}\alpha$ radiation, the reconstructed 'film' will be nearly five feet high and eighteen feet long - all covered with numbers. The reflections, once indexed, can be manually integrated.

Thus it can be easily seen that the diffractometer yields intensities more rapidly, with less tedium and for far less cost than film methods can. To process 2000 reflections to get integrated intensities would cost a mere \$10 - \$20 (at the MIT computation center) for diffractometer data but nearly \$1000 for film data. The time involved for diffractometer data is that needed to punch the computer cards while film data requires a minimum of several exhaustive days per level (depending on the number of reflections). The accuracy of the diffractometer is well determined by counting statistics but that of film data has yet to be determined on any mathematical basis. As final proof of the 'goodness' of the diffractometer data, the final R values of the film data and the diffractometer data are submitted: $R_{\text{film}} = 18.9\%$ (plus misplaced and missing sulfurs) while $R_{\text{diff.}} = 10.0\%$ - a correct structure.

In complete fairness this test of the film technique was particularly severe. With a small weakly-diffracting crystal and utilization of the Weissenberg camera without monochromated radiation, all the disadvantages of the film methods are amplified. If the precession camera could have been used, data reduction would have been somewhat simplified. Thus until improved methods of evaluation of the photodensity are found - the diffractometer method (with good electronics) must be said to be superior to the film method and the equipment employed in this study when used in these sulfosalt structure determinations.

Appendix B

The Concept of the Direct Method

One of the basic problems of the crystallographer is determining the phase factor of the structure factor. The structure factor, F_{hkl} , is

$$F_{hkl} = \sum_{j=1}^N f_j e^{2\pi i(hx_j + ky_j + lz_j)} \quad (1)$$

where there are N atoms in the unit cell with scattering factors f_j and atomic coordinates $x_j y_j z_j$. Only the intensity (proportional to $|F|^2$) can be measured. While the Patterson method extracts interatomic distance information from $|F|^2$, the direct methods are a means of getting information about phases from $|F|$'s.

Harker and Kasper (1948) initially found several relationships among the structure factors. One can apply the Cauchy Inequality:

$$\left| \sum_{i=1}^N a_i b_i \right|^2 < \left(\sum_{i=1}^N |a_i|^2 \right) \left(\sum_{i=1}^N |b_i|^2 \right)$$

to the structure factor relationship (1) yielding:

$$|F_{hkl}|^2 < \sum_{j=1}^N (\sqrt{f_j})^2 \sum_{j=1}^N (\sqrt{f_j} e^{2\pi i(hx_j + ky_j + lz_j)})^2.$$

This is more simply:

$$|F_{hkl}|^2 < \left(\sum_{j=1}^N f_j \right)^2 = F_{000}^2 .$$

Defining the unitary structure factor as

$$U_{hk\ell} = F_{hk\ell} / \sum_{j=1}^N f_j \quad (2)$$

one then obtains the fundamental inequality relationship

$$|U_{hk\ell}|^2 < 1. \quad (3)$$

All this work presupposes only symmetry 1. Now if an inversion center is considered at the origin,

$$F_{hk\ell}^2 < F_{000} [0.5 F_{000} + 0.5 F_{2h-2k-2\ell}] .$$

Recalling that $F_{000} = \sum_i f_i$ and using the unitary structure factor yields:

$$U_{hk\ell}^2 < 0.5(1 \pm |U_{2h2k2\ell}|) . \quad (4)$$

If the magnitude of $U_{hk\ell}$ and $U_{2h2k2\ell}$ are sufficiently large, then the sign of $U_{2h2k2\ell}$ must be positive. A study of some examples presented in Table 1 reveals the importance of relationship (4). With the consideration of additional symmetry, more relationships similar to (3) and (4) can provide further clues to the phase factors.

As is apparent in Table 1 only in a small number of cases is it possible to predict with certainty the sign of $U_{hk\ell}$. However Sayre (1952) lead the development of a means of probabilistically determining the phase factor. He showed that

$$F_{hk\ell} = \phi_{hk\ell} \sum_{h'} \sum_{k'} \sum_{\ell'} F_{h'k'\ell'} F_{h-h'k-k'\ell-\ell'} \quad (5)$$

with $\phi_{hk\ell}$ being a scaling term. The implication is that the sign of $F_{hk\ell}$ can be calculated from a set of other known structure factors. Practically, however, it is simply impossible

TABLE 1

Phase Determination By An Inequality

U_{hkl}^2	$ U_{2h,2k,2l} $	Phase +	Phase -	Comment
0.60	0.20	0.60	0.40	$u(2h,2k,2)$ must be +
0.50	0.10	0.55	0.45	Must be +
0.40	0.10	0.55	0.45	Could be either
0.40	0.30	0.65	0.35	Must be +
0.25	0.50	0.75	0.25	Almost certainly +
0.25	0.30	0.65	0.35	Could be either

(after Stout & Jensen, 1968)

to know a large enough number of $F_{h-h'k-k'\ell-\ell'}$ signs to obtain the sign of $F_{hk\ell}$. Sayre also demonstrated that when the magnitude of $F_{hk\ell}$ is large and the structure centrosymmetric, the series tended strongly in one direction (i.e. + or -). This direction he proposed is determined by

$$\mathcal{S}(F_{hk\ell}) \sim \mathcal{S}(F_{h'k'\ell'}) \cdot \mathcal{S}(F_{h-h'k-k'\ell-\ell'}) \quad (6)$$

where \mathcal{S} means sign of. Hauptmann and Karle (1953) proposed for centrosymmetric space groups, the phase relations were better given as

$$\mathcal{S}(F_{hk\ell}) \sim \Sigma \mathcal{S}(F_{h'k'\ell'}) \cdot \mathcal{S}(F_{h-h'k-k'\ell-\ell'}) \quad (7)$$

which resembles the basic relation (5). They also showed that the probability that equation (7) was true is given as

$$P_{\pm}(E_{hk\ell}) = 0.5 + 0.5 \tanh\left[\frac{\sigma_3}{\sigma_2^{3/2}} |E_{hk\ell}| \Sigma_{h'k'\ell'} E_{h'k'\ell'} E_{h-h'k-k'\ell-\ell'}\right] \quad (8)$$

where $\sigma_n = \frac{\sum_{j=1}^n n_j^n}{\sum_{j=1}^n n_j}$ and $n_i = f_i / \sum_{j=1}^N f_j$ and $E_{hk\ell}^2 = U_{hk\ell}^2 / \bar{U}^2$.

\bar{U}^2 , the average of all unitary structure factors including systematically absent reflections (if any) is expressed by

$$\bar{U}^2 = \frac{\sum_{i=1}^N n_i^2}{\sum_{i=1}^N n_i} .$$

It should be remembered that F's, U's, and E's all have the same sign or phase although they possess different magnitudes. For the U's and E's each atom is assumed to be a point in the structure factor calculation. Applying these relationships yields

$$E_{hkl}^2 = |F_{hkl}|^2 / \epsilon \sum f_i^2$$

where ϵ is an integer which equalizes the importance of E_{hkl} 's and is dependent on the space group. For general reflections ϵ is 1 but in classes where systematic extinctions occur it is greater than unity.

In practice crystallographers use these relations probabilistically in a process called Symbolic Addition (SAP). The essence of the procedure is to assign literal (A,B,C,) signs to several reflections with E_{hkl} 's greater than some large value (like 2.0). Then further signs can be assigned by relation (7) with probability of being correct calculated by equation (8). The choice of starting hkl reflections can not be arbitrary. The following criteria must be applied:

- 1) the magnitude of E must be large,
- 2) the reflections must have many interactions with the rest of the data set - e.g. if all even hkl 's are chosen then only reflections with hkl even will be signed. Contradictions may occur after several cycles of symbolic addition, e.g. E_{451} may be assigned + in an earlier cycle but later be signed - . Therefore conditions must be established for the acceptance of the sign. These usually involve:

- 1) the minimum acceptance probability for sign correctness,
- 2) the minimum number of affirmative contributions to each individual sign,
- 3) the maximum number of inconsistencies acceptable, and

4) the minimum ratio of contributors to inconsistencies. At the conclusion of the iterations the contrast ratios are calculated for all sign combinations in which positive or negative signs are assigned to the literal (ABC) ones. The sign combination with the smallest index is selected for the assignment of E_{hkl} .

In current practice the program FAME (Dewar and Stone) takes an arbitrarily scaled data set and converts it to normalized structure factors. This is done by making a Wilson plot to determine a scale factor and overall temperature factor. Subsequently it calculates the statistical distribution of E_{hkl} 's and makes a comparison with theoretical values for both centric and acentric models. Lastly the whole list of E_{hkl} 's is examined to determine a specific number of E_{hkl} 's to initialize Symbolic Addition. These reflections are selected on the basis of the conditions discussed previously.

MAGIC, a program also written by Dewar and Stone, performs SAP for centric space groups. The E_{hkl} 's selected by FAME initialize MAGIC with arbitrary literal signs and through iterative cycles the signs of the remaining E_{hkl} 's are determined using symbols and signs previously determined. All the contradictions are summed as

$$\sum 1/((1 + \text{PARAM} - P)(\text{ITER.NO.}))$$

where PARAM is a damping factor usually of the order of 10^{-6} , P is the probability of the sign to be true, and ITER.NO. is

the number of the iterative cycle where the contradiction occurs. Therefore, sign contradictions with high probability occurring in earlier cycles have greater weight than later ones.

When it is determined that more cycles will not generate appreciable numbers of new signs, SAP is discontinued. An initial structure can be determined with the aid of an E-map (an electron density synthesis with E's not F's). The remaining unsigned reflections can now be signed with the knowledge of the atomic positions.

Appendix C

The Program - INTEN

The following is a listing of the computer program INTEN written for the IBM 370 in Fortran 4. This program enables the digitized densities of the Weissenberg film to be converted into intensities.

```

C      MAIN PROGRAM
      REAL*4 TITLE(20),WAVE(2)
      INTEGER*2 IXC(2),IYC(2)
      INTEGER*2 IH(3,1600),IXX1(1600),IXX2(1600),IYY1(1600),IYY2(1600)
      COMMON/BLKA/XLIM,YLIM,RS,LREC,NREC,IXC,IYC
      COMMON/BLKB/ UR,CR,XR,YR,C1,C2, ISET,KOUNT,IDX,IDY
      COMMON/BLKC/A,B,C,AL,BE,GA,WAVE,EQUI
      COMMON/BLKD/OMS,OML,J,UPS,OM,HH,HK,HL,ICLK,STH,L,CEQS
      COMMON/BLKE/IDT,IST1,ITEMP
      COMMON/BLKX/TK2,TL2,OMD
      COMMON/BLKL/IH,IXX1,IXX2,IYY1,IYY2
      READ (5,899) NFILM
899   FORMAT (I2)
      NLOOP=0
      1   READ (5,901) TITLE
901   FORMAT (20A4)
      WRITE (6,900) TITLE
900   FORMAT (1H,20A4)
      READ(5,905) IDT,IST1,ITEMP,IDX,IDY,ISHORT,XLIM,YLIM,RS
905   FORMAT(6I3,3F5.0)
      LREC = XLIM/RS
      NREC = YLIM/RS
      WRITE (6,990) XLIM,YLIM,RS,LREC,NREC
990   FORMAT(1H0,'DENSITOMETER CONSTANTS'/10X,'XLIM = ',F7.2,' MM.'/
1   10X,'YLIM = ',F7.2,' MM.'/10X,'RASTER SIZE = ',F5.2,' MM.'/10X,
2   2 'LENGTH OF RECORD = ',I5,/10X,'NUMBER OF RECORDS = ', I5)
30   READ (5,920) A,B,C,AL,BE,GA,WAVE(1),WAVE(2),EQUI
      WRITE (6,940) A,AL,B,BE,C,GA
      WRITE (6,945) WAVE(1),WAVE(2),EQUI
      IDX2 = IDX * 2
      IDY2 = IDY * 2
      WRITE (6,946) IDX2,IDY2
      IF (ISHORT) 35,40,35
35   LREC = (LREC/2) - 4
      READ (5,995) IXC(1),IYC(1),IXC(2),IYC(2)
      GO TO 50

```

```

40  CALL REFLOC(IERR)
    GO TO 897
    IF(IERR) 898,50,898
50  CALL CAMCON
    IKL=4
    CALL SET(IKL)
    WRITE(6,1020)KOUNT
    WRITE(6,950)
    CALL SORT
897  CONTINUE
    CALL INTEN
    REWIND IST1
898  NLOOP = NLOOP + 1
    IF(NLOOP - NFILM) 1,1000,1000
1000 REWIND IDT
945  FORMAT(' WAVELENGTH OF RADIATION USED'/10X,'ALPHA(1) = ',F8.6,
1 2X,'ANGSTROMS'/10X,'ALPHA(2) = ',F8.6,2X,'ANGSTROMS'/'EQUINCLINA
2TICN ANGLE = ',F10.6,2X,'DEGREES')
1020 FORMAT(' KOUNT = ',I6)
995  FORMAT(4I5)
920  FORMAT(9F8.6)
940  FORMAT(' RECIPROCAL CELL DIMENSIONS'/10X,'A* = ',F10.6,2X,
1 'ALPHA* = ',F10.6/10X,'B* = ',F10.6,3X,'BETA* = ',F10.6/10X,
2 'C* = ',F10.6,2X,'GAMMA* = ',F10.6/)
950  FORMAT(' END OF PART ONE')
946  FORMAT(' SIZE OF LARGEST REFLECTION ON FILM',/10X,'X = ',I6,/,
1 10X,'Y = ',I6)
    STOP
    END
C    SUBROUTINE INTEN
C    THIS IS THE PART THAT READS THE DENSITY DATA AND ORGANIZES IT.
C    SUBROUTINE INTEN
C    INTEN SUBROUTINE
    INTEGER*2 LDEN(776,50),RECNUM,IXC(2),IYC(2)
    INTEGER*2 IY1,IY2,IUF
    INTEGER*2 IH,IK,IL,IX1,IX2,NY1,NY2
    REAL*8 OD(194,60)
    COMMON/BLKB/ UR,OR,XR,YR,C1,C2,ISET,KOUNT,IDX,IDY
    COMMON/BLKA/XLIM,YLIM,RS,LREC,NREC,IXC,IYC
    COMMON/BLKE/IDT,IST1,ITEMP
    COMMON/LIST/IH,IK,IL,IX1,IX2,NY1,NY2,IY1,IY2,IUF
    COMMON/BLKY/LDEN
    EQUIVALENCE(OD(1,1),LDEN(1,1))
C    THE VALUE OF IEND1 IS DETERMINED BU THE LDEN(1550,IEND1) DIMENSION
    IEND1=50
    ID=0
    IC = 0
    I1=0
    I2=0
    I3=0
3    LR2=LREC/2
    MT = LR2 * 2
    IF(LREC-MT) 102,103,102
102  LR2= LR2 + 1

```

```

103   LREC = LR2
      NR2= NREC/2
      MT= NR2*2
      IF(NREC-MT) 321,3201,321
321   NREC = MT + 1
      GO TO 3202
3201   NREC= MT
3202   CCONTINUE
      DO 5 I=1,IEND1
5     READ(ITEMP)(OD(J,I),J=1,194)
      IYBEG = C
      LERR= 0
      DO 130 NINT=1,22
      ICHK = 0
      READ (IST1) IH,IK,IL,IX1,NY1,IX2,NY2
323   FORMAT(3I3,2X,4I4)
C     TEST IF REFLECTION TOO CLOSE TO EDGE
C     TEXT X DIRECTION
      IF(IX1-IDX) 120,120,10
10    IF((LREC-IX2)-IDX) 120,120,20
20    IY1 = NY1-IYBEG
      IY2=NY2-IYBEG
22    IF(IY1-8) 120,120,30
30    IF(IEND1-(IY2 + 12)) 40,60,60
40    IF(LERR) 120,50,120
C     UPDATE LDEN MATRIX
50    INC = IY1-10
      ISTOP = IEND1 - INC
C     DOES NEXT REFLECTION APPEAR AT A GREATER DISTANCE THAN IDEN1
      IF (ISTOP) 502,502,504
502   DO 503 J=1,IEND1
503   READ(ITEMP,END=320) (OD(I,J),I=1,194)
      IYBEG = IYBEG + IEND1
      IY1= IY1 -IEND1
      IY2= IY2-IEND1
      GO TO 22
C     ELIMINATE USED PORTION OF LDEN MATRIX
504   DO 305 I =1,ISTOP
      II = I + INC
      DO 305 J = 1,LREC
305   LDEN(J,I)=LDEN(J,II)
C     READ IN NEW VALUES TO REPRACE THOSE DISCARDED
      DO 310 J=1,INC
      JJ = ISTOP + J
310   READ(ITEMP,END=320)(OD(I,JJ),I=1,194)
      GO TO 55
320   IEND2=J-1
      LERR= -1
55    IYBEG = IYBEG + INC
      IY1=IY1-INC
      IY2=IY2-INC
60    INTSUM =0
      IERR=C
      CALL DISPLA

```

```

120 CONTINUE
130 CONTINUE
RETURN
END
C SUBROUTINE REFLOC
SUBROUTINE REFLOC(IERR)
C REFLOC SUBROUTINE
INTEGER *2 RECNUM
LOGICAL*1 OA(1552),OB(3104)
REAL*8OP(194),LIST(194)
INTEGER*2LDEN(1552),LCDEN(776),IY(50),IX(50),IXC(2),IYC(2)
INTEGER*4 IXMAX(50),IXMIN(50)
EQUIVALENCE(OA(1),OP(1))
COMMON/BLKA/XLIM,YLIM,RS,LREC,NREC,IXC,IYC
COMMON/BLKE/IDT,IST1,ITEMP
EQUIVALENCE(LDEN(1),OB(1))
EQUIVALENCE(LCDEN(1),LIST(1))
IERR = 0
DO 10 J=1,1552
10 LDEN(J)=0
NREC = 0
MM=C
M=0
LREC = LREC-4
LR=LREC/8
LR8= LR*8
DO 19 I=1,776
19 LCDEN(I)=0
NRC = 0
20 READ (IDT,920,END=70) RECNUM,(OP(J),J=1,LR)
NREC=NREC+1
DO 30 J=1,LR8
JJ=J+J
30 OB(JJ)= CA(J)
DO 50 I=1,LR8
IF(LDEN(I)) 50,40,50
40 M = M + 1
IX(M)= I
50 CONTINUE
NRC=NRC + 1
IKK = 1
DO 501 KK = 1,LR8,2
LCP=LDEN(KK) + LDEN(KK+1)
LCDEN(IKK)= LCP + LCDEN(IKK)
IKK = IKK + 1
501 CONTINUE
IF(NRC-2) 503,502,504
503 GO TO 5031
504 WRITE(6,5041)
5041 FORMAT(' CALLING EXITE ERROR IN COMPACTION PROCESS')
CALL EXIT
502 WRITE (ITEMP) LIST
NRC = 0
DO 5021 JK=1,IKK

```



```

5021 LCDEN(JK)=0
5031 CONTINUE
      IF(M) 60,20,60
60    MM=MM+1
      IXMAX(MM)= IX(M)
      IXMIN(MM)=IX(1)
      IY(MM) = NREC
      M=0
      GO TO 20
70    WRITE (6,970)      NREC
210   CONTINUE
      END FILE ITEMP
      REWIND ITEMP
      GO TO 999
      WRITE (6,930)
      DO 220 JJ=1,MM
220   WRITE(6,940)IY(JJ), IXMIN(JJ), IXMAX(JJ)
      KK=0
      L=0
230   MIN=5000
      MAX=0
      KY=0
240   L = L + 1
      IF (IY(L)-(IY(L+1)-1)) 270,250,270
250   MAX = MAX0(IXMAX(L),MAX)
      MIN = MIN0(IXMIN(L),MIN)
      KY = KY + 1
      IF (L+1-MM) 240,260,260
260   L = L + 1
270   BMAX= AMAX0(IXMAX(L),MAX)
      BMIN=AMINO(IXMIN(L),MIN)
      KY=KY+1
      KK = KK +1
      IF(BMAX-BMIN) 290,280,290
280   IXC(KK)=BMAX
      GO TO 300
290   IXC(KK) = BMIN + ((BMAX-BMIN) + 0.5)/2.0
300   MID = L-(KY-2)
      IYC(KK)= IY(MID)
      IF(L-MM) 230,310,310
310   IF(KK-2) 320,330,320
320   WRITE (6,950)'KK
      IERR = 1
      GO TO 1000
330   WRITE (6,960)
      WRITE(6,965)(IXC(J),IYC(J),J=1,KK)
999   CONTINUE
      LREC = LR8
      GO TO 1000
1000  RETURN
920   FCRMAT(A2,2X,200A8)
940   FORMAT(1X,I6,3X,I6,3X,I6)
930   FORMAT(' RECNUM',5X,'XMIN',5X,'XMAX')
950   FORMAT(' CALLING EXIT',I6,2X,'CENTERS FOUND')
960   FORMAT('CENTERS OF REFERENCE REFLECTIONS AT',/10X,'X',10X,'Y')

```

```

965  FORMAT(2(5X,I6))
970  FORMAT(' END OF FILE ON IDT, NREC CHANGED TO ',I6)
    END
C    SUBROUTINE CAMCON  CALCULATES CAMERA CONSTATNS
C    CAMCON SUBROUTINE
    SUBROUTINE CAMCON
    REAL*4 RIX(2),RIY(2),O(2),U(2),X(2),Y(2)
    INTEGER*2 IXC(2),IYC(2),IUPS(2)
    COMMON/BLKA/XLIM,YLIM,RS,LREC,NREC,IXC,IYC
    COMMON/BLKB/ UR,OR,XR,YR,C1,C2,ISET,KOUNT,IDX,IDY
    COMMON/BLKE/IDT,IST1,ITEMP
    C1C=2.0
    C2C = 2.0
    IKL=1
    CALL SET(IKL)
    READ(5,900) IUPS(1),IUPS(2)
    WRITE (6,899)
    DO 10 I=1,2
    RIX(I)=IXC(I)
10   RIY(I)=IYC(I)
    IF(IXC(1)-IXC(2)) 30,20,20
20   X(1)=RIX(1)*RS
    X(2)=RIX(2)*RS
    Y(1)=RIY(1)*RS
    Y(2)= RIY(2)*RS
    GO TO 40
30   X(1)=RIX(2)*RS
    X(2)=RIX(1)*RS
    Y(1)=RIY(2)*RS
    Y(2)=RIY(1)*RS
40   DO 110 J=1,2
    IF(ISET-2) 50,60,70
50   READ(IST1) HH,HK,HL,UPS,OMEGU,OMEGL
    GO TO 80
60   READ(IST1) HL,HH,HK,UPS,OMEGU,OMEGL
    GO TO 80
70   READ(IST1) HK,HL,HH,UPS,OMEGU,OMEGL
80   IF (IUPS(J)) 90,90,100
90   O(J)=OMEGU
    U(J)=UPS
    GO TO 110
100  O(J)=OMEGL
    U(J)= -UPS
110  WRITE(6,905) HH,HK,HL,U(J),O(J),X(J),Y(J)
    DX=X(1)-X(2)
    DY=Y(1)-Y(2)
    DU = U(1)-U(2)
    IF (DY) 200,290,210
200  IF (O(1)-O(2)) 220,290,230
220  DO = O(1)-O(2)
    GO TO 300
230  DO=(360.-O(1))+O(2)
    GO TO 300
210  IF(O(1)-O(2)) 250,290,220

```

```

250  DO = (360. -O(2)) + O(1)
      GO TO 300
290  WRITE(6,930)
      CALL EXIT
300  C1=ABS(DU/DX)
      C2=ABS(DG/DY)
      GO TO 301
      IF(C1-(C1C+ 0.1*C1C)) 401,402,402
401  IF(C1-(C1C-0.1*C1C)) 402,402,403
403  IF(C2-(C2C+0.1*C2C))           404,402,402
404  IF(C2-(C2C-0.1*C2C)) 402,402,301
402  WRITE(6,999)
999  FORMAT('REFERENCE REFLECTION IMPROPERLY INDEXED START AGAIN')
      WRITE(6,9991) C1,C2
9991 FORMAT (2F8.5)
      CALL EXIT
301  WRITE(6,910) C1,C2
      UR=U(1)
      OR=O(1)
      XR=X(1)
      YR=Y(1)
      WRITE (6,920) UR,OR,XR,YR
      REWIND IST1
899  FORMAT(' REFLECTIONS USED IN CALCULATING CAMERA CONSTANTS'/13X,'H'
',3X,'K',3X,'L',5X,'UPSILON',7X,'OMEGA',5X,'X',10X,'|')
900  FORMAT(2I1)
905  FORMAT(10X,3F4.0/4(2X,F10.5))
910  FORMAT(' CAMERA CONSTANTS'/10X,'C1 = ',F10.5,2X,'DEGREES/MM.'/
1 10X,'C2 = ',F10.5,2X,'DEGREES/MM.')
```

```

920  FORMAT(' POSITION OF REFERENCE REFLECTION',10X,'UPSILON = ',F10.5,
12X,'DEGREES'/10X,'OMEGA = ',F10.5,2X,'DEGREES'/10X,'X = ',
2F10.5,2X,'MM.'/10X,'Y = ',F10.5,2X,'MM.')
```

```

930  FORMAT(' OY(2) EQUAL TO Y(1), NO SOLUTION FOR C2***CALLING EXIT')
      RETURN
      END
C  SUBROUTINE SET /SETS UP HLKS IN PROPER ORDER TO BE READ
C  SUBROUTINE SET(IKL)
C  SET SUBROUTINE
      INTEGER*2 IXC(2),IYC(2)
      REAL*4 WAVE(2),WSQ(2),AXIS(3),UPS(2),OMEGU(2)
      COMMON/BLKA/XLIM,YLIM,RS,LREC,NREC,IXC,IYC
      COMMON/BLKB/ UR,OR,XR,YR,C1,C2,ISET,KCUNT,IDX,IDY
      COMMON/BLKC/A,B,C,AL,BE,GA,WAVE,EQUI
      COMMON/BLKD/OMS,OML,J,UPS,OM,HH,HK,HL,ICLK,STH,L,CEQS
      COMMON/BLKE/IDT,IST1,ITEMP
      COMMON/BLKX/TK2,TL2,OMD
      DATA AXIS/'C ','B ','A '/
      KCUNT = C
      JMP=1
      IF (IKL-4) 40,10,40
C  CALCULATE STARTING AND ENDING VALUES OF OMEGA
10  OMS= OR-(YR*C2)
      IF (OMS) 20,30,30
20  OMS = OMS + 360.0
30  OML=OMS + YLIM*C2
```

```

32   IF(CML-360.0) 36,36,34
34   OML = OML-360.0
      GO TO 32
36   WRITE (6,2010) CMS, OML
      OMD=Y LIM*C2
      GO TO 500
40   IF (IKL-2) 60,50,60
50   IKL=1
      GO TO 250
60   READ(5,1000) STHN,ISET,MH2,MK2,ML2
1000  FCRMAT(F10.5,4I3)
      WRITE(6,1020) AXIS(ISET), STHN
      PI=3.14159
      PIH= PI/2.0
      RAD = PI/180.0
      WSQ(1)= WAVE(1)*WAVE(1)
      WSQ(2)=WAVE(2)*WAVE(2)
      EQUI = EQUI * RAD
      SEC= SIN(EQUI)
      CEQ = COS(EQUI)
      LEQS=CEQ*CEQ
      IF (ISET-2) 201,202,203
C     CRYSTAL MOUNTED CN C AXIS
201  AP = A
      BP=B
      CP=C
      ALP = AL * RAD
      BEP = BE * RAD
      GAP = GA*RAD
      GO TO 204
C     CRYSTAL MOUNTED ALONG B AXIS
202  AP = C
      BP = A
      CP = B
      ALP = GA * RAD
      BEP = AL * RAD
      GAP = BE * RAD
      GO TO 204
C     CRYSTAL MOUNTED CN A AXIS
203  AP = B
      BP = C
      CP = A
      ALP = BE * RAD
      BEP = GA * RAD
      GAP = AL * RAD
204  A = AP
      B = BP
      C = CP
      AL = ALP
      BE = BEP
      GA = GAP
      CAL = COS(AL)
      CBE= COS(BE)
      CGA = COS(GA)
      CCA = SIN(CA)

```

```

SGA = SIN(GA)
ABG= 2.0*A*B*CGA
BCA = 2.0*B*C*CAL
CAB = 2.0*C*A*CBE
AA = A*A
BB = B*B
CC= C*C
BCG= B*CGA
CCB = C*CBE
BSG= B*SGA
DC = C*(CAL-CBE*CGA)/SGA
R = CEQ
ZETA = 2.0*SEQ
ZETA2=ZETA*ZETA
IEOF = 0
250   IF(IKL-1) 300,300,500
C     READ HKL FROM CARDS
300   READ(5,301) MH,MK,ML,IEOF
301   FORMAT(4I3)
      IF (IEOF) 904,800,904
C     GENERATE HKLS FROM EXTINCTION RULES - NOT USED
C     INSTEAD GENERATE FROM CARDS
500   GO TO 300
C     COMPUTE DIFFRACTION SETTINGS
800   IF (ISET-2) 801,802,803
801   TH=MH
      TK = MK
      TL = ML
      GO TO 804
802   TH = ML
      TK = MH
      TL = MK
      GO TO 804
803   TH = MK
      TK = ML
      TL = MH
804   TLC= TL*TL*CC
      QA= TH*TH*AA + TK*TK*BB + TLC
      QB = TH*TK*ABG
      QC = TK*TL*BCA
      QD = TH*TL*CAB
C     HKL
      Q= QA+QB+QC+QD
      STH=(WAVE(1))/2.0*SQRT(Q)
      IF (STH-STHN) 810,990,990
810   HL = TL
850   HH = TH
860   HK = TK
870   XIX = HH*A + HK*BCG + TL*CCB
      XIY = HK*BSG + HL*CC
      IF (XIX) 890,880,890
880   IF(XIY) 884,882,884
882   PHI =PIH
      GO TO 920
884   PHI=PIH -(XIY/ABS(XIY))*PIH

```

```

GO TO 920
890   IF (XIY) 894,892,894
892   PSI = 0.0
      GO TO 91C
894   XY = ABS(XIY/XIX)
      PSI = ATAN(XY)
      IF (XIY) 900,910,91C
900   PSI = -PSI
910   PHI=PI-((XIX/ABS(XIX)))*(PIH+PSI)
920   PHI = PHI/RAD
      IF (IKL-1) 924,922,924
922   CALL RTEST(PHI,HH,HK,HL,Q,WSQ(1),ZETA2,R,PI)
      GO TO 250
924   ICHK = 0
      DO 930 J=1,2
      L = J
      XI2= WSQ(J)*Q-ZETA2
      IF (XI2) 9240,9240,9241
9240  WRITE(6,1030) MH,MK,ML,I,XI2
1030  FORMAT(' THE VALUE OF XI**2 FOR REFLECTION', 3I4,' SIGN GROUP',
1I4,' IS',F10.8/' THIS REFLECTION WILL BE IGNORED')
      GO TO 990
9241  XI=SQRT(XI2)
      XXI=XI/(2.0*R)
      IF(XXI-1.0) 9242,99C,990
9242  U = 2.0*ARSIN(XXI)
      UPS(J) = U/RAD
      OMEGU(J) = PHI+UPS(J)/2.0
      IF (ICLK) 940,926,940
926  OM=OMEGU(J)
      CALL TEST
930  CONTINUE
940  ICHK = 0
      DO 980 J = 1,2
      L = 3-J
      OMEGL = OMEGU(L) + 180.0 - UPS(L)
      UPS(L) = -UPS(L)
950  IF(CMEGL-360.0) 970,960,960
960  OMEGL = OMEGL - 360.0
      GO TO 950
970  OM = OMEGL ,
      CALL TEST
      IF (ICLK) 990,980,990
980  CONTINUE
990  CONTINUE
      GO TO 250
904  END FILE IST1
      REWIND IST1
2010  FORMAT(' OMEGA START = ',F15.8/' OMEGA LIMIT = ',F15.8)
1020  FORMAT(' CRYSTAL MOUNTED ON',A2,' AXIS'/' UPPER LIMIT OF SIN(THETA
1) = ',F15.8)
      RETURN
      END
C      SUBROUTINE RTEST

```

```

SUBROUTINE RTEST(PHI,HH,HK,HL,Q,WSQ,ZETA2,R,PI)
COMMON/BLKE/IDT,IST1,ITEMP
XI= SQRT(WSQ*Q-ZETA2)
UPS=2.0*ARSIN(XI/(2.0*R))
UPS = UPS* (180.0/PI)
OMEGU = PHI + UPS/2.0
OMEGL = OMEGU + 180.0 -UPS
10  IF (OMEGL - 360.0) 30,20,20
20  OMEGL = OMEGL - 360.0
GO TO 10
30  WRITE (IST1) HH,HK,HL,UPS,OMEGU, OMEGL
RETURN
END
C  SUBROUTINE TEST
C  TEST SUBROUTINE
SUBROUTINE TEST
REAL*4 UPS(2),YY(3),H(3)
INTEGER*2 IH(3,1600),IXX1(1600),IXX2(1600),IYY1(1600),IYY2(1600)
INTEGER*2 IXC(2),IYC(2)
COMMON/BLKA/XLIM,YLIM,RS,LREC,NREC,IXC,IYC
COMMON/BLKB/ UR,OR,XR,YR,C1,C2,ISET,KOUNT,IDX,IDY
COMMON/BLKD/OMS,OML,J,UPS,OM,HH,HK,HL,ICLK,STH,L,CEQS
COMMON/BLKE/IDT,IST1,ITEMP
COMMON/BLKL/IH,IXX1,IXX2,IYY1,IYY2
COMMON/BLKX/TK2,TL2,OMD
H(1) = HH
H(2) = HK
H(3) = HL
UP = UPS(L)
C  CALCULATE Y
SOM = OM-OMS
10  IF (SOM) 20,30,30
20  SOM = SOM + 360.0
GO TO 10
C  IS Y WITHIN LIMITS
30  IF(SOM-OMD) 40,40,90
40  Y = SOM/C2
IY = (Y/RS) + 0.5
C  CALCULATE X
DU = UR-UP
DX= DU/C1
X = XR + DX
C  IS X WITHIN LIMITS
IF (X) 90,50,50
50  IF(XLIM-X) 90,60,60
60  IX=(X/RS) + 0.5
IF (J-1) 80,70,80
70  IY1 = IY + 1 -IDY
IX2 = IX + IDX
IF (IY1) 95,95,85
80  IY2 = IY + IDY
IX1 = IX + 1 - IDX
IF (IY2-NREC) 82,82, 100
82  KOUNT = KOUNT + 1
XX = 0.0

```

```

C      COMPACT COORDINATES
      MT = (IX1/2)*2
      IF(MT-IX1) 101,102,101
C      IX1 ODD
101      IX1 = (IX1 +1)/2
      GO TO 103
C      IX1 EVEN
102      IX1 = (IX1/2)
103      MT=(IX2/2)*2
      IF(MT-IX2)104,105,104
C      IX2 IS ODD
104      IX2=(IX2+1)/2
      GO TO 106
C      IX2 IS EVEN
105      IX2 = IX2/2
C      CHECK Y COORDINATES
106      MT=(IY1/2)*2
      IF(MT-IY1) 107,108,107
107      IY1=(IY1+1)/2
      GO TO 109
108      IY1=IY1/2
109      MT= (IY2/2)*2
      IF(MT-IY2) 110,111,110
110      IY2=(IY2+1)/2
      GO TO 112
111      IY2 = IY2/2
112      CONTINUE
      DO 240 I=1,3
240      IH(I,KOUNT)=H(I)
      IXX1(KOUNT) = IX1
      IXX2(KOUNT) = IX2
      IYY1(KOUNT) = IY1
      IYY2(KOUNT)=IY2
85      ICHK = 0
      GO TO 100
90      IF(J-2) 95,100,95
95      ICHK=1
100      RETURN
      END

C      SUBROUTINE SORT
C      NREC NOW COMPACTED
SUBROUTINE SORT
C      SORT SUBROUTINE
      INTEGER*2 IH(3,1600),IXX1(1600),IXX2(1600),IYY1(1600),IYY2(1600)
      INTEGER*2 IXC(2),IYC(2)
      COMMON/BLKA/XLIM,YLIM,RS,LREC,NREC,IXC,IYC
      COMMON/BLKB/ UR,OR,XR,YR,C1,C2,ISET,KOUNT,IDX,IDY
      COMMON/BLKE/IDT,IST1,ITEMP
      COMMON/BLKL/IH,IXX1,IXX2,IYY1,IYY2
      L=0
      MM=(NREC/2)*2
      IF(MM-NREC) 1,2,1
1      NREC=(NREC+1)/2

```



```

      GO TO 3
2     NREC= NREC/2
3     CONTINUE
      DO 100 J=1,NREC
      DO 100 K=1,KOUNT
      IF(IYY1(K)-J) 100,90,100
90    L = L+1
      IF (ISET-2) 10,20,30
C     CRYSTAL MOUNTED ON C AXIS
10    WRITE(IST1)(IH(JJ,K),JJ=1,3),IXX1(K),IYY1(K),IXX2(K),IYY2(K)
      GO TO 100
C     CRYSTAL ON B AXIS

20    WRITE(IST1)IH(2,K),IH(3,K),IH(1,K),IXX1(K),IYY1(K),IXX2(K),
1    IYY2(K)
      GO TO 100
C     CRYSTAL ON A AXIS
30    WRITE(IST1)IH(3,K),IH(1,K),IH(2,K),IXX1(K),IYY1(K),IXX2(K),
1    IYY2(K)
100   CONTINUE
      END FILE IST1
      REWIND IST1
      WRITE(6,900) KOUNT, L
      KOUNT = L
      RETURN
900   FORMAT( 1H0, 20X, I6, ' REFLECTIONS CALCULATED ', I6, ' REFLECTIONS
1    IERED' )
      END

C     SUBROUTINE DISPLA
C     THIS SUBROUTINE DISPLAYS THE INTENSITY DATA AND THE PARTIAL SUMS
      SUBROUTINE DISPLA
C     DISPLA SUBROUTINE
      INTEGER*2 IH,IK,IL,IX1,IX2,NY1,NY2,IY1,IY2,IUF
      INTEGER*2 LDEN(776,50),RECNUM,IXC(2),IYC(2)
      REAL*8 OD(194,60)
      EQUIVALENCE (OD(1,1),LDEN(1,1))
      COMMON/BLKE/IDT,IST1,ITEMP
      COMMON/LIST/IH,IK,IL,IX1,IX2,NY1,NY2,IY1,IY2,IUF
      COMMON/BLKY/LDEN
      WRITE(6,900) IH,IK,IL
      WRITE(6,910) IX1,IX2,IY1,IY2
      IB1=0
      J1=IX1
      J2=IX2
      IBKR=IY2
      IBKL=IY1
      WRITE(6,920) NY1,NY2
      IDI=IBKR-IBKL
      IF(IDI-28) 20,20,10
10    IB2=IBKL + 28
      IB1 = IB2 +1
      GO TO 25
20    IB2=IBKR
25    DO 30 J=J1,J2

```

```
30  WRITE(6,930)(LDEN(J,I),I=IBKL,IB2)
    IF(IBM) 40,60,40
40  WRITE (6,940)
    DO 50 J =J1,J2
50  WRITE(6,930)(LDEN(J,I),I=IB1,IBKR)
60  RETURN
900  FORMAT(' DISPLAY OF REFLECTION',5X,3I4)
910  FORMAT(' COORDINATES OF REFLECTION ARE '/10X,'X',I6,'TO',I6/
110X,'Y',I6,'TO',I6/)
920  FORMAT(' DISPLAY STARTS 4 POSITIONS ABOVE REFLECTION AND ENDS J
1POSITIONS BELOW',10X,'DISPLAY GOES FROM',I6,'TO',I6)
930  FORMAT(1X,29I4,2X,I6)
940  FORMAT(//////)
    END
```

```

C   TAPE SET UP CARDS FOR IBM 370
    TAPE = UNIT 9, DISK SET UP IST1 = 12, ITEMP=13
G.FTC9FC01 DD DDNAME=TAPE
G.TAPE DD DSNAM=USERFILE.M6569.6541.DATA,UNIT=24009, X
        DCB=(RECFM=U,BLKSIZE=1500,OPTCD=Z),
        VOLUME=SER=000439,DISP=(OLD,PASS),LABEL=(3,NL)
G.FT12FO01 DD DSNAM=&&LC,UNIT=SYSDA,DISP=(NEW,DELETE),
        SPACE=(2408,(1000,9)),DCB=(RECFM=VS,BLKSIZE=2408)
G.FT13FO01 DD DSNAM=&&LD,UNIT=SYSDA,DISP=(NEW,DELETE), X
        SPACE=(2408,(1000,9)),DCB=(RECFM=VS,BLKSIZE=2408)
G.SYSIN DD *
C   INPUT DECK
1.   NUMBER OF FILMS (I2) NFILM
2.   TITLE CARD (20A4)
3.   TAPE CONTROL CARD (6I3,3F5.0)
1-3  IDT TAPE UNIT # = 9
4-6  IST1 FIRST DISK UNIT # = 12
7-9  ITEMP SECOND DISK NUMBER = 13
10-12  IDX - HALF WIDTH IN X DIRECTION OF LARGEST PEAK IN MM/RASTER
        SIZE(MM)
13-15  IDY - HALF WIDTH IN Y DIRECTION OF LARGEST PEAK
        IN MM/RASTER SIZE(MM)
16-18  ISFORT - PROCESSNG INDICATOR ALWAYS =0
19-23  XLIM - X-LENGTH SCANNED IN MM
24-28  YLIM - Y LENGTH SCANNED IN MM
29-33  RS - RASTER SIZE IN MM
4.   CELL CARD (9F8.6)
1-8   A*      A
9-16  B*      B
17-24 C*      C
25-32 *      AL
33-40 *      BE
41-48 *      GA
49-56 1 WAVE(1)
57-64 2 WAVE(2)
65-72 EQUI
5.   MAXIMUM LIMITS (F10.5,4I3)
1-10  SIN THETA MAX
11-13 ISET - ROTATION AXIS C=1,B=2,A=3
14-16 MAXIMUM H
17-19 MAXIMUM K
20-22 MAXIMUM L
6.   REFERENCE REFLECTIONS (4I3)
1-3   H
4-6   K
7-9   L
10.12 IEOF =1 LAST CARD, =0 MORE FOLLOWS
      NOTE **** 3 CARDS, FKL LOWEST ON THE FILM
      (LARGEST X VALUE) INPUTED FIRST

```

7. TOP BTTGM INDICATOR

1 IUPS(1) FIRST REFERENCE REFLECTION IS ON TOP(=0)
OR BOTTOM(=1) HALF OF FILM

2 IUPS(2) SECOND REFERENCE REFLECTION IS ON TOP(=0)
OR ON BOTTOM(=1) HALF OF FILM

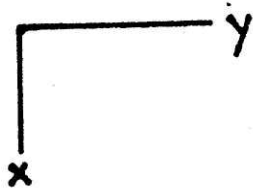
8. REFLECTIONS TO BE INDEXED (413)

1-3 H

4-6 K

7-9 L

10.12 IEOF =1 LAST CARD, =0 MORE FOLLOWS



Bibliography

- LeBihan, M.-Th. (1962), Bull. Soc. Franc. Min. Crystallogr., 85, 15-47.
- Bond, A. (1951), Rev. Sci. Inst. 22 344-345.
- Born, L. and Hellner, E. (1960), Am. Mineral. 45, 1266-1371.
- Buerger, M. J. (1959) Vector Space, John Wiley and Son, Inc. N.Y.
- Burnham, C., (1961), Lattice Constant Refinement, Carnegie Inst. Washington Year Book, 61 133-135.
- Cho, S. A. (1969) "Determination of the Crystal Structure of Plagioclase, $Pb_5Sb_8S_{17}$, by Direct Methods" Ph.D thesis, M.I.T. Department of Metallurgy and Materials Science.
- Dewar, R. and Stone, A. Fortran Program for Automatic Manufacture of E's. University of Chicago.
- Dewar, R. and Stone, A. Multiphase Automatic Generation from Intensities in Centric Crystals. University of Chicago.
- Engel, P. and Nowacki, W. (1969), Zeit. Kristallogr. 129, 178-202.
- Hall, H. T. (1967), Am. Mineral. 52, 1311-1321.
- Harker, D. and Kasper, J. S. (1948) Acta Cryst. 1, 70-75.
- Horiuchi, H., Tokonami, M., Morimoto, N. (1972) Acta Cryst. B 28, 1404-1410.
- Iitaka, Y. and Nowacki, W. (1961), Acta Cryst. 14 1291-1292.
- Jambor, J. (1969), Mineral. Mag. 37 442-446
- Karle, J. and Hauptmann, H. (1953) Amer. Cryst. Assoc. Monograph #3 Edward Brothers, Ann Arbor, Michigan.
- Kohatsu, I. (1971) "The Crystal Chemistry of some Lead-Copper-Bismuth Sulfides, $PbCuBiS_3$, $PbCuBi_5S_9$, $Pb_5Cu_2Bi_5S_{14}$ ", Ph.D. thesis M.I.T. Department of Metallurgy and Materials Science.
- Marumo, F. and Nowacki, W. (1967), Zeit. Kristallogr. 124, 409-419.

- Nowacki,W. and Bayliss,P.(1971) Zeit.Kristallogr. 135, 308-315.
- Peacock,M. and Nuffield,E.(1945),University of Toronto Series 49,
17-39.
- Prewitt,C.T.(1962),"Structures and Crystal Chemistry of Wol-
tonstonite and Pectolite",Ph.D.M.I.T. Depart-
ment of Geology.
- Ribar,B. and Nowacki,W (1969) Zeit.Kristallogr. 128, 321-338.
- Rosch,H.(1963) N. Jb. Mineral. 99, 307-337.
- Sayre,D.(1952) Acta Crystal. 5, 60
- Stout,G.H. and Jensen,L.H.(1968) X-Ray Structure Determination,
The McMilliam Co. N.Y.
- Takeda,H. and Sadanaga,R.(1964) Min.Jour.Japan 4 159-171.
and Horiuchi,H.(1971) Ibid 10, 283-295.
- Wuensch,B.J. and Prewitt,C.T.(1965) Zeit.Kristallogr. 122, 24-59.
and Nowacki,W.(1966) Schweiz.Min.Petrogr.Mitt.
46, 89-96.
and Cho,S.A.(1970) Nature 225 , 444-445.
- Zalkin,A. FORDAP-II unpublished.

Biographical Note

The author was born in Washington D.C. on July 16, 1947. She graduated from Ocean City High School, Ocean City, New Jersey June, 1965 and entered M.I.T. September, 1965. She graduated with a Bachelor of Science in Metallurgy and Materials Science, June, 1969. After completing her bachelor's thesis with Professor B.J.Wuensch, she continued to study the crystal chemistry of sulfosalt minerals with him.

The author is a member of the American Crystallographic Association. She has also been elected to Sigma Xi and Tau Beta Pi. Her bachelor's thesis won the Dow Award for outstanding senior research (1969). She is married to Iwao Kohatsu of Okinawa, Japan.